UNIVERSIDADE DA CORUÑA

PhD. Thesis

Contributions to the mathematical analysis and numerical simulation of stochastic models of general equilibrium with heterogeneous agents and fixed costs

AUTOR:

Jonatan Ráfales Pérez

DIRECTOR:

Carlos Vázquez Cendón

TESE PRESENTADA PARA A OBTENCIÓN DO TÍTULO DE DOUTOR NA UNIVERSIDADE DA CORUÑA

DEPARTAMENTO DE MATEMÁTICAS

FACULTADE DE INFORMÁTICA, A CORUÑA (SPAIN)

2023

UNIVERSIDADE DA CORUÑA

El abajo firmante hace constar que es director de la Tesis Doctoral titulada **"Contributions to the mathematical analysis and numerical simulation of stochastic models of general equilibrium with heterogeneous agents and fixed costs"** desarrollada por Jonatan Ráfales Pérez, cuya firma también se incluye, dentro del programa de doctorado **"Métodos Matemáticos y Simulación Numérica en Ingeniería y Ciencias Aplicadas"** en el Departamento de Matemáticas (Universidade da Coruña), dando su consentimiento para su presentación y posterior defensa.

The undersigned hereby certify that he is supervisor of the Thesis entitled **"Contributions to the mathematical analysis and numerical simulation of stochastic models of general equilibrium with heterogeneous agents and fixed costs"** developed by Jonatan Ráfales Pérez, whose signature is also included, inside the Ph.D Program **"Mathematical Methods and Numerical Simulation in Applied Sciences and Engineering"** at the Department of Mathematics (University of A Coruña), consenting to its presentation and posterior defense.

Diciembre, 2023

Director:

VAZQUEZ CENDON CARLOS - 34946083K

Firmado digitalmente por VAZQUEZ CENDON CARLOS -
Fecha: 2023.12.15 10:04:59 +01'00'

Carlos Vázquez Cendón

Doctorando:

Jonathan Ráfales Pérez

Firmado digitalmente por Jonathan Ráfales Pérez
Fecha: 2023.12.15 10:01:55 +01'00'

Jonatan Ráfales Pérez

Funding

This research has been partially funded by the following projects:

- FPI grant with reference PRE2020-094645 associated with project PID2019-108584RB-I00 from Ministerio de Ciencia e Innovación.
- Project PID2019-108584RB-I00 from Ministerio de Ciencia e Innovación.
- Project MTM2016-76497-R from Ministerio de Economía y Competitividad.
- Project ED431C 2018/033 from Xunta de Galicia.
- Project ED431G 2019/01 from Xunta de Galicia.
- Project ED431C 2022/47 from Xunta de Galicia.

All previous projects include FEDER funding.

A mi familia

Agradecimientos

Al culminar una tarea tan exigente y llena de desafíos como la elaboración de una tesis doctoral, deseo expresar mi gratitud a todas aquellas personas que me han brindado su apoyo de diversas maneras.

En primer lugar, quiero extender un agradecimiento especial y sincero a mi director de tesis, Carlos Vázquez Cendón. A lo largo de estos años, me ha transmitido su entusiasmo y dedicación en cada aspecto de su labor, especialmente su pasión por la investigación y las Matemáticas Aplicadas. Sus conocimientos, ideas y orientaciones han sido fundamentales en esta tesis, convirtiéndose en un referente para mí. Además, agradezco su apoyo constante y la confianza que depositó en mí, así como la energía positiva que siempre me ha brindado. Por todo ello, muchas gracias, Carlos.

También debo agradecer al profesor Kees Oosterlee por su colaboración durante mi formación predoctoral. Durante mi estancia de tres meses en Utrecht, tuve la oportunidad de enriquecerme con su amplio conocimiento y vivir una experiencia sumamente provechosa, tanto a nivel profesional como personal. No puedo olvidar mencionar a mis compañeros Luis, Felix, Balint, Zhipeng, Thomas y Leonardo, quienes me hicieron sentir como en casa.

En estos años, he tenido la fortuna de impartir clases en la Facultad de Informática en A Coruña, contribuyendo en las asignaturas de Cálculo en Ingeniería Informática y Cálculo Multivariable en el Grado en Ciencia e Ingeniería de Datos. Por ello, agradezco enormemente a los profesores Luís Hervella y Marta Benítez por su invaluable ayuda. Me considero afortunado de poder trabajar y, sobre todo, aprender de ellos. Muchas gracias.

No puedo dejar de mencionar al Departamento de Matemáticas y sus profesores, así como a mis compañeros del grupo de investigación M2NICA. Especialmente, debo destacar al profesor Íñigo Arregui por su interés y respaldo durante esta etapa. Además, un reconocimiento especial a mis compañeros Álvaro, Alberto y Joel, con quienes he compartido momentos muy enriquecedores. Han sido un gran apoyo en todo momento.

Gracias también a Luis Rodríguez por estar siempre disponible para ayudarme con cualquier problema informático.

Si bien han sido varios los compañeros que han formado parte del Laboratorio 2.1., primero, y luego del CITIC, debo resaltar a Bea, Eva, Silvia, Dani, Rebeca, Isa y María, con quienes he compartido la mayoría de este tiempo. Con ellos, he disfrutado de muchos cafés, charlas diversas y vivencias que han facilitado sin duda este proceso.

A lo largo de mi etapa como estudiante, he establecido vínculos especiales con algunos profesores. Uno de ellos es el profesor Francisco Gaspar, a quien debo agradecer mi primer acercamiento a las Matemáticas Aplicadas. Gracias a él, esta tesis comenzó a tomar forma.

No puedo olvidar el apoyo incondicional de mis amigos y mi familia. Siempre han estado ahí, interesados en mi trabajo y dispuestos a escucharme y ayudarme. Aunque en ocasiones el tiempo fue limitado o la distancia un obstáculo, siempre encontarón un momento para mí.

A Zai, quien ha sido fundamental en este proceso, mi más sincero agradecimiento. Su constante presencia, disposición para escucharme y esfuerzo por comprenderme han sido invaluables. Gracias por ser un pilar en este camino.

Estas palabras finales de agradecimiento están dirigidas a las personas más importantes en mi vida: mis padres. Les agradezco infinitamente su apoyo incondicional y cariño. Gracias a ellos, sin duda alguna, he logrado alcanzar mis metas, y esta tesis es una más. Muchísimas gracias.

A Coruña, 2023.

Table of Contents

List of Tables

List of Figures

Abstract

In the framework of general equilibrium models for heterogeneous agents under rational expectations, we analyze different problems to establish their mathematical model and numerical solution. The productivity is the only stochastic underlying factor, the dynamics of which either follows an Ito process or a Levy one. We assume the possibility of exit and entry of new firms in the sectors and we consider the case of one sector or two sectors.

In this setting, for the problems of incumbent firms, the mathematical models are mainly formulated in terms of Hamilton-Jacobi-Bellman (HJB) PDEs or PIDEs, with obstacle inequality constraints on the solution. For the probability distribution of firms, the mathematical models are based on Kolmogorov-Fokker-Plank (KFP) PDEs or PIDEs. The global equilibrium models are completed with the household problem and the feasibility conditions. For the numerical solution, the appropriate discretizations of the involved PDEs or PIDEs are combined with an augmented Lagrangian active set (ALAS) method to treat the free boundaries in the incumbent problems. A fixed point iteration that sequentially solves the different subproblems included in the global one is applied. For the time-dependent models, a Crank-Nicolson method for the time discretization is incorporated.

The numerical examples illustrate the performance of the proposed models and numerical methods for different problems and show the convergence of the solutions of the evolutive problems to the ones of the corresponding steady state problems.

Resumen

En el marco de modelos de equilibrio general para agentes heterogéneos bajo expectativas racionales, analizamos diferentes problemas para obtener sus modelos matemáticos y soluciones numéricas. La productividad es el único factor estocástico, cuya dinámica sigue un proceso de Ito o de Levy. Además, consideramos el caso de uno o dos sectores, asumiendo la posibilidad de salida y entrada de nuevas empresas en los sectores.

En este contexto, para los problemas de empresas existentes, los modelos matemáticos se formulan principalmente en términos de ecuaciones en derivadas parciales (EDPs) o ecuaciones integro-diferenciales parciales (EIDPs) de Hamilton-Jacobi-Bellman (HJB), con restricciones de tipo obstáculo en las soluciones. Para la distribución de probabilidad de empresas, los modelos matemáticos se basan en EDPs o EIDPs de Kolmogorov-Fokker-Planck (KFP). Además, los modelos de equilibrio global se completan con el problema de los hogares y las condiciones de viabilidad. Para la solución numérica, adecuadas discretizaciones de las EDPs o EIDPs se combinan con métodos de conjunto activo de tipo Lagrangiano aumentado para tratar las fronteras libres en los problemas de empresas existentes. Además, se aplica una iteración de punto fijo que resuelve secuencialmente los diferentes subproblemas involucrados en el problema global. Para el modelo evolutivo, se incorpora el método de Crank-Nicolson para la discretización temporal.

Los ejemplos numéricos ilustran el rendimiento de los modelos propuestos y los métodos numéricos para los diferentes problemas, y muestran la convergencia de las soluciones de los problemas evolutivos a sus correspondientes problemas estacionarios.

Resumo

No marco dos modelos de equilibrio xeral para axentes heteroxéneos baixo expectativas racionais, analizamos diferentes problemas para obter os seus modelos matemáticos e solucións numéricas. A produtividade é o único factor estocástico, cuxa dinámica segue un proceso de Ito ou de Levy. Ademais, consideramos o caso dun ou dous sectores, asumindo a posibilidade de saída e entrada de novas empresas nos sectores.

Neste contexto, para os problemas de empresas existentes, os modelos matemáticos formúlanse principalmente en termos de ecuacións en derivadas parciais (EDPs) ou ecuacións integro-diferenciais parciais (EIDPs) de Hamilton-Jacobi-Bellman (HJB), con restricións de tipo obstáculo nas solucións. Para a distribución de probabilidade de empresas, os modelos matemáticos baséanse en EDPs ou EIDPs de Kolmogorov-Fokker-Planck (KFP). Ademais, os modelos de equilibrio global complétanse co problema dos fogares e as condicións de viabilidade. Para a solución numérica, discretizacións adecuadas das EDPs ou EIDPs combínanse con métodos de conxunto activo de tipo Lagrangiano aumentado para tratar as fronteiras libres nos problemas de empresas existentes. Ademais, aplícase unha iteración de punto fixo que resolve secuencialmente os diferentes subproblemas involucrados no problema global. Para o modelo evolutivo, incorpórase o método de Crank-Nicolson para a discretización temporal.

Os exemplos numéricos ilustran o funcionamento dos modelos propostos e os métodos numéricos para os diferentes problemas, e mostran a converxencia das solucións dos problemas evolutivos aos seus correspondentes problemas estacionarios.

Introduction

In this thesis we study a class of continuous time heterogeneous agent models with idiosyncratic shocks and incomplete markets under rational expectations in a macroeconomic framework. As in Hopenhayn [30], we consider a continuous time formulation in which firms face with idiosyncratic productivity shocks. The productivity evolution is the only underlying source of uncertainty, which is modelled by a stochastic Itô process or a Lévy one. We assume that the industry is operated by heterogeneous agents to relate (expected) future opportunity benefits for firms, allowing the possibility of exit or entry of new establishments. In this setting, we consider problems posed in the presence of one or two productive sectors. In the case of one sector, the establishments that exit the sector just leave the economy and receive the subsidy. Nevertheless, in the case of two sectors, the firms operating in the sector associated to small establishments can either leave the economy or move to the sector with large establishments after the payment of the conversion costs.

In a general equilibrium macroeconomic framework, the main objective of this thesis is to provide the mathematical modeling for both the steady-state and the time-dependent equilibrium problems, as well as suitable numerical methods in order to solve the different subproblems that are involved in the global equilibrium problem.

Firstly, our study centers on the equilibrium problem that involves one productive sector of the economy in a country. As in Weninger and Just [55], we assume that the abilities of individual firms follow a stochastic process and that there is a fixed operating cost for firms to remain in the industry. These two last assumptions generate the evolution of firm dynamics over time. Therefore, individual rational decisions are not only based on current profits and the whole transitional dynamics must be computed to capture the behavior of firms and its consequences on economic variables. Also, in view of their shocks, firms decide to remain or exit. Exit decisions are endogenously determined by the optimal decision where the opportunity cost of remaining is taken into account by firms through the existence of a scrap value at which firms exit the industry. This decision is formulated in terms of an optimal stopping time problem. Moreover, exit firms are replaced by the entry of new firms such that exit and entry rates are balanced. In this way, the rate of the entry of firms is also endogenous at prescribed levels of productivity. In this respect, we consider two examples, one case where entry takes place at a given productivity above the optimal exit productivity in line with Luttmer [40], and a second one where firms enter at a finite set of productivities with their corresponding probabilities. More general cases could be incorporated by using suitable probability distributions for the productivity of entry firms. Also, in some industries, these entry productivities are exogeneously provided by suitable models to incorporate the income, and therefore the wages and labor (see [16], for an example in the case of fisheries). Unlike in the work by Guzzini and Pallestrini [29], we do not consider the interaction between the idiosyncratic shock of firms and their network structure, which would require to use adjacency matrices from graph theory to represent links between firms.

As in Achdou et al. [3], we assume that individuals interact in markets and make choices for given prices. These prices are determined in a general equilibrium and depend on the entire distribution of individuals in the economy and its evolution. Individuals' choices jointly with idiosyncratic shocks in turn determine the evolution of this distribution. Mathematical models for such economies can be mainly formulated in terms of a system of two coupled partial differential equations (PDEs). More precisely, they involve a Hamilton-Jacobi-Bellman (HJB) PDE for the incumbents problem, with obstacle inequality constraints on the solution. This backward in time HJB equation characterizes the optimal value of the utility function associated with the profit of the firm over time with a given stochastic process evolution for labor productivity. Additionally, a forward in time Kolmogorov-Fokker-Planck (KFP) PDE governs the evolution of the firm distribution. Note that the coupling of these two equations for modelling heterogeneous agents behaviour can be framed into the mathematical theory of Mean Field Games (MFG) developed by Lasry and Lions in [39] and the coupled system is know as a *backward-forward MFG system*. For example, this coupling also arises in the Aiyagari-Bewley-Hugget model to characterize the optimal saving and consumption behaviour of individuals with a stochastic income (see Hugget [31] and Aiyagari [4], for example). Additional references of mean field games are [8, 28, 27], for example. Numerical methods for the MFG system are proposed in [2]. Furthermore, the global equilibrium models are completed with the household problem and the feasibility conditions.

In our model, individual firms assess the expected value of remaining in the industry at each time moment and compare it to the present discounted value of profits associated with exiting the industry. Based on this comparison, individual firms decide to stay in or exit the industry. Note that these models with endogenous firms' exit are also investigated in the so called real options framework (see Dixit et al. [21], for example). Analogous problems arise in mathematical finance, when pricing financial derivatives with early exercise opportunities, such us the American options (see Wilmott et al. [56], for example).

In previous works, such as Luttmer [40] or Da-Rocha and Sempere [16], it was assumed that the stochastic productivity process follows a geometric Brownian motion and new firms enter at a given productivity above the exit productivity, so that in the steady-state case we can adapt our model to get an analytical solution for the one productive sector KFP PDE and a semi-analytical solution for their equilibria. In general, (semi-)analytical solutions to these PDEs are not available. In Achdou et al. [1], the authors point out that the development of numerical methods for solving both stationary and time-dependent equilibria is an open question when more general stochastic processes than geometric Brownian motion for the one productive sector problem are considered. Therefore, we focus on the development of effective numerical solutions. Thus, in the incumbent problem we consider the use of the augmented Lagrangian active set (ALAS) algorithm developed in Kärkkäinen et al. [35] for solving the linear complementarity problem associated with the HJB PDE. For example, in the context of financial problems, this algorithm has been used in Bermúdez et al. [9] for the pricing of Amerasian options, in Calvo et al. [13] for pricing pension plans with early retirement and in Calvo et al. [11] for the pricing of swing options in electricity markets. For the KFP PDE we propose a suitable numerical method and for the equilibrium problem we consider a Steffensen method, developed in [50], to speed up the fixed point iteration, which provides second order convergence in the global algorithm. Moreover, time-dependent models require suitable additional numerical methods, so we incorporate a Crank-Nicolson for the time discretization to be combined with the previously indicated methods for the steady-state models (see Strikwerda [52], for example).

In addition, the incorporation of jumps in the productivity dynamics serves to model significant and abrupt events that can have a profound impact on economic systems. Such events might include global crises, as witnessed in recent years, such as the COVID-19 pandemic since 2020, or geopolitical events like the invasion of Ukraine in 2022, or bubbles in specific sectors of the economy, which have had repercussions on global markets and energy sectors. This modeling approach, employing jump-diffusion processes, is motivated by the need to account for these unexpected, discrete events within the economic framework. Jump-diffusion models have already been introduced in [22] to model the size evolution of an economic unit, like a firm or a city, when analyzing the presence of power laws in economy and finance. Also in [23], a jump-diffusion process is considered for the income dynamics (actually for the logarithm of the income) when studying the dynamics of inequality. These models trace their roots to the seminal work of Merton [42] in 1976. In this classical model, relative jump sizes are typically assumed to follow a lognormal distribution. Since then, a wide variety of jump-diffusion processes have been introduce in the literature, including exponential Lévy processes such as Variance Gamma (VG), Normal Inverse Gaussian (NIG), and Carr–Geman–Madan–Yor (CGMY) models (see [15, 45, 49], for example). This thesis explores two specific jump-diffusion models: Merton's classical model [42] and Kou's model [38]. In the latter, relative jump sizes follow a log-double-exponential distribution. These models give rise to time-dependent partial integro-differential equations (PIDEs) that govern the equilibrium.

As in the case of PDEs models, (semi-)analytical solutions to these general PIDEs are not available. Therefore, we focus on the development of effective numerical solutions for the equilibrium PIDEs associated with both the Merton and Kou models. As the HJB PDE problem, we use the ALAS algorithm to treat the free boundaries in the incumbent problems. This algorithm has proven effective in solving the linear complementarity problem associated with PIDEs and has been applied in various contexts, including the pricing of fixed-rate mortgages, insurance and coinsurance, and swing options in electricity markets, as demonstrated in Calvo et al. [14] and Calvo et al. [12], respectively. For the KFP PIDE, we propose a suitable numerical method, and for the equilibrium problem, we consider the Steffensen algorithm as for the PDE problem. Moreover, we also incorporate a Crank-Nicolson method for time discretization, which is combined with the previously mentioned methods designed for steady-state models. Additionally, we incorporate an explicit treatment of the integral term, following the IMEX approach proposed in [48], which utilizes the Adams-Bashforth scheme.

On the other hand, our study focuses on the equilibrium problem that involves the interaction between two productive sectors of the economy in a country. Companies of the first sector have the option of abandoning it to enter in the second sector (for example, when the first enters into crisis), facing the corresponding costs of conversion. Also those companies in the second sector have the option to exit the sector either by charging a subsidy and leaving the economy, or moving to the first sector by facing the required conversion costs. Recent examples of these situations appeared for example during the last world pandemia, where different companies adapted their production teams in sectors affected by the crisis to produce masks or medical dresses of great demand during Covid-19 spread. Other examples related to companies from one sector that moved to another one are ship building companies who entered in the production of big structures (jackets) highly demanded by off shore wind mills when they became not so competitive in the naval sector. Also, the transition in the car industry from manufacturing diesel/gasoline fuel cars to electric ones could be another example.

In order to model the evolution of the two productive sector problems, our approach needs extending and adapting the modeling strategies formulated for one productive sector problems. This adaptation centers not only the modeling approach but also the incorporation of suitable numerical methodologies, ensuring compatibility and effectiveness within the context of two sector dynamics.

Exit decisions in both sectors are internally determined through optimal decision-making processes. This needs considering the opportunity cost of remaining within a sector, factored in by a scrap value indicating the threshold at which companies opt to exit each sector. Mathematical models governing such economies can be mainly formulated in the form of a system of four coupled PDEs or PIDEs. More precisely, these models require a couple of backward-in-time HJB PDEs or PIDEs, characterizing the incumbent firm problems per each sector. Additionally, another couple of forward-in-time KFP PDEs or PIDEs govern the evolution of the firm distribution within each sector. These coupled equations involve the dynamics of the firms within the two productive sector landscape.

For the equilibrium solution of the PDEs or PIDEs problems, similar numerical strategies to the one productive sector case are considered. For addressing the incumbent problem within small establishments, we consider the application of the ALAS algorithm adapted for bilateral obstacle problems. Similar obstacle problems arise when solviing optimal investment problems under transaction costs (see [7, 18, 19], for example). Moreover, in handling the incumbent problem within large establishments, we propose employing the ALAS algorithm designed for unilateral obstacle problems. Both methodologies, developed by Kärkkäinen et al. [35], offer effective solutions for resolving linear complementarity problems associated with PDEs and PIDEs. Furthermore, concerning the numerical solution of KFP PDEs or PIDEs, we consider the use of appropriate numerical techniques. The implementation of a Steffensen acceleration technique is proposed in solving the equilibrium problem. For the time-dependent models, we incorporate additional numerical strategies. As in previous cases, for this purpose we propose a Crank-Nicolson scheme for time discretization. Additionally, in order to address the PIDEs problems, we incorporate an explicit handling of the integral term, involving a AB scheme.

The outline of this thesis is as follows.

In Chapter 1, we propose the mathematical models for the equilibrium problems in the case of one sector, both with productivity following an Itô process and a Lévy process. These models involve HJB equations with free boundary problems of single obstacle type and KFP equations.

Chapter 2 contains the description of the set of numerical methodologies to approximate the solution of the models described in the previous chapter. Moreover, we present different numerical examples that illustrate the performance of the methods and the models.

In Chapter 3, we propose the modelling approach for the equilibrium problems in the case of two sectors with the two dynamics for the productivity. In this case, the models involve HJB equations with single and double obstacle free boundary problems and KFP equations.

Chapter 4 describes the set of numerical methods to solve the models proposed in Chapter 3 and includes several numerical simulation examples related to the different equilibrium problems in the two sectors case.

Finally, some conclusions and possible future lines of research are briefly indicated.

Chapter 1

Mathematical models for one productive sector

First, we assume that there are two markets in the economy: final goods and labor markets. Labor is used to produce the final goods. By choosing the output price as the numeraire, we denote the wages at time t by $\omega(t)$. We also assume that there exists a continuum of identical households who own the firms, consume the final goods and supply labor by solving a consumption-leisure maximization problem.

Secondly, we assume that firms are heterogeneous. Let $g(t, z)$ denote the probability distribution of firms with productivity z at time t. The decision rules of incumbent firms at time t depend on the productivity z. For a given productivity z and time t, we denote the optimal choices of output and labor by $y(t, z)$ and $l(t, z)$, respectively.

As in Weninger and Just [55], we assume that the uncertain productivity of firms evolves in time according to a stochastic process z_t and that firms must pay the fixed operating cost c_f to remain active in the industry. These two assumptions imply that individual firms change over time in the transition problem. At each particular time t, some of them expand production, hiring staff, while others contract production, firing staff, and others exit the industry. When a firms exits, it receives a scrap value s that may depend on time, but it can never re-entry in the future. The firms that exit are instantaneously replaced by a group of entry firms, in such a way that the exit and entry rates are balanced. In the present work, the productivity of firms that enter the industry is assumed to be random and governed by a probability function g^e. For example, if this probability function is defined by a Dirac delta centered at a particular productivity z_0^e, then all firms enter with this productivity at a rate that balances the exit rate.

The decision problem of incumbent firms involves two types of decision rules. There are continuous decision rules for the optimal choice of output $y(t, z)$ and labor $l(t, z)$, and there is a discrete decision rule for the optimal stay/exit decision that takes into account the scrap value which involves the opportunity cost of remaining in operation.

Therefore, we have an endogenous exit decision. This decision depends on $l(t, z)$ and $y(t, z)$ in each period. Conditioned by the choices of functions l and y in each period, the firms must compare the expected value of remaining in the industry with the discounted value of profits associated with exiting the industry. Note that unlike to the standard framework, the distribution of the productivity of firms is not exogenous. In our model it is endogenously determined by their decisions on exiting. Therefore, the distribution g changes over time in the transition model. In the steady-state case, the balance between entry and exit of firms allows to understand entry and exit as job creation and destruction. In this case, we obtain stationary probability functions of firms size and values, as well as in the other equilibrium magnitudes.

1.1 The coupled PDEs problem

In this section, we assume that the productivity z is a stochastic process which satisfies the following stochastic differential equation (SDE):

$$dz_t = \mu(t, z_t)dt + \sigma(t, z_t)dW_t, \tag{1.1}$$

where μ and σ represent the drift and volatility of the productivity, while W_t denotes a standard Brownian motion. Thus, the productivity follows a Itô process, where μ and σ satisfy the conditions that guarantee the existence and uniqueness of solution of equation (1.1), see [43] for example. As we mainly are interested in the convergence of evolutive problems to the corresponding steady-state ones, we assume the following SDE:

$$dz_t = \mu(z_t)dt + \sigma(z_t)dW_t. \tag{1.2}$$

Note that the geometric Brownian motion is a particular case for (1.1) and (1.2). Also Ornstein-Uhlenbeck processes with mean reversion to a long term productivity are included in (1.1) or (1.2), see some models in Stokey [51]. We refer the reader to [44] for an introduction to stochastic differential equations and to [37] as a classical reference for their numerical solution.

However, if we would like to incorporate jumps in productivity then a jump-diffusion models need to be considered, where a Poisson process or a more general Lévy process must be introduced (see Pascucci [45], for example). For example, jump-diffusion models have been included in Gabaix et al. [23] for income dynamics in the modelling of random growth theories for income inequalities.

Next, we analyze the coupled model in three steps. First, we consider the individual problems of firms and households, which establishes the optimal stay/exit decisions. Secondly, we specify the dynamics of the distribution of firms and the feasibility conditions. Finally, we define the equilibrium coupled problem. In all cases, the transition and steady-state problems are presented.

1.1.1 Problem of incumbent firms

In the first continuous decision rule inside this problem, we assume that firms maximize at each time $t \in [0, T]$ their profits, $\pi(t, z)$, with respect to the labor force $l(t, z)$ and the revenues $y(t, z)$ provided by their available technology, which satisfy the relation $y(t, z) = \sqrt{zl(t, z)}$. Therefore, at each time $t \in [0, T]$, the profit maximization problem is formulated in the form

$$\begin{aligned} \max_{l(t,z),\, y(t,z)} \quad & \pi(t,z) = y(t,z) - \omega(t)l(t,z) - c_f, \\ \text{s.t.} \quad & y(t,z) = \sqrt{zl(t,z)}, \end{aligned} \tag{1.3}$$

where profits are given as the difference between revenues $y(t,z)$ and the sum of labor costs $\omega(t)l(t,z)$ plus fixed operation costs c_f.

By analytically solving problem (1.3) for each time $t \in [0,T]$, we find that the labor force and revenues that maximize the profit are given by:

$$l(t,z) = \frac{z}{4\omega(t)^2}, \qquad y(t,z) = \frac{z}{2\omega(t)}, \tag{1.4}$$

so that the optimal profit is given by:

$$\pi(t,z) = \frac{z}{4\omega(t)} - c_f\,. \tag{1.5}$$

For a time horizon $T > 0$ and the set of positive productivities, we consider the domain $\Omega = [0,T] \times \mathbb{R}^+$. Assuming the option of firms to exit, the dynamic incumbents problem is posed as the optimal stopping time problem:

$$\begin{aligned} v_t &= \max_{\tau_l} \mathbb{E}_0 \left[\int_0^{\tau_l} \pi(t,z_t) e^{-\rho t} dt + s(\tau_l) e^{-\rho \tau_l} \right], \\ \text{s.t.} \quad dz_t &= \mu(t,z_t)dt + \sigma(t,z_t)dW_t, \end{aligned}$$

where $v_t = v(t,z_t)$ is the optimal firm value for the productivity z_t and time t, τ_l is a stopping time, $\mathbb{E}_0$ is the expectation conditional on the initial state, $\pi(t,z)$ is given by (1.5) from the solution of maximization problem (1.3) and ρ is a discount rate. By using the tools of stochastic control, we obtain that the function v satisfies the following Hamilton-Jacobi-Bellman (HJB) equation in Ω:

$$\min\left\{ -\frac{\partial v}{\partial t} - \mu(t,z)\frac{\partial v}{\partial z} - \frac{1}{2}\sigma^2(t,z)\frac{\partial^2 v}{\partial z^2} + \rho v - \pi(t,z), v - s \right\} = 0. \tag{1.6}$$

Problem (1.6) and analogous incumbent problems will be referred as HJB problems. Moreover, it can be written as the linear complementarity problem:

$$\mathcal{L}^H[v] \geq \pi, \quad v \geq s, \quad \left(\mathcal{L}^H[v] - \pi\right) \cdot (v - s) = 0, \tag{1.7}$$

with the involved parabolic differential operator of second order in the space variable z given by:

$$\mathcal{L}^H[v] = -\frac{\partial v}{\partial t} - \mu(t,z)\frac{\partial v}{\partial z} - \frac{1}{2}\sigma^2(t,z)\frac{\partial^2 v}{\partial z^2} + \rho v. \tag{1.8}$$

Note that (1.7) can also be formulated as a parabolic variational inequality of obstacle type, see Kinderlehrer-Stampacchia [36] for example. Therefore, we are handling the concept of weak solution of a variational inequality, whose regularity can be further studied. Note that the concept of viscosity solution for HJB equation has been also handled in the literature (see [39] and references therein, for example).

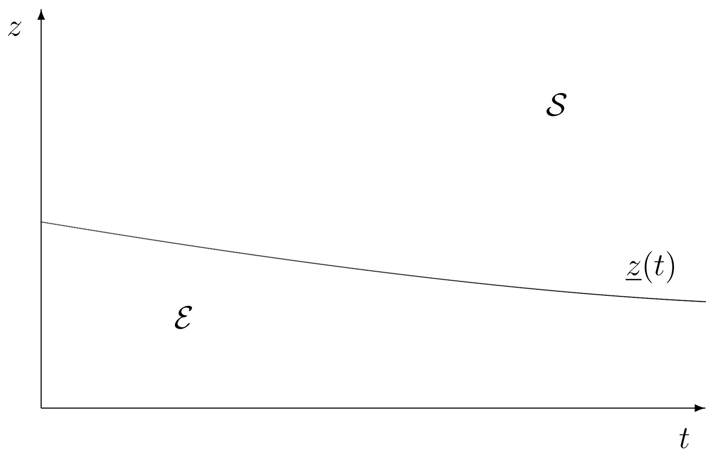

Figure 1.1: Exit region ($\mathcal{E}$), stay region ($\mathcal{S}$) and the free boundary between them ($\underline{z}(t)$)

In Fig. 1.1, we can identify the exit and stay regions defined by:

$$\mathcal{E} = \{(t,z) \in \Omega \,|\, v(t,z) = s(t)\}, \qquad \mathcal{S} = \{(t,z) \in \Omega \,|\, v(t,z) > s(t)\}, \tag{1.9}$$

which are unknowns of the incumbent problem. The following smooth pasting conditions hold at the unknown boundary separating these regions:

$$v = s, \qquad \frac{\partial v}{\partial z} = 0, \qquad \text{on } \partial\mathcal{E} \cap \partial\mathcal{S}. \tag{1.10}$$

Note that $\partial\mathcal{E} \cap \partial\mathcal{S}$ can be understood as an optimal exit boundary and can be parameterized in the (t, z)-plane as $\partial\mathcal{E} \cap \partial\mathcal{S} = \{(t, \underline{z}(t)),\ t \in [0, T]\}$. Therefore, the function v satisfies the equations:

$$\mathcal{L}^H[v] = \pi \quad \text{in } \mathcal{S}, \qquad v = s \quad \text{in } \mathcal{E}, \tag{1.11}$$

jointly with the smooth pasting conditions (1.10).

By considering the dynamics in (1.2), the steady-state version of (1.7) for the incumbents problem is:

$$\hat{\mathcal{L}}^H[v] \geq \pi, \quad v \geq s, \quad \left(\hat{\mathcal{L}}^H[v] - \pi\right) \cdot (v - s) = 0, \tag{1.12}$$

with the involved differential operator given by:

$$\hat{\mathcal{L}}^H[v] = -\mu(z)\frac{\partial v}{\partial z} - \frac{1}{2}\sigma^2(z)\frac{\partial^2 v}{\partial z^2} + \rho v. \tag{1.13}$$

Moreover, the steady-state formulation analogous to (1.11) reads:

$$\hat{\mathcal{L}}^H[v] = \pi(z) \quad \text{in } \hat{\mathcal{S}}, \qquad v = s \quad \text{in } \hat{\mathcal{E}}, \tag{1.14}$$

jointly with the smooth pasting conditions:

$$v(z) = s, \qquad \frac{\partial v}{\partial z}(z) = 0, \qquad \text{on } \partial\hat{\mathcal{E}} \cap \partial\hat{\mathcal{S}}, \tag{1.15}$$

where $\hat{\mathcal{E}} = \{z \in \mathbb{R}^+ \,|\, v(z) = s\}$, $\hat{\mathcal{S}} = \{z \in \mathbb{R}^+ \,|\, v(z) > s\}$ and $\partial\hat{\mathcal{E}} \cap \partial\hat{\mathcal{S}} = \{\underline{z}\}$. Note that in the steady-state problem, the optimal exit boundary is given by the productivity $\underline{z}$, which separates the region $\hat{\mathcal{S}} = (\underline{z}, +\infty)$ where is optimal to remain from the region $\hat{\mathcal{E}} = [0, \underline{z}]$ where it is optimal to exit.

1.1.2 Household problem

Each representative household supplies labor (L) and consumes goods (C). If we consider given prices as numeraire and denote wages by ω, each household at each time t solves a static consumption-leisure maximization problem:

$$\max_{L(t),\, C(t)} \left[\log C(t) - eL(t)\right],$$

where e is a utility parameter, subject to the constraint $C(t) = \omega(t)L(t)+\Pi(t)$, where the budget C is the sum of wage income ωL and the aggregated profits of operating firms, Π. If we replace the constraint in the function to be maximized and apply the first order condition for the maximum we get the equation:

$$\omega(t) = e\big[\omega(t)L(t) + \Pi(t)\big]. \tag{1.16}$$

1.1.3 Problem of the dynamics of firm distribution

In order to compute the prices, the dynamics of firms must be obtained. For this purpose, the probability distribution of firms is denoted by g, which is endogenously determined by stay/exit decisions made by firms and the distribution of entry firms. The function g satisfies the following Kolmogorov-Fokker-Planck (KFP) equation with a source term related to the entry of firms:

$$\mathcal{L}^K[g] = \alpha(t)g^e(t,z), \quad \text{in } \mathcal{S}, \tag{1.17}$$

with the involved differential operator given by:

$$\mathcal{L}^K[g] = \frac{\partial g}{\partial t} + \frac{\partial\big(\mu(t,z)g\big)}{\partial z} - \frac{1}{2}\frac{\partial^2\big(\sigma^2(t,z)g\big)}{\partial z^2}. \tag{1.18}$$

Additionally, $\alpha(t)$ represents the new establishment entry rate and g^e denotes the probability function of the new establishments. More precisely, g^e is a probability density (pdf) or a probability mass (pmf) function for a continuous or discrete random variable, respectively. We assume that the support of $g^e(t,\cdot)$ is contained in $(\underline{z}(t), +\infty)$ to be consistent with the solution of the incumbent problem. Although alternative probability functions could be considered, here we consider that new firms enter either at a given productivity z_0^e, so that $g^e(t,z) = \delta(z - z_0^e)$ with δ being the Dirac function centered at $z = 0$, or randomly among a set of given productivities with their associated probabilities, so that

$$g^e(t,z) = \sum_{i=1}^{I} p_i^e \delta(z - z_i^e), \qquad \text{with} \quad z_i^e > \underline{z}, \quad p_i^e \geq 0, \quad \sum_{i=1}^{I} p_i^e = 1. \tag{1.19}$$

Note that the productivity process has a reflecting barrier at the optimal productivity boundary, so that equation (1.17) is satisfied on $\mathcal{S}$. Moreover, we consider the boundary conditions at the spatial boundaries of $\mathcal{S}$:

$$g(t, \underline{z}(t)) = 0 \qquad \text{and} \qquad \lim_{z \to +\infty} g(t, z) = 0. \tag{1.20}$$

By integrating (1.17) between $\underline{z}(t)$ and $+\infty$, applying boundary conditions (1.20) and using the Leibniz integral rule, we obtain

$$\alpha(t) = \frac{1}{2}\sigma^2\big(t, \underline{z}(t)\big)\frac{\partial g}{\partial z}\big(t, \underline{z}(t)\big),$$

which states that the entry rate $\alpha(t)$ is equal to the exit rate at point $z = \underline{z}(t)$, so that the entry rate is endogenous. In Gabaix et al. [23], the same argument is used to pose a KFP equation to model income inequality.

Moreover, we can write the steady-state version of equation (1.17) as follows:

$$\hat{\mathcal{L}}^K[g] = \frac{1}{2}\sigma^2(\underline{z})\frac{\partial g}{\partial z}(\underline{z})\, g^e(z), \quad \text{in } \hat{\mathcal{S}}, \tag{1.21}$$

with the involved differential operator given by:

$$\hat{\mathcal{L}}^K[g] = \frac{\partial\big(\mu(z)g\big)}{\partial z} - \frac{1}{2}\frac{\partial^2\big(\sigma^2(z)g\big)}{\partial z^2}, \tag{1.22}$$

where the entry of firms does not depend on time.

1.1.4 Feasibility conditions

In order to close the model we need to define feasibility conditions in the labor and output markets. These conditions are respectively given by:

$$L(t) = \int_{\underline{z}(t)}^{+\infty} l(t,z)g(t,z)\,\mathrm{d}z, \quad Q(t) = \int_{\underline{z}(t)}^{+\infty} y(t,z)g(t,z)\,\mathrm{d}z,$$

where $l(t, z)$ and $y(t, z)$ are given by (1.4).

Note that in [16], the quantity $Q(t)$ represents the fishing opportunities and it is exogenously obtained from a stocks dynamics model. Moreover, the household budget constraint implies that the final output market is in equilibrium, i.e.

$$\begin{aligned} C(t) &= \omega(t)L(t) + \Pi(t) \\ &= \omega(t) \int_{\underline{z}(t)}^{+\infty} l(t,z)g(t,z)\,\mathrm{d}z + \int_{\underline{z}(t)}^{+\infty} \left(y(t,z) - \omega(t)l(t,z) - c_f\right) g(t,z)\,\mathrm{d}z \\ &= \int_{\underline{z}(t)}^{+\infty} y(t,z)g(t,z)\,\mathrm{d}z - c_f\,. \end{aligned}$$

After some calculus, we can write (1.16) in the form

$$\omega(t) = e\left(\int_{\underline{z}(t)}^{+\infty} \frac{z}{2\omega(t)} g(t,z)\,\mathrm{d}z - c_f\right), \tag{1.23}$$

where $\underline{z}(t)$ depends on ω.

Moreover, the steady-state formulation analogous to (1.23) is:

$$\omega = e\left(\int_{\underline{z}}^{+\infty} \frac{z}{2\omega} g(z)\,\mathrm{d}z - c_f\right). \tag{1.24}$$

1.1.5 Equilibrium model

In a general dynamic equilibrium framework, the economy can be represented by the time-varying solution $\underline{z}(t)$, $v(t,z)$, $g(t,z)$ and $\omega(t)$ to the HJB and KFP PDEs (1.7) and (1.17), we rewrite as follows:

$$\mathcal{L}^H[v] \geq \pi, \quad v \geq s, \quad \left(\mathcal{L}^H[v] - \pi\right) \cdot (v - s) = 0, \tag{1.25}$$

$$\mathcal{L}^K[g] = \frac{1}{2}\sigma^2\big(t, \underline{z}(t)\big) \frac{\partial g}{\partial z}\big(t, \underline{z}(t)\big)\, g^e(t,z), \tag{1.26}$$

jointly with (1.23). Moreover, domains for (1.7) and (1.17) are Ω and $\mathcal{S}$, respectively, with appropriate boundary and final or initial conditions.

The stationary equilibrium is represented by the time-independent solution $\underline{z}$, $v(z)$, $g(z)$ and ω to the corresponding steady-state HJB and KFP PDEs (1.12) and (1.21):

$$\hat{\mathcal{L}}^H[v] \geq \pi, \quad v \geq s, \quad \left(\hat{\mathcal{L}}^H[v] - \pi\right) \cdot (v - s) = 0, \tag{1.27}$$

$$\hat{\mathcal{L}}^K[g] = \frac{1}{2}\sigma^2(\underline{z}) \frac{\partial g}{\partial z}(\underline{z})\, g^e(z), \tag{1.28}$$

jointly with (1.24). In this case, the domains of the HJB and KFP PDEs are the productivity intervals $[0, +\infty)$ and $(\underline{z}, +\infty)$, respectively. Note that the steady-state HJB problem admits an equivalent formulation as an elliptic variational inequality (see [36], for example).

1.1.6 A particular stationary model for productivity evolution

In this section, we assume that the productivity follows a geometric Brownian motion, so that equation (1.2) with $\mu(z_t) = \mu z_t$ and $\sigma(z_t) = \sigma z_t$ is satisfied, where constants $\mu < 0$ and σ are the expected growth rate and the per-unit time volatility, respectively. Moreover, we consider that all new establishments enter with a given productivity $z_0^e > \underline{z}$, so that $g^e(z) = \delta(z - z_0^e)$.

1.1.6.1 The particular steady-state incumbent firm problem

The steady-state incumbent firm problem can be formulated by equations (1.14) and (1.15). By using analogous techniques to the ones in Da-Rocha and Sempere [17], the exact solution is given in Proposition 1.1.1.

Proposition 1.1.1. *Given wages w, the exit threshold $\underline{z}$ and the value function v(z) that solve the particular incumbent firm problem are given by:*

$$\underline{z} = \frac{4\omega\beta(\rho - \mu)}{1 + \beta}\left(s + \frac{c_f}{\rho}\right), \tag{1.29}$$

and

$$v(z) = \begin{cases} s, & z \leq \underline{z}, \\ \dfrac{s + \frac{c_f}{\rho}}{1 + \beta}\left(\dfrac{\underline{z}}{z}\right)^{\beta} + \dfrac{z}{4\omega(\rho - \mu)} - \dfrac{c_f}{\rho}, & z > \underline{z}, \end{cases} \tag{1.30}$$

where $\beta = \left(\frac{\mu}{\sigma^2} - \frac{1}{2}\right) + \sqrt{\left(\frac{\mu}{\sigma^2} - \frac{1}{2}\right)^2 + \frac{2\rho}{\sigma^2}}$.

Proof: First, assuming a solution of the form $v(z) = A_1 z^{-\beta} + A_2 z + A_3$ in the domain

$\mathcal{S}$, its substitution in the HJB equation (1.14) leads to

$$-\mu z\big(-\beta A_1 z^{-\beta-1}+A_2\big)-\frac{\sigma^2}{2}z^2\big(\beta(\beta+1)A_1 z^{-\beta-2}\big)+\rho\big(A_1 z^{-\beta}+A_2 z+A_3\big)=\pi(z),$$

where $\pi(z)=\dfrac{z}{4w}-c_f$. If we rearrange terms, we get the following equation for β: $\sigma^2\beta^2-(2\mu-\sigma^2)\beta-2\rho=0$, the positive solution of which is given by $\beta=\left(\frac{\mu}{\sigma^2}-\frac{1}{2}\right)+\sqrt{\left(\frac{\mu}{\sigma^2}-\frac{1}{2}\right)^2+\frac{2\rho}{\sigma^2}}$. Moreover, we also obtain $A_2=(4w(\rho-\mu))^{-1}$ and $A_3=-c_f/\rho$.

Next, we use the smooth pasting conditions (1.15), so that

$$v(\underline{z})=A_1\underline{z}^{-\beta}+\frac{1}{4w(\rho-\mu)}\underline{z}-\frac{c_f}{\rho}=s,\quad \frac{\partial v}{\partial z}(\underline{z})=-\beta A_1\underline{z}^{-\beta-1}+\frac{1}{4w(\rho-\mu)}=0,$$

from which we obtain expression (1.29) for $\underline{z}$ and $A_1=\dfrac{\underline{z}^{\beta+1}}{4w\beta(\rho-\mu)}$. Finally, expression (1.30) for v is obtained.

$\square$

1.1.6.2 The particular steady-state problem of firm distribution

As we have chosen $g^e(z)=\delta(z-z_0)$, we can rewrite the steady-state version of the KFP equation (1.21) as follows:

$$\overline{\mu}z\frac{\partial g}{\partial z}(z)-\frac{\sigma^2 z^2}{2}\frac{\partial^2 g}{\partial z^2}(z)+\overline{\lambda}g(z)=\frac{\sigma^2\underline{z}^2}{2}\frac{\partial g}{\partial z}(\underline{z})\delta(z-z_0^e),\quad \text{in } \hat{\mathcal{S}}, \tag{1.31}$$

where $\overline{\mu}=\mu-2\sigma^2$ and $\overline{\lambda}=\mu-\sigma^2$.

Luttmer [41] shows that equation (1.31) can be solved explicitly for all z, except at the entry point $z=z_0^e$. The solution is continuous and there is a kink that reflects the entry of firms at $z=z_0^e$. In Proposition 1.1.2 we characterize the stationary distribution g that solves (1.31).

Proposition 1.1.2. *Given the exit and entry productivities $\underline{z}$ and z_0^e, respectively, the stationary size distribution in $z\in[\underline{z},z_0^e)\cup(z_0^e,+\infty)$ is given by:*

$$g(z)=c\min\left\{\left(\frac{z}{\underline{z}}\right)^{\zeta+\zeta_*}-1,\left(\frac{z_0^e}{\underline{z}}\right)^{\zeta+\zeta_*}-1\right\}\times\left(\frac{z}{\underline{z}}\right)^{-\zeta}, \tag{1.32}$$

where $c = \frac{\underline{z}^{\zeta_*}}{\underline{z}^{\zeta_*+1} - (z_0^e)^{\zeta_*+1}} \frac{(1-\zeta)(1+\zeta_*)}{\zeta+\zeta_*}$ *and the tail indexes* $-\zeta$ *and* ζ_* *are the roots of the characteristic equation:*

$$\frac{\sigma^2}{2} r^2 - \left(\overline{\mu} - \frac{\sigma^2}{2}\right) r - \overline{\lambda} = 0.$$

Proof: Let $x = \log(z/\underline{z})$ be the logarithmic normalized productivity and let $x_0 = \log(z_0^e/\underline{z})$. For $x \in [0, x_0) \cup (x_0, +\infty)$, the KFP equation (1.31) can be equivalently written in the form:

$$\frac{\partial^2 \hat{g}}{\partial x^2}(x) - \gamma_1 \frac{\partial \hat{g}}{\partial x}(x) - \gamma_2 \hat{g}(x) = 0, \tag{1.33}$$

where $\gamma_1 = (2\overline{\mu} - \sigma^2)/\sigma^2$ and $\gamma_2 = 2\overline{\lambda}/\sigma^2$. Moreover, the boundary conditions are transformed into

$$\hat{g}(0) = 0, \qquad \lim_{x \to +\infty} \hat{g}(x) = 0. \tag{1.34}$$

By applying Laplace transform in equation (1.33), we obtain:

$$(u^2 - \gamma_1 u - \gamma_2)\mathcal{L}[\hat{g}](u) - (u - \gamma_1)\hat{g}(0) - \frac{\partial \hat{g}}{\partial x}(0) = 0,$$

so that we have

$$\mathcal{L}[\hat{g}](u) = \frac{\frac{\partial \hat{g}}{\partial x}(0) + (u - \gamma_1)\hat{g}(0)}{(u^2 - \gamma_1 u - \gamma_2)}. \tag{1.35}$$

As $\gamma_1 < 0$, $\gamma_2 < 0$ and $\gamma_1^2 + 4\gamma_2 > 0$, the two negative roots of the characteristic equation are $r_\pm = \frac{\gamma_1 \pm \sqrt{\gamma_1^2 + 4\gamma_2}}{2}$ and expression (1.35) turns into

$$\mathcal{L}[\hat{g}](u) = \frac{\frac{\partial \hat{g}}{\partial x}(0) + (u - \gamma_1)\hat{g}(0)}{(u - r_+)(u - r_-)}.$$

Next, we obtain the following Laplace inverses:

$$\mathcal{L}^{-1}\left[\frac{1}{(u - r_+)(u - r_-)}\right] = \frac{1}{r_+ - r_-}\left(e^{r_+ x} - e^{r_- x}\right),$$
$$\mathcal{L}^{-1}\left[\frac{u - \gamma_1}{(u - r_+)(u - r_-)}\right] = \frac{1}{r_+ - r_-}\left((r_+ - \gamma_1)e^{r_+ x} - (r_- - \gamma_1)e^{r_- x}\right).$$

From them, for $x \in [0, x_0) \cup (x_0, +\infty)$ we get:

$$\hat{g}(x) = \frac{\frac{\partial \hat{g}}{\partial x}(0)}{r_+ - r_-}\left(e^{r_+ x} - e^{r_- x}\right) + \frac{\hat{g}(0)}{r_+ - r_-}\left((r_+ - \gamma_1)e^{r_+ x} - (r_- - \gamma_1)e^{r_- x}\right).$$

Next, we use the boundary conditions (1.34) and obtain that

$$\hat{g}(x) = \frac{\frac{\partial \hat{g}}{\partial x}(0)}{r_+ - r_-}\left(e^{r_+ x} - e^{r_- x}\right) = \frac{\frac{\partial \hat{g}}{\partial x}(0)}{r_+ - r_-}\left(e^{(r_+ - r_-)x} - 1\right) \cdot e^{r_- x}. \tag{1.36}$$

Therefore, we can get the expression:

$$g(z) = c\left[\left(\frac{z}{\underline{z}}\right)^{\zeta+\zeta_*} - 1\right] \cdot \left(\frac{z}{\underline{z}}\right)^{-\zeta},$$

where $\zeta = -r_-$ and $\zeta_* = r_+$.

By applying that $\int_{\underline{z}}^{+\infty} g(z)dz = 1$, we get:

$$c\left[\frac{1}{\underline{z}^{\zeta_*}} \lim_{z\to+\infty} \frac{z^{\zeta_*+1}}{\zeta_*+1} - \frac{\underline{z}}{\zeta_*+1} - \frac{1}{\underline{z}^{-\zeta}} \lim_{z\to+\infty} \frac{z^{-\zeta+1}}{-\zeta+1} + \frac{\underline{z}}{-\zeta+1}\right] = 1. \tag{1.37}$$

The condition for the expression (1.37) to be finite is $\zeta_* < -1$ and $\zeta > 1$. As in Luttmer [41], we assume that $\zeta > 1$, but we cannot guarantee $\zeta_* < -1$. Thus, we can narrow $\left(\frac{z}{\underline{z}}\right)^{\zeta+\zeta_*} - 1$ with the expression

$$\min\left\{\left(\frac{z}{\underline{z}}\right)^{\zeta+\zeta_*} - 1, \left(\frac{z_0^e}{\underline{z}}\right)^{\zeta+\zeta_*} - 1\right\}.$$

Therefore, we finally obtain expression (1.32) and conclude the proof.

□

In view of the result in the previous proposition, we note that the solution of the steady-state KFP equation with source term exhibits a power law behaviour in right hand side tail, which actually corresponds to a Pareto distribution. This is in agreement with previous results from Luttmer [41] and the review article of Gabaix [22] which highlights the presence of power laws in the solution of many problems arising in economics and finance. This behaviour will be better illustrated by graphical representations in Section 2.1.2.1.

Note that in the KFP models we assume the existence of a weak solution g, i.e. a function g such that g, $\frac{\partial g}{\partial z}$ and $\frac{\partial^2 g}{\partial z^2}$ are square integrable in variable z. This is in line with the kind of solutions considered in [23] for income inequality problems, for example. In a more general MFG setting, an alternative concept of measure-valued solution for the KFP PDE has been introduced in [39].

1.1.6.3 The particular steady-state equilibrium problem

In this particular stationary equilibrium problem, we aim to find the functions v and g, and the values $\underline{z}$ and ω that solve the system of equations:

$$\min\left\{-\mu z\frac{\partial v}{\partial z}(z)-\frac{\sigma^2 z^2}{2}\frac{\partial^2 v}{\partial z^2}(z)+\rho v(z)-\pi(z), v(z)-s\right\}=0, \tag{1.38}$$

$$\overline{\mu}z\frac{\partial g}{\partial z^2}(z)-\frac{\sigma^2 z^2}{2}\frac{\partial^2 g}{\partial z^2}(z)+\overline{\lambda}g(z)=\frac{\sigma^2\underline{z}^2}{2}\frac{\partial g}{\partial z}(\underline{z})\delta(z-z_0^e), \tag{1.39}$$

$$\omega=e\left[\int_{\underline{z}}^{+\infty}\frac{zg(z)}{2\omega}dz-c_f\right]. \tag{1.40}$$

From the previous computations, the wage ω that solves (1.40) also satisfies

$$\omega=e\left[\frac{\big((z_0^e)^{\zeta_*+2}-\underline{z}(\omega)^{\zeta_*+2}\big)(1-\zeta)(1+\zeta_*)}{2\omega\big((z_0^e)^{\zeta_*+1}-\underline{z}(\omega)^{\zeta_*+1}\big)(2-\zeta)(2+\zeta_*)}-c_f\right].$$

In Proposition 1.1.3 we formally characterize the solution of (1.38)–(1.40).

Proposition 1.1.3. *The solution of the stationary equilibrium problem defined by equations* (1.38)–(1.40) *is given by:*

$$\underline{z}(\omega)=\frac{4\omega\beta(\rho-\mu)}{1+\beta}\left(s+\frac{c_f}{\rho}\right),$$

$$v(z)=\begin{cases} s, & z\le\underline{z},\\ \dfrac{s+\frac{c_f}{\rho}}{1+\beta}\left(\dfrac{\underline{z}}{z}\right)^{\beta}+\dfrac{z}{4\omega(\rho-\mu)}-\dfrac{c_f}{\rho}, & z>\underline{z},\end{cases}$$

$$g(z)=c\min\left\{\left(\frac{z}{\underline{z}}\right)^{\zeta+\zeta_*}-1,\left(\frac{z_0^e}{\underline{z}}\right)^{\zeta+\zeta_*}-1\right\}\times\left(\frac{z}{\underline{z}}\right)^{-\zeta}, \qquad z\ge\underline{z},$$

and the implicit equation for ω*:*

$$\omega=e\left[\frac{\Big((z_0^e)^{\zeta_*+2}-\big[\frac{4\omega\beta(\rho-\mu)}{1+\beta}(s+\frac{c_f}{\rho})\big]^{\zeta_*+2}\Big)(1-\zeta)(1+\zeta_*)}{2\omega\Big((z_0^e)^{\zeta_*+1}-\big[\frac{4\omega\beta(\rho-\mu)}{1+\beta}(s+\frac{c_f}{\rho})\big]^{\zeta_*+1}\Big)(2-\zeta)(2+\zeta_*)}-c_f\right]. \tag{1.41}$$

Finally, note that the contents of Section 1.1 have already been published in our work [46].

1.2 The coupled PIDEs problem

In the previous section, we have developed a model to describe the dynamics of productivity without taking into account the possibility of sudden spikes or jumps. However, in this section, we expand upon that model to make it more realistic by incorporating the possibility of such spikes, which is a common feature in real-world productivity dynamics.

In this section, we assume that the stochastic evolution of the productivity is described by the following SDE:

$$dz_t = \mu(t, z_t)dt + \sigma(t, z_t)dW_t + \beta(t, z_t)dN_t, \tag{1.42}$$

where μ is the drift or the expected rate of change of productivity and σ represents the volatility of productivity, while W_t is a standard Brownian motion. The Brownian motion is associated to the continuous random fluctuations in productivity, as the paths of the Brownian motion are continuous.

The last term is the new addition to our model and it aims to model the possibility of sudden random jumps or spikes in productivity. More precisely, the parameter β represents the jump size and N_t denotes a compound Poisson process with intensity λ, which captures the occurrence of jumps. Note that a compound Poisson process is a process where events occur at random times and these events have a size distribution given by β.

As our main focus is on studying the convergence of time-dependent problems to their corresponding steady-state solutions, we simplify the SDE (1.42) as follows:

$$dz_t = \mu(z_t)dt + \sigma(z_t)dW_t + \beta(z_t)dN_t, \tag{1.43}$$

where a time-independent drift, volatility and jump size are assumed. This makes the model more amenable to study steady-state behaviors.

In addition, we must specify the distribution of jump sizes. For this purpose, we consider either Merton model [42] or Kou model [38]. More precisely, under Merton model (β) are taken from the normal distribution $\big(\mathcal{N}(\nu_m, \gamma_m^2)\big)$, with the density:

$$f(x) = f_m(x) = \frac{1}{\gamma_m\sqrt{2\pi}} \exp\left(-\frac{(x-\nu_m)^2}{2\gamma_m^2}\right), \tag{1.44}$$

where ν_m is the mean jump size and γ_m is the standard deviation of the jump size, whereas under Kou model the set (β) corresponds to a distribution with double-exponential density:

$$f(x) = f_k(x) = \begin{cases} p\alpha_1 \exp(\alpha_1 x), & x < 0, \\ q\alpha_2 \exp(-\alpha_2 x), & x \geq 0, \end{cases} \tag{1.45}$$

where p, q, α_1 and α_2 are positive constants such that $p + q = 1$ and $\alpha_2 > 1$. Note that p and q represent the probabilities of downward and upward jumps, respectively.

Since $f(x)$ is the probability density function of the jump amplitude β, then

$$\int_{-\infty}^{\infty} f(x)\mathrm{d}x = 1.$$

Moreover, we can compute the expectations for Merton and Kou models:

$$\overline{\kappa} = \mathbb{E}_m[\beta] = \nu_m, \qquad \overline{\kappa} = \mathbb{E}_k[\beta] = \frac{q}{\alpha_2} - \frac{p}{\alpha_1}. \tag{1.46}$$

Therefore, within this context, we formulate a set of mathematical equations to model the dynamics of firms in the presence of jumps, leading to a partial integro-differential equation (PIDE) model. The PIDE system involves two main equations: the HJB PIDE for the incumbent problem and the KFP PIDE that describes the distribution of firms.

1.2.1 Problem of incumbent firms

Let $\Omega = [0,T] \times \mathbb{R}^+$, the incumbent problem can be written as a linear complementarity problem. Given the optimal profit π defined by (1.5), if we denote by $v(t,z)$ the optimal firm value for the productivity z and time t, then standard techniques based on Itô formulas for jump-diffusion processes prove that the function v satisfies the following PIDE problem:

$$\begin{cases} \mathcal{L}_J^H[v] \geq \pi, \quad v \geq s, \quad \big(\mathcal{L}_J^H[v] - \pi\big) \cdot (v - s) = 0, & \forall (t,z) \in \Omega, \\ v(t,0) = -c_f/\rho, \qquad \lim_{z\to\infty} \dfrac{\partial^2 v}{\partial z^2}(t,z) = 0, & \forall t \in [0,T], \\ v(T,z) = v^T(z), & \forall z \in \mathbb{R}^+, \end{cases} \tag{1.47}$$

where v^T is the final condition of the HJB PIDE problem and $\mathcal{L}_J^H[\cdot]$ is the parabolic PIDE operator of second order given by:

$$\mathcal{L}_J^H[v] = \mathcal{L}^H[v] - \lambda \int_{-\infty}^{+\infty} \left[v\big(t, z + \beta(t,z,x)\big) - v(t,z) - \beta(t,z,x) \frac{\partial v}{\partial z} \right] f(x)\,\mathrm{d}x, \tag{1.48}$$

such that the HJB PDE operator $\mathcal{L}^H[\cdot]$ is defined in (1.8).

Note that (1.47) can also be formulated as a parabolic variational inequality of obstacle type, [36]. In this way, we can identify the exit and stay regions as in (1.9). Thus, $\partial\mathcal{E} \cap \partial\mathcal{S} = \{(t, \underline{z}(t)), t \in [0,T]\}$ such that conditions (1.10) are satisfied.

Therefore, the value function v satisfies the following equations:

$$\mathcal{L}_J^H[v] = \pi \quad \text{in } \mathcal{S}, \qquad v = s \quad \text{in } \mathcal{E},$$

jointly with the smooth pasting conditions (1.10).

Moreover, we can write the steady-state version of (1.47) as follows:

$$\begin{cases} \hat{\mathcal{L}}_J^H[v] \geq \pi, \quad v \geq s, \quad \Big(\hat{\mathcal{L}}_J^H[v] - \pi\Big) \cdot (v - s) = 0, & \forall z \in \mathbb{R}^+, \\ v(0) = -c_f/\rho, \qquad \lim_{z\to\infty} \dfrac{\partial^2 v}{\partial z^2}(z) = 0, \end{cases} \tag{1.49}$$

where the involved differential operator is given by:

$$\hat{\mathcal{L}}_J^H[v] = \hat{\mathcal{L}}^H[v] - \lambda \int_{-\infty}^{+\infty} \left[v\big(z + \beta(z,x)\big) - v(z) - \beta(z,x) \frac{\partial v}{\partial z} \right] f(x)\,\mathrm{d}x, \tag{1.50}$$

such that the steady-state HJB PDE operator $\hat{\mathcal{L}}^H[\cdot]$ is defined in (1.13).

1.2.2 Problem of the dynamics of firm distribution

As Section 1.1.3, we consider companies opt to exit the industry, when they determine that their low productivity can no longer offset the costs. Consequently, the productivity process features a reflecting barrier at the optimal productivity boundary. Following the methodology presented in Section 1.1.3, these departing companies are promptly replaced by new entrants. Therefore, the dynamics of firm distribution can be mathematically formulated as a KFP equation with a source term.

Let $g(t,z)$ represent the probability distribution of firms concerning productivity z at time t. Given the entry rate of new establishments $\alpha(t)$ and the probability function governing new establishment entries $g^e(t,z)$, the objective is to determine the distribution g that satisfies the following PIDE problem:

$$\begin{cases} \mathcal{L}_J^K[g] = \alpha(t) g^e(t,z), & & \forall (t,z) \in \mathcal{S}, \\ g(t,\underline{z}(t)) = 0, & \lim\limits_{z\to\infty} g(t,z) = 0, & \forall t \in [0,T], \\ g(0,z) = g^0(z), & & \forall z \in \mathbb{R}^+, \end{cases} \tag{1.51}$$

where g^0 is the initial condition of the KFP PIDE problem and $\mathcal{L}_J^K[\cdot]$ is the involved PIDE operator of second order in the space variable z given by:

$$\mathcal{L}_J^K[g] = \mathcal{L}^K[g] - \lambda \int_{-\infty}^{+\infty} \big[g\big(t, z - \beta(t,z,x)\big) - g(t,z) \big] f(x)\,\mathrm{d}x, \tag{1.52}$$

such that the KFP PDE operator $\mathcal{L}^K[\cdot]$ is defined in (1.18).

As the previous context, we assume that the range of $g^e(t,\cdot)$ falls within the interval $(\underline{z}(t), +\infty)$, aligning with the solution for the incumbent firms. Moreover, we also consider two scenarios: new firms enter either at a predefined productivity z_0^e, giving rise to $g^e(t,z) = \delta(z - z_0^e)$ where δ represents the Dirac delta function centered at $z = 0$, or new firms enter randomly from a predefined set of productivities with their corresponding probabilities, so that g^e satisfies (1.19).

By integrating the PIDE of (1.51) between $\underline{z}$ and $+\infty$, applying their boundary conditions and using the Leibniz integral rule, we obtain:

$$\alpha(t) = \frac{1}{2}\sigma^2(t,\underline{z}) \frac{\partial g}{\partial z}(t,\underline{z}),$$

which state that the entry rate $\alpha(t)$ is equal to the exit rate at point $z = \underline{z}(t)$, so that the entry rate is also endogenous.

Moreover, we can write the steady-state version of the problem (1.51) as follows

$$\begin{cases} \hat{\mathcal{L}}_J^K[g] = \alpha g^e(z), & \forall z \in \hat{\mathcal{S}}, \\ g(\underline{z}) = 0, \qquad \lim_{z\to\infty} g(z) = 0, \end{cases} \tag{1.53}$$

with the involved differential operator given by:

$$\hat{\mathcal{L}}_J^K[g] = \hat{\mathcal{L}}^K[g] - \lambda \int_{-\infty}^{+\infty} \big[g\big(z - \beta(z,x)\big) - g(z)\big] f(x)\, \mathrm{d}x, \tag{1.54}$$

where the steady-state KFP PDE operator $\hat{\mathcal{L}}^K[\cdot]$ is defined in (1.22). Note that the entry of new firms does not depend on time.

1.2.3 Equilibrium model

The equilibrium solution pertaining to the PIDE problems can be described by the time-dependent solutions: $\underline{z}(t)$, $v(t,z)$, $g(t,z)$ and $\omega(t)$. These solutions correspond to the HJB and KFP PIDEs, specifically denoted as equations (1.47) and (1.51), we rewrite as follows:

$$\mathcal{L}_J^H[v] \geq \pi, \quad v \geq s, \quad \big(\mathcal{L}_J^H[v] - \pi\big) \cdot (v - s) = 0, \tag{1.55}$$

$$\mathcal{L}_J^K[g] = \frac{1}{2}\sigma^2\big(t, \underline{z}(t)\big) \frac{\partial g}{\partial z}\big(t, \underline{z}(t)\big)\, g^e(t,z), \tag{1.56}$$

along with the supplementary equation (1.23). Moreover, domains for (1.55) and (1.56) are Ω and $\mathcal{S}$, respectively, with appropriate boundary and final or initial conditions.

The stationary equilibrium is represented by the time-independent solution $\underline{z}$, $v(z)$, $g(z)$ and ω to the corresponding steady-state HJB and KFP PIDEs (1.49) and (1.53):

$$\hat{\mathcal{L}}_J^H[v] \geq \pi, \quad v \geq s, \quad \Big(\hat{\mathcal{L}}_J^H[v] - \pi\Big) \cdot (v - s) = 0, \tag{1.57}$$

$$\hat{\mathcal{L}}_J^K[g] = \frac{1}{2}\sigma^2(\underline{z}) \frac{\partial g}{\partial z}(\underline{z})\, g^e(z), \tag{1.58}$$

jointy with (1.24). In this case, the domains of the HJB and KFP PIDEs are the productivity intervals $[0, +\infty)$ and $(\underline{z}, +\infty)$, respectively.

Finally, we note that the contents of Section 1.2 are included in the article [47].

Chapter 2

Numerical simulation for one productive sector

This chapter mainly focuses on explaining the methodologies proposed to treat both the steady-state and time-dependent equilibrium problems. Additionally, it aims to show a set of results that serve to prove the efficacy and robustness of the suggested numerical approaches.

The first part of the chapter is dedicated to the presentation of the numerical methodologies and examples for both the steady-state and time-dependent PDEs problems. Subsequently, numerical techniques employed in resolving the steady-state and time-dependent PIDEs problems and different tests are presented.

2.1 Numerical solution for the steady-state PDEs problem

This section focuses on solving the steady-state equilibrium problem, mainly characterized by the PDEs denoted as (1.27) and (1.28), along with equation (1.24). Our approach involves a fixed-point iteration technique to compute the numerical solution for problems defined by these equations.

Firstly, we present the numerical methods employed in this process. Subsequently, we showcase several numerical examples to prove the effectiveness and performance of the proposed methodology.

2.1.1 Numerical methods

As the semianalytical solution is not available for the general steady-state problem, in this section we propose a set of numerical techniques to approximate the solution. The main point is the numerical discretization of the HJB and KFP equations governing the incumbent and firm distribution problems.

2.1.1.1 Problem of stationary incumbent firms

A previous step to apply numerical methods is the truncation of the unbounded domain to a bounded one. Thus, we choose a fixed large enough value Z and consider the fixed domain $\hat{\Omega}_Z = [0, Z]$ to pose the stationary incumbent problem (1.27) jointly with the boundary conditions:

$$v(0) = -c_f/\rho \quad \text{and} \quad \frac{\partial^2 v}{\partial z^2}(Z) = 0. \tag{2.1}$$

Different classical alternatives for solving linear complementarity problems or its equivalent formulation in terms of variational inequalities can be found in Glowinski et al. [25, 26] or Glowinski [24], for example. Among these classical alternatives are those ones based on penalization, projection or duality algorithms, see for example in [54] for the pricing problem of American vanilla options.

In the present work, we have chosen the augmented Lagrangian active set (ALAS) method proposed in Kärkkäinen et al. [35] and we apply it to the diffferent fully discretized problem of incumbent firms that arise along this thesis. For example, this method has been compared in Bermúdez et al. [9] with a duality method proposed by Bermúdez and Moreno for the pricing of Amerasian options, i.e., financial options on certain average value of the underlying asset with early exercise oportunity. Note that the ALAS algorithm can also be identified as as a semi-smooth Newton method (see [32, 33, 34], for example).

For the spatial discretization, we use a uniform grid, with stepsize $\Delta z = Z/N_z$, for a given natural number N_z. The grid nodes are $z_k = k\Delta z$, for $k = 0, ..., N_z$, so that we denote $v_k \approx v(z_k)$ the approximation to the solution.

Next, in order to approximate problem (1.27) at the grid point z_k, $k = 1, \ldots, N_z - 1$, we consider the approximations:

$$\frac{\partial v}{\partial z}(z_k) \approx \frac{v_k - v_{k-1}}{\Delta z} \qquad \text{and} \qquad \frac{\partial^2 v}{\partial z^2}(z_k) \approx \frac{v_{k+1} - 2v_k + v_{k-1}}{(\Delta z)^2}. \tag{2.2}$$

After some reordering of terms, we get for $k = 1, \ldots, N_z - 1$ the expressions:

$$\mathcal{L}_k^H[v] \geq \pi_k, \quad v_k \geq s, \quad \left(\mathcal{L}_k^H[v] - \pi_k\right) \cdot (v_k - s) = 0,$$

where

$$\mathcal{L}_k^H[v] = \left[\frac{\mu(z_k)}{\Delta z} - \frac{\sigma^2(z_k)}{2(\Delta z)^2}\right] v_{k-1} + \left[-\frac{\mu(z_k)}{\Delta z} + \frac{\sigma^2(z_k)}{(\Delta z)^2} + \rho\right] v_k - \frac{\sigma^2(z_k)}{2(\Delta z)^2} v_{k+1}. \tag{2.3}$$

Moreover, boundary conditions (2.1) are approximated by:

$$v_0 = -c_f/\rho \quad \text{and} \quad \frac{2v_{N_z} - 5v_{N_z-1} + 4v_{N_z-2} - v_{N_z-3}}{(\Delta z)^2} = 0. \tag{2.4}$$

Thus, the fully discretized linear complementarity problem can be written in matrix form:

$$AV \geq f, \quad V \geq S, \quad (AV - f)^t \cdot (V - S) = 0, \tag{2.5}$$

where $V = (v_0, \ldots, v_{N_z})^t$ is the unknown vector of nodal values of v, $S \in \mathbb{R}^{N_z+1}$ is the vector with all components equal to the scrap value s and vector $f \in \mathbb{R}^{N_z+1}$, such that $f_0 = -c_f/\rho$ and $f_{N_z} = 0$, while $f_k = \pi_k$, $k = 1, \ldots, N_z - 1$. Matrix A is given by

$$A = \begin{pmatrix} 1 & 0 & 0 & 0 & \cdots & \cdots & 0 & 0 & 0 & 0 \\ a_1 & b_1 & c_1 & 0 & \cdots & \cdots & 0 & 0 & 0 & 0 \\ 0 & a_2 & b_2 & c_2 & \ddots & & 0 & 0 & 0 & 0 \\ \vdots & \vdots & \ddots & \ddots & \ddots & \ddots & \vdots & \vdots & \vdots & \vdots \\ \vdots & \vdots & \vdots & \ddots & \ddots & \ddots & 0 & 0 & 0 & 0 \\ \vdots & \vdots & \vdots & \vdots & \ddots & \ddots & c_{N_z-4} & 0 & 0 & 0 \\ \vdots & \vdots & \vdots & \vdots & & \ddots & b_{N_z-3} & c_{N_z-3} & 0 & 0 \\ 0 & 0 & 0 & 0 & \cdots & \cdots & a_{N_z-2} & b_{N_z-2} & c_{N_z-2} & 0 \\ 0 & 0 & 0 & 0 & \cdots & \cdots & 0 & a_{N_z-1} & b_{N_z-1} & c_{N_z-1} \\ 0 & 0 & 0 & 0 & \cdots & \cdots & e_{N_z} & d_{N_z} & a_{N_z} & b_{N_z} \end{pmatrix}$$

such that

$$a_k = \frac{\mu(z_k)}{\Delta z} - \frac{\sigma^2(z_k)}{2(\Delta z)^2}, \quad b_k = -\frac{\mu(z_k)}{\Delta z} + \frac{\sigma^2(z_k)}{(\Delta z)^2} + \rho, \quad c_k = -\frac{\sigma^2(z_k)}{2(\Delta z)^2},$$

for $k = 1, \ldots, N_z - 1$, and,

$$a_{N_z} = \frac{-5}{(\Delta z)^2}, \quad b_{N_z} = \frac{2}{(\Delta z)^2}, \quad d_{N_z} = \frac{4}{(\Delta z)^2}, \quad e_{N_z} = \frac{-1}{(\Delta z)^2}.$$

As previously indicated, we propose the ALAS algorithm from [35] to solve (2.5), which can be written with the equivalent mixed formulation

$$AV + P = f,$$

where P denotes the vector of the multiplier values associated with the inequality constraint. The basic iteration of the ALAS algorithm consists of two steps. In the first one, the nodes are decomposed into active and inactive nodes (depending on whether the constraints are active or not), and in the second step, a reduced linear system associated with the inactive nodes is solved.

First, for any decomposition of nodes $\mathcal{N} = \mathcal{I} \cup \mathcal{J}$, where $\mathcal{N} = \{0, 1, 2, \ldots, N_z\}$, let us denote by $[A]_{\mathcal{I}\mathcal{I}}$ the main diagonal block of matrix A indexed by $\mathcal{I}$ and let us denote by $[A]_{\mathcal{I}\mathcal{J}}$ the codiagonal block indexed by $\mathcal{I}$ and $\mathcal{J}$. Thus, the ALAS algorithm computes not only V and P, but also updates the decomposition $\mathcal{N} = \mathcal{I} \cup \mathcal{J}$ such that

$$\begin{aligned} &AV + P = f, && \\ &P_j + \beta(V_j - S_j) \leq 0, && \text{for all } j \in \mathcal{J}, \\ &P_i = 0, && \text{for all } i \in \mathcal{I}, \end{aligned}$$

for a given positive parameter β. In the above equations, $\mathcal{I}$ and $\mathcal{J}$ are the inactive and the active sets, respectively. More precisely, the iterative algorithm builds sequences $\{V^m\}$, $\{P^m\}$, $\{\mathcal{I}^m\}$ and $\{\mathcal{J}^m\}$, converging to V, P, $\mathcal{I}$ and $\mathcal{J}$, by means of the steps described in Algorithm 1 that appears in the Appendix.

It is important to note that actually (A.1) reduces to solving

$$\begin{aligned} [A]_{\mathcal{I}\mathcal{I}}[V]_{\mathcal{I}} &= [f]_{\mathcal{I}} - [A]_{\mathcal{I}\mathcal{J}}[S]_{\mathcal{J}}, \\ [V]_{\mathcal{J}} &= [S]_{\mathcal{J}}, \\ P &= \min\{f - AV,\ 0\}, \end{aligned}$$

where we have denoted $\mathcal{I} = \mathcal{I}^m$ and $\mathcal{J} = \mathcal{J}^m$.

2.1.1.2 Problem of stationary firm distribution

In this problem, the computational domain will be $\hat{\Omega}_Z = \hat{\mathcal{E}}_Z \cup \hat{\mathcal{S}}_Z$, where $\hat{\mathcal{E}}_Z = [0, \underline{z}]$ and $\hat{\mathcal{S}}_Z = (\underline{z}, Z]$. Moreover, we will consider $g(z) = 0$ on $\hat{\mathcal{E}}_Z$, pose equation (1.28) on $\hat{\mathcal{S}}_Z$ and the boundary condition $g(Z) = 0$.

Let us denote by $g_k \approx g(z_k)$ the approximation obtained with the numerical method. Let $z_{\widetilde{k}}$ be the approximation of the optimal exit productivity, where $\widetilde{k} = \max\{j : j \in \mathcal{J}\}$ is obtained in terms of the sets defined in the numerical solution of the incumbent problem. Next, we discretize equation (1.28) at the grid points z_k,

$k = \widetilde{k}+1, \ldots, N_z - 1$, by introducing the approximations:

$$\begin{aligned} \frac{\partial\big(\mu(z_k)g(z_k)\big)}{\partial z} &\approx \frac{[\mu(z_k)]^+ g_k - [\mu(z_{k-1})]^+ g_{k-1}}{\Delta z} + \frac{[\mu(z_{k+1})]^- g_{k+1} - [\mu(z_k)]^- g_k}{\Delta z}, \\ \frac{\partial^2\big(\sigma^2(z_k)g(z_k)\big)}{\partial z^2} &\approx \frac{\sigma^2(z_{k+1})g_{k+1} - 2\sigma^2(z_k)g_k + \sigma^2(z_{k-1})g_{k-1}}{(\Delta z)^2}. \end{aligned} \tag{2.6}$$

After some reordering of terms, for $k = \widetilde{k}+1, \ldots, N_z - 1$, we get the expression:

$$\mathcal{L}_k^K[g] = \frac{\sigma^2(z_{\widetilde{k}})}{2}\frac{\partial g}{\partial z}(z_{\widetilde{k}})g^e(z_k), \tag{2.7}$$

where

$$\begin{aligned} \mathcal{L}_k^K[g] = &-\frac{1}{\Delta z}\left[\frac{\sigma^2(z_{k-1})}{2\Delta z} + [\mu(z_{k-1})]^+\right] g_{k-1} \\ &+ \frac{1}{\Delta z}\left[\frac{\sigma^2(z_k)}{\Delta z} + [\mu(z_k)]^+ - [\mu(z_k)]^-\right] g_k \\ &- \frac{1}{\Delta z}\left[\frac{\sigma^2(z_{k+1})}{2\Delta z} - [\mu(z_{k+1})]^-\right] g_{k+1}. \end{aligned} \tag{2.8}$$

In order to maintain the structure of matrices to make an efficient solution of tridiagonal systems, we make a fixed point iteration in the term involving $\frac{\partial g}{\partial z}(z_{\widetilde{k}})$ to approximate $\frac{\partial g}{\partial z}(z_{\widetilde{k}}) \approx \frac{\partial g^p}{\partial z}(z_{\widetilde{k}})$, where g^p comes from the previous fixed point iteration. Thus, equation (2.7) is replaced by:

$$\mathcal{L}_k^K[g] = \frac{\sigma^2(z_{\widetilde{k}})}{2}\frac{\partial g^p}{\partial z}(z_{\widetilde{k}})g^e(z_k),$$

which is completed with $g_{N_z} = 0$ provided by the boundary condition and $g_k = 0$, for $k = 0, \ldots, \widetilde{k}$ as $g = 0$ in $\hat{\mathcal{E}}_Z$.

Therefore, the discretized problem can be written as the linear system:

$$BG = b, \tag{2.9}$$

where $G = (g_0,\, g_1, \ldots, g_{N_z})^t$ is the solution vector and $b \in \mathbb{R}^{N_z+1}$, such that $b_k = 0$, $k = 0, \ldots, \widetilde{k}$ and $b_{N_z} = 0$, while

$$b_k = \frac{\sigma^2(z_{\widetilde{k}})}{2}\frac{\partial g^p}{\partial z}(z_{\widetilde{k}})g^e(z_k), \qquad k = \widetilde{k}+1, \ldots, N_z - 1.$$

In order to impose that $g_k = 0$ for $k = 0, \ldots, \widetilde{k}$ and $k = N_z$, we consider

$$B = \begin{pmatrix} 1 & 0 & 0 & 0 & 0 & \cdots & 0 & 0 & 0 & 0 \\ \vdots & \ddots & \vdots & \vdots & \vdots & \cdots & 0 & 0 & 0 & 0 \\ 0 & 0 & 1 & 0 & 0 & \cdots & 0 & 0 & 0 & 0 \\ \vdots & \vdots & \hat{a}_{\widetilde{k}+1} & \hat{b}_{\widetilde{k}+1} & \hat{c}_{\widetilde{k}+1} & & \vdots & \vdots & \vdots & \vdots \\ \vdots & \vdots & \vdots & \ddots & \ddots & \ddots & \vdots & \vdots & \vdots & \vdots \\ \vdots & \vdots & \vdots & \vdots & \ddots & \ddots & \ddots & \vdots & \vdots & \vdots \\ \vdots & \vdots & \vdots & \vdots & & \ddots & \ddots & \ddots & \vdots & \vdots \\ 0 & 0 & 0 & 0 & 0 & \cdots & \hat{a}_{N_z-2} & \hat{b}_{N_z-2} & \hat{c}_{N_z-2} & 0 \\ 0 & 0 & 0 & 0 & 0 & \cdots & 0 & \hat{a}_{N_z-1} & \hat{b}_{N_z-1} & \hat{c}_{N_z-1} \\ 0 & 0 & 0 & 0 & 0 & \cdots & 0 & 0 & 0 & 1 \end{pmatrix},$$

where for $k = \widetilde{k}+1, \ldots, N_z - 1$, we have

$$\begin{aligned} \hat{a}_k &= -\frac{1}{\Delta z}\left[\frac{\sigma^2(z_{k-1})}{2\Delta z} + [\mu(z_{k-1})]^+\right], \ \hat{b}_k = \frac{1}{\Delta z}\left[\frac{\sigma^2(z_k)}{\Delta z} + [\mu(z_k)]^+ - [\mu(z_k)]^-\right], \\ \hat{c}_k &= -\frac{1}{\Delta z}\left[\frac{\sigma^2(z_{k+1})}{2\Delta z} - [\mu(z_{k+1})]^-\right]. \end{aligned}$$

As g is a probability density function, its integral must be equal to one, so that discretizing this condition with the composed trapezoidal rule we get:

$$\sum_{i=0}^{N_z-1} \frac{g_i + g_{i+1}}{2}\Delta z = 1. \tag{2.10}$$

Moreover, we take into account that the probability density function of a $\mathcal{N}(z_i^e, \kappa^2)$ random variable tends to $\delta(z - z_i^e)$ when $\kappa \to 0$, so that we consider the approximation

$$\delta(z - z_i^e) \approx \frac{1}{\kappa\sqrt{2\pi}} e^{-\frac{(z-z_i^e)^2}{2\kappa^2}}. \tag{2.11}$$

in the expression of g^e by choosing κ small enough. In all examples we verified that the choice $\kappa = 10^{-6}$ is suitable.

Remark 2.1.1. *Note that as stated in [23], for example, under certain boundary conditions the differential operator that defines the KFP equation is the adjoint* *operator of the one that defines the HJB equation. So, the numerical solution can take advantage of this result, as the matrix of the discretized KFP equation is just the trasposed matrix of the the one of the HJB equations. However, this is not the case in the models used in the present thesis.*

2.1.1.3 Stationary equilibrium problem

In this section we briefly describe how we calculate the steady-state equilibrium given specified functions $\mu(z)$ and $\sigma(z)$; and values for the parameters s, ρ, e and c_f. We propose a Steffensen method [50], which is specifically designed to speed up the convergence of fixed-point algorithms with linear convergence. Therefore, we start with ω^0 given and for $m = 0, 1, 2, \ldots$ we follow:

1. Given the wage ω^m, solve the stationary HJB equation (1.27) to obtain v^m and $\underline{z}^m$ with the method described in Section 2.1.1.1.

2. Given $\underline{z}^m$, solve the stationary KFP equation (1.28) for g^m using the method detailed in Section 2.1.1.2.

3. Given g^m, we compute the wages ω_1^m by using the equation (1.24).

4. Given the wages ω_1^m, we repeat Steps 1 to 4 for calculating ω_2^m and generate a new guess using the Steffensen formula:

$$\omega^{m+1} = \omega^m - \frac{(\omega_1^m - \omega^m)^2}{\omega_2^m - 2\omega_1^m + \omega^m}. \tag{2.12}$$

Remark 2.1.2. *In [3], for a PDE system of HJB and KFP equations, the authors use that differential operators associated with HJB and KFP PDEs are selfadjoint, so that they propose a numerical method where the matrix associated with the discretized KFP PDE is the trasposed of the one associated with the HJB problem. In our approach, the discretization of the boundary conditions and the blocking of the KFP solution to zero at the nodes in the exit region implies that associated matrices to HJB and KFP PDEs are not trasposed each other.*

2.1.1.4 The particular productivity model

Note that (1.41) allows to characterize ω as a fixed point of the function

$$f(\omega) = e\left[\frac{\left((z_0^e)^{\zeta_*+2} - \left[\frac{4\omega\beta(\rho-\mu)}{1+\beta}(s+\frac{c_f}{\rho})\right]^{\zeta_*+2}\right)(1-\zeta)(1+\zeta_*)}{2\omega\left((z_0^e)^{\zeta_*+1} - \left[\frac{4\omega\beta(\rho-\mu)}{1+\beta}(s+\frac{c_f}{\rho})\right]^{\zeta_*+1}\right)(2-\zeta)(2+\zeta_*)} - c_f\right],$$

so that $\omega = f(\omega)$ is equivalent to (1.41).

The $\omega^{m+1} = f(\omega^m)$ fixed-point iteration technique appears to be a straightforward numerical method. We opt for a particular version of the technique described to compute the general steady-state equilibrium problem. The Steffensen method begins with a given ω^0 and employs the following updating formula:

$$\omega^{m+1} = \omega^m - \frac{(f(\omega^m) - \omega^m)^2}{f \circ f(\omega^m) - 2f(\omega^m) + \omega^m}.$$

When the difference between two consecutive values is below a prescribed tolerance, we consider ω^m jointly with $\underline{z}(\omega^m)$, $v(\omega^m)$ and $g(\omega^m)$ given by Proposition 1.1.3 as the semianalytical solution of the steady-state equilibrium problem.

2.1.2 Numerical results

In this section, we begin with numerical results derived from the semianalytical solution in Section 2.1.1.4. Then, we showcase the effectiveness of our proposed numerical methods in Section 2.1.1 through two examples. One example concerns to the problem in Section 1.1.6, while the second involves randomness in entry productivity using discrete random variables. The first example validates against the semianalytical solution. All examples use the economic data in Table 2.1

More precisely, we take μ and σ^2 from [55] and [17], respectively. Once the geometric Brownian motion parameters have been fixed, it remains to provide s, c_f, e and ρ. We select the annual discount rate $\rho = 0.05$, which is standard in the macroeconomic literature and assume that there are no decommissioning schemes, so that we choose the scrap value $s = 0$. Finally, we obtain the utility parameter e by solving the model when the economy is non-distorted in order to match a labor

Table 2.1: Macroeconomic parameters for one productive sector

Symbol	Value	Description
e	1.53	Utility parameter
ρ	0.05	Discount rate
μ	-0.04	Productivity drift
σ^2	0.01	Productivity volatility
s	0	Scrap value
c_f	0.31	Fixed cost

supply of $L = 1/3$, which is a standard normalization in macroeconomic literature. We consider fixed costs $c_f = 0.31$.

2.1.2.1 Semianalytical solution of the particular productivity model

In this section, we consider the particular model described in Section 1.1.6, for which a semianalytical solution has been obtained (see Proposition 1.1.3). For this aim, the numerical strategy described in Section 2.1.1.4 is performed.

Once the Steffensen numerical method has been applied, we consider the absolute error and the experimental order of convergence

$$E^m(\omega) = |\omega^m - \omega^{m-1}|, \quad p^m(\omega) = \frac{\log\left(\frac{E^m(\omega)}{E^{m-1}(\omega)}\right)}{\log\left(\frac{E^{m-1}(\omega)}{E^{m-2}(\omega)}\right)}. \tag{2.13}$$

In Table 2.2 we can see how the computed values of p^m tend to the expected order of convergence equal two for the case $z_0^e = 3$. The same order of convergence has been observed in all choices of z_0^e.

Next, we illustrate the behaviour of the solution in terms of the productivity at which entry of firms takes place. In Table 2.3 we observe how the values of ω and $\underline{z}$ increase with respect to z_0^e.

Figure 2.1 shows the value function and firms distribution for the values of z_0^e in Table 2.3. Note that the value function decreases when z_0^e increases. As pointed

Table 2.2: Wages approximations, absolute errors and experimental order of convergence for $z_0^e = 3$ obtained with the semianalytical solution

m	ω^m	$E^m(\omega)$	$p^m(\omega)$
0	1	–	–
1	1.090294666372	0.090294666372	–
2	1.087567512305	0.002501300016	–
3	1.087565071168	0.000002244584	1.956364106225
4	1.087565071166	0.000000000002	2.000629506675

Table 2.3: Entry productivity, wages and optimal exit productivity obtained with the semianalytical solution

z_0^e	ω	$\underline{z}$
2	0.904284	1.009181
3	1.087565	1.213723
4	1.237616	1.381179

in Gabaix [22], the empirical regularity of distribution of firms fails at the entry productivity z_0^e and exhibits a singular behaviour at that point, where a kind of kink is observed. At the right tail (i.e. for $z > z_0^e$) an expected power law behaviour is observed. As soon as we increase the value of z_0^e, the firms distribution is more spread up along a larger set of productivities, thus reaching a lower maximum. Actually, the kink is better observed for the higher values of z_0^e.

2.1.2.2 Example 1: The steady-state equilibrium with a prescribed entry productivity

In this example, we also consider the particular model described in Section 1.1.6. However, we use the numerical methods described in Section 2.1.1 to obtain the full

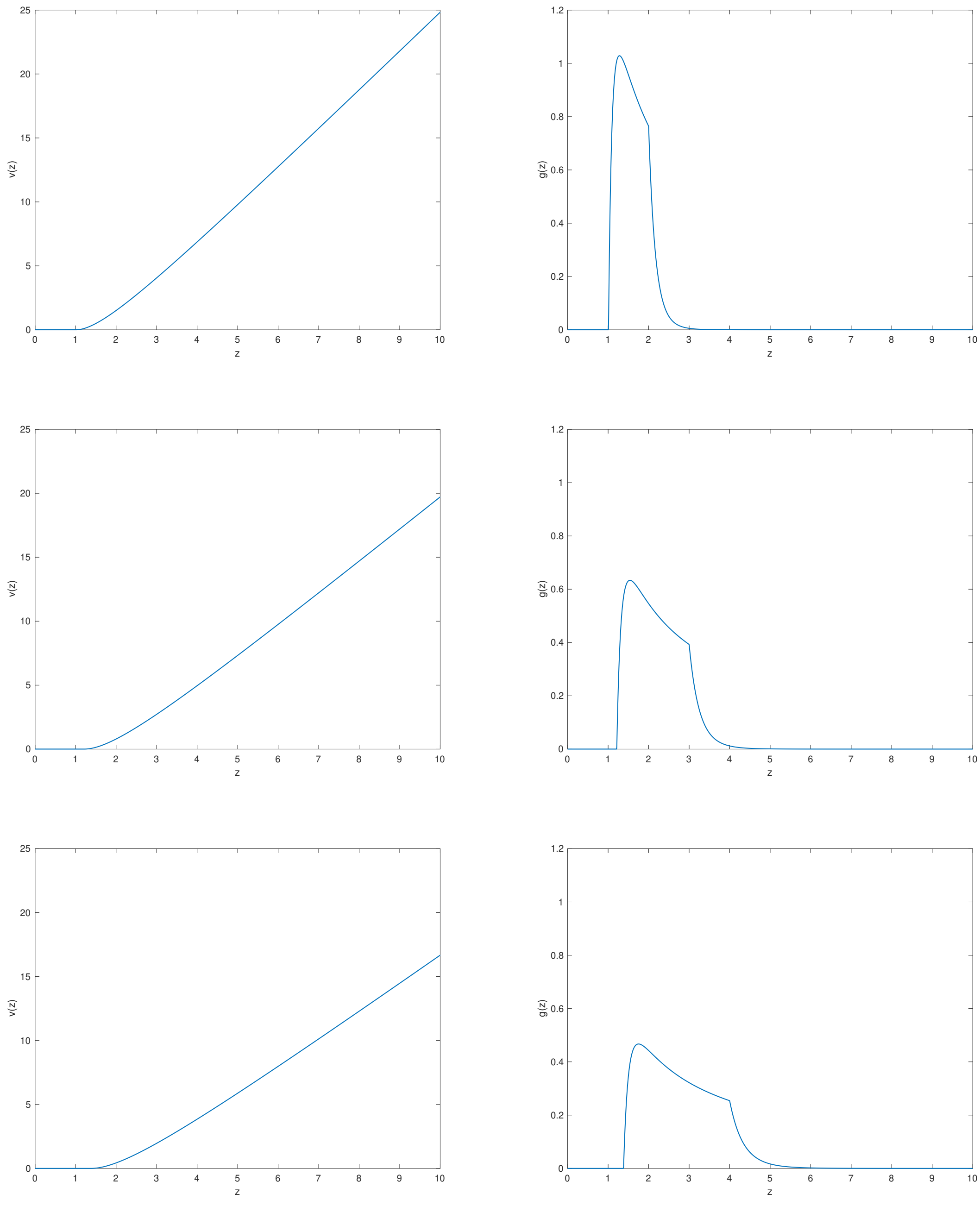

Figure 2.1: The value function (left) and the firm distribution (right) with $z_0^e = 2$ (top), $z_0^e = 3$ (middle) and $z_0^e = 4$ (bottom), obtained with the semianalytical solution

numerical solution of all the involved models. Numerical results are validated with the semianalytical solution obtained in Section 2.1.2.1.

We first show the results for $v_{\Delta z}$ that solves the HJB equation for different mesh steps Δz. Table 2.4 shows the order of convergence of the proposed numerical strategy. For $z_0^e = 3$ we consider the wages value $\omega = 1.087565$ showed in Table 2.2 and we use in all forthcoming examples the upper limit $Z = 10$ in the productivity interval.

In order to study convergence, we use the absolute error between the approximations in the common nodes with meshes with stepsize $2\Delta z$ and Δz, i.e. $E_{\Delta z}(v) = ||v_{2\Delta z} - \overline{v}_{\Delta z}||_\infty$, where $\overline{v}_{\Delta z}$ only contains the approximations of $v_{\Delta z}$ at the nodes that also belong to the coarser mesh with step $2\Delta z$. Next, we compute the convergence ratio $R_{\Delta z}(v) = \frac{E_{2\Delta z}(v)}{E_{\Delta z}(v)}$ and the experimental order of convergence $p_{\Delta z}(v) = \log_2(R_{\Delta z}(v))$. Note that the proposed method achieves linear convergence. In Table 2.4 we can see how the computed values of p tend to the expected order of convergence one. Also the obtained optimal exit productivity for each mesh is shown. Note its convergence to the value obtained from the semianalytical solution in Section 2.1.2.1.

Table 2.4: Absolute errors, convergence ratios and order of convergence in the value function approximation, jointly with computed optimal exit productivity

N_z	$E_{\Delta z}(v)$	$R_{\Delta z}(v)$	$p_{\Delta z}(v)$	$\underline{z}$
4000	–	–	–	1.212500
8000	0.000533	–	–	1.213750
16000	0.000266	2.002788	1.002009	1.213750
32000	0.000133	2.000222	1.000160	1.213750
64000	0.000067	2.000168	1.000121	1.213594

Let $g_{\Delta z}$ be the solution of the KFP equation with mesh step Δz. Using analogous notations as in previous section, Table 2.5 shows the order of convergence of the proposed numerical strategy for solving the KFP model. Note that the proposed method achieves linear convergence. Table 2.5 shows that the computed values of p tend to the expected order of convergence one.

Table 2.5: Absolute errors, convergence ratios and order of convergence in the firm distribution approximation

N_z	$E_{\Delta z}(g)$	$R_{\Delta z}(g)$	$p_{\Delta z}(g)$
4000	–	–	–
8000	0.001780	–	–
16000	0.000883	2.002788	1.010898
32000	0.000440	2.000222	1.005370
64000	0.000220	2.000168	1.002679

Once the algorithm in Section 2.1.1.3 has been applied, Table 2.6 shows the order convergence for the entry productivity $z_0^e = 3$. For this purpose, we consider the absolute error and the experimental order of convergence defined in (2.13). Table 2.6 shows that the computed values of p tend to the expected order of convergence equal two for $z_0^e = 3$ (the same order has been observed for all choices of z_0^e).

Table 2.6: Computed wages, absolute errors and experimental order of convergence for $z_0^e = 3$ in Example 1

m	ω^m	$E^m(\omega)$	$p^m(\omega)$
0	1	–	–
1	1.090007559278	0.090007559278	–
2	1.087563949290	0.002443609989	–
3	1.087547943192	0.000016006098	1.394254099212
4	1.087547942992	0.000000000199	2.245891561217

Next, we choose three values of z_0^e to illustrate the behaviour of the solution in terms of the productivity at which entry of firms takes place. Table 2.7 shows the different values we obtain for the equilibrium ω and $\underline{z}$. Note that all results are very close to the ones obtained from the semianalytical solution in Section 2.1.2.1 (see Table 2.3).

Table 2.7: Equilibrium wages and optimal exit productivity for different entry productivities in Example 1

z_0^e	ω	$\underline{z}$
2	0.904223	1.009063
3	1.087548	1.213594
4	1.237583	1.381094

Figure 2.2 shows the corresponding value function and density of firms for $z_0^e = 3$. In order to illustrate the behavior of the proposed numerical strategy, we also show the semianalytical solution obtained in Section 2.1.2.1.

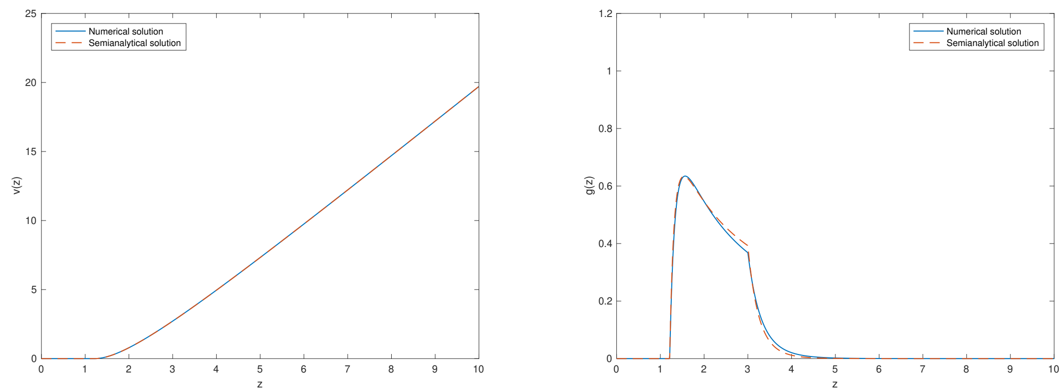

Figure 2.2: The value function (left) and the firm distribution (right) for $z_0^e = 3$ in Example 1

2.1.2.3 Example 2: The steady-state equilibrium with random entry productivities

In this example, we incorporate to the model in Section 1.1.6 the randomness in the entry productivity by means of a discrete random variable. For this purpose, we consider a probability function of new establishments given by expression (1.19) with $I = 3$. In this case, we can rewrite a similar version of the KFP equation (1.31) as follows:

$$\overline{\mu} z \frac{\partial g}{\partial z}(z) - \frac{\sigma^2 z^2}{2} \frac{\partial^2 g}{\partial z^2}(z) + \overline{\lambda} g(z) = \frac{\sigma^2 \underline{z}^2}{2} \frac{\partial g}{\partial z}(\underline{z}) \sum_{i=1}^{3} p_i^e \delta(z - z_i^e), \quad \text{in } \hat{\mathcal{S}}.$$

For this equation, an analytical solution is not available as in the particular model of Section 2.1.2.1. In this setting we will consider different choices for the productivities z_i^e and the associated probabilities p_i^e. Although we have solved the different subproblems separately to validate the different numerical methods, we prefer to present just those results corresponding to the equilibrium problem, which requires the solution of each subproblem at each iteration of the fixed point algorithm. Moreover, for an easier presentation of the results we will consider a vector notation for entry productivities $\mathbf{z^e} = (z_1^e,\, z_2^e,\, z_3^e)$ with the associated probabilities $\mathbf{p^e} = (p_1^e,\, p_2^e,\, p_3^e)$.

As a first data set, we use $\mathbf{z^e} = (2,\, 3,\, 4)$ and $\mathbf{p^e} = (0.25,\, 0.5,\, 0.25)$. In this way, we assume that entry productivity is random and assign probabilities to each of the entry productivities considered in Example 1. Once the Steffensen numerical method has been applied to solve the equilibrium problem, Table 2.8 clearly shows how the order of convergence obtained by equations (2.13) tends to the expected order of convergence equal two for the case $\mathbf{z^e} = (2,\, 3,\, 4)$ and $\mathbf{p^e} = (0.25, 0.5, 0.25)$. The same order of convergence has been observed in all choices of $\mathbf{z^e}$ and $\mathbf{p^e}$ we show in this section.

Next, we have chosen two additional data sets for $\mathbf{p^e}$ to illustrate the behaviour of the solution of the equilibrium problem in terms of the productivity at which entry of firms takes place and their associated probabilities. These computations allow us

Table 2.8: Wages approximations, absolute errors and experimental order of convergence for $\mathbf{z^e} = (2, 3, 4)$ and $\mathbf{p^e} = (0.25, 0.5, 0.25)$ in Example 2

m	ω^m	$E^m(\omega)$	$p^m(\omega)$
0	1	–	–
1	1.121165977662	0.121165977662	–
2	1.116987872017	0.004178105645	–
3	1.117000129288	0.000012257271	1.731799380392
4	1.117000129176	0.000000000112	1.988838781379

to obtain the equilibrium values of ω and $\underline{z}$ for these sets of parameters. In Table 2.9 these equilibrium values are shown.

Table 2.9: Probabilities, wages and optimal exit productivities for $\mathbf{z^e} = (2, 3, 4)$ in Example 2

$\mathbf{p^e}$	ω	$\underline{z}$
$(0.25, 0.5, 0.25)$	1.117000	1.246563
$(0.1, 0.8, 0.1)$	1.098930	1.226406
$(0.1, 0.1, 0.8)$	1.213797	1.354531

Next, in Figures 2.3, 2.4 and 2.5 we show the corresponding value functions and probability densities of firms for the different sets $\mathbf{p^e}$ that appear in Table 2.9.

First, Figure 2.3 shows the computed value function and firms distribution when we assign probabilities $\mathbf{p^e} = (0.25, 0.5, 0.25)$ to the three cases of entry productivity we considered in Section 2.1.2.2. In the probability density of firms we observe a kink at each possible entry productivity, three kinks in total, being more steep the one at the productivity with higher probability. If we compare with Figure 2.2, we observe that the value function decreases and a change in the distribution of firms.

Note that we could consider the example in Figure 2.2 as associated with the case with $\mathbf{p^e} = (0, 1, 0)$ instead of $\mathbf{p^e} = (0.25, 0.5, 0.25)$.

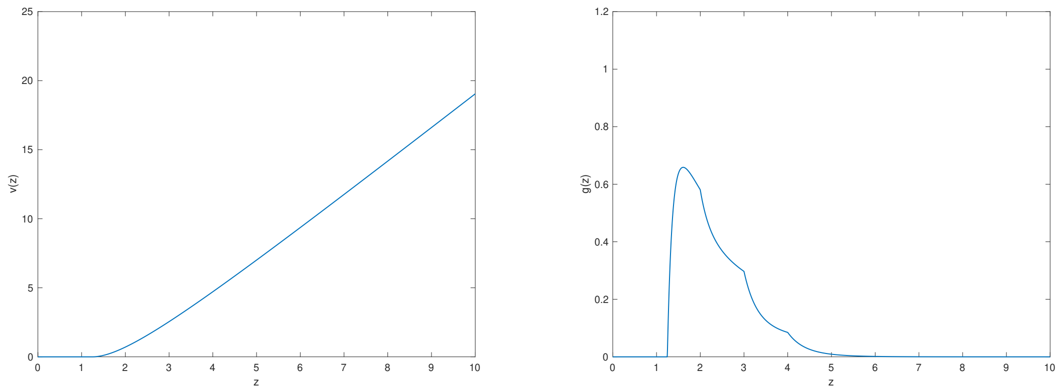

Figure 2.3: The value function (left) and the firm distribution (right) with $\mathbf{z^e}$ = (2, 3, 4) and $\mathbf{p^e}$ = (0.25, 0.5, 0.25) in Example 2

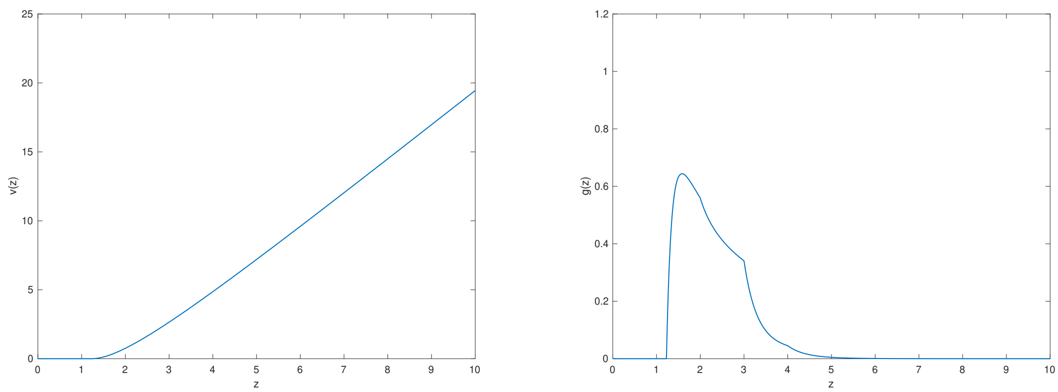

Figure 2.4: The value function (left) and the firm distribution (right) with $\mathbf{z^e}$ = (2, 3, 4) and $\mathbf{p^e}$ = (0.1, 0.8, 0.1) in Example 2

In Table 2.9, for the fixed set $\mathbf{z^e}$ = (2, 3, 4), in the second row we change the probabilities to make $z_2^e = 3$ much more probable than the others, thus giving rise to Figure 2.4. Next, we make $z_3^e = 4$ more probable than the others and obtain results in Figure 2.5. Figures 2.4 and 2.5 illustrate how the kink in the probability density function is more steep at the entry productivity where the associated probability is higher, as expected. Moreover, it seems that the parts of the density functions at the right tails of the different entry productivities z_i^e exhibit a power law behavior with a different exponent in each case. We conjecture that these power laws correspond to Pareto distributions. Also at each z_i^e the density function becomes singular, which is a consequence of using combinations of delta functions in the source term g^e.

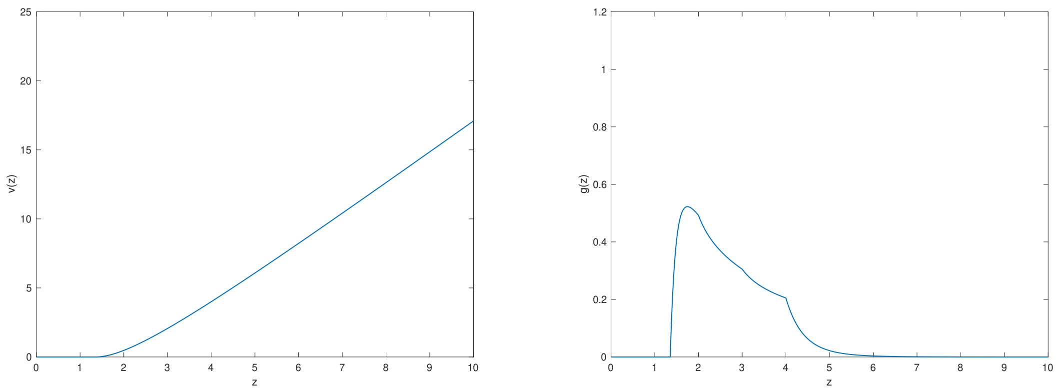

Figure 2.5: The value function (left) and the firm distribution (right) with $\mathbf{z^e} = (2, 3, 4)$ and $\mathbf{p^e} = (0.1, 0.1, 0.8)$ in Example 2

In Example 2 the semianalytical solution of the equilibrium problem is not available so that the numerical solution of all involved PDEs is mandatory.

The contents of Section 2.1 have been previously published in our article [46].

2.2 Numerical solution for the time-dependent PDEs problem

In this section we address the numerical solution of the time-dependent equilibrium problem, which is mainly defined by equations (1.25), (1.26) and (1.23). As in the steady-state problem, in the time-dependent equilibrium we pose a fixed point iteration between the numerical solution of the involved problems.

As we aim to show the convergence of the solution of the time-dependent problem to the solution of the corresponding steady-state one, we consider as final condition for (1.25) the solution of the steady-state problem. Concerning the initial condition to complete equation (1.26), we assume that it is related to the productivities at which new establishments enter the industry.

We first describe the additional numerical methods we incorporate in the time-dependent problems and secondly we show some numerical examples to illustrate the performance of the proposed methodology.

2.2.1 Numerical methods

For the numerical solution of problems defined by equations (1.25) and (1.26), we propose a Crank-Nicolson scheme for the time discretization, which will be combined with the finite difference methods we used for the spatial discretization in the steady-state problems. At each time step, the fully discretized problems will be solved with the same techniques as in the discretized steady-state ones.

2.2.1.1 Problem of evolutionary incumbent firms

The evolutionary incumbent's problem is posed in terms of the complementarity problem (1.25) on the computational domain $\Omega_Z = [0,T] \times [0,Z]$, where Z is a large enough productivity and T is a large enough time horizon to enter in the steady-state regime at $t = T$. Additionally, we assume the following final and boundary conditions:

$$v(T,z) = v_T(z), \quad v(t,0) = -c_f/\rho \quad \text{and} \quad \frac{\partial^2 v}{\partial z^2}(t,Z) = 0, \tag{2.14}$$

where $v_T(z)$ is the solution of the steady-state problem.

For the time discretization we introduce a uniform mesh, with time step $\Delta t = T/N_t$ for a given natural number N_t, so that the nodes are given by $t^n = n\Delta t$, with $n = 0, 1, ..., N_t$. For the productivities we use a uniform mesh with the same notation as in the steady-state case, so that we define v_k^n as the approximation of the solution of problem (1.25) at $\big(n\Delta t, k\Delta z\big)$, i.e. $v_k^n \approx v(t^n, z_k)$.

Next, in order to approximate problem (1.25) at the point (t_θ^n, z_k), with $k = 1, \ldots, N_z - 1$ and $n = 0, 1, \ldots, N_t - 1$, we introduce the following approximations of $\dfrac{\partial v}{\partial t}$, $\dfrac{\partial v}{\partial z}$ and $\dfrac{\partial^2 v}{\partial z^2}$ at (t_θ^n, z_k), where $t_\theta^n = \theta t^n + (1-\theta)t^{n+1}$, with $0 \leq \theta \leq 1$:

$$\begin{aligned}
&\frac{\partial v}{\partial t}(t_\theta^n, z_k) \approx \frac{v_k^{n+1} - v_k^n}{\Delta t}, \quad \frac{\partial v}{\partial z}(t_\theta^n, z_k) \approx \theta \frac{v_k^n - v_{k-1}^n}{\Delta z} + (1-\theta)\frac{v_k^{n+1} - v_{k-1}^{n+1}}{\Delta z}, \\
&\frac{\partial^2 v}{\partial z^2}(t_\theta^n, z_k) \approx \theta \frac{v_{k+1}^n - 2v_k^n + v_{k-1}^n}{(\Delta z)^2} + (1-\theta)\frac{v_{k+1}^{n+1} - 2v_k^{n+1} + v_{k-1}^{n+1}}{(\Delta z)^2}.
\end{aligned} \tag{2.15}$$

Previous approximations correspond to the so called θ-method ($0 \leq \theta \leq 1$) applied to the backward in time HJB PDE, where $\theta = 0$ and $\theta = 1$ correspond to the explicit and implicit methods, respectively. In practice we consider $\theta = 0.5$, which defines the Crank-Nicolson scheme and exhibits second order convergence in time and space for linear PDEs [52].

Once expressions (2.15) are introduced in (1.25) at points (t_θ^n, z_k) and after some reordering of terms, we obtain, for $n = N_t - 1, N_t - 2, \ldots, 1, 0$ and $k = 1, \ldots, N_z - 1$, the following inequalities:

$$\mathcal{L}_\theta^H[v] \geq \pi_k^\theta, \quad v_k^\theta \geq s^\theta, \quad \left(\mathcal{L}_\theta^H[v] - \pi_k^\theta\right) \cdot (v_k^\theta - s^\theta) = 0$$

such that $v_k^\theta = \theta v_k^n + (1-\theta)v_k^{n+1}$, $\pi_k^\theta = \theta \pi_k^n + (1-\theta)\pi_k^{n+1}$ and $s^\theta = \theta s^n + (1-\theta)s^{n+1}$, where $\pi_k^n = \pi(t^n, z_k)$ and $s^n = s(t^n)$. Moreover, the involved operator is defined by:

$$\mathcal{L}_\theta^H[v] = \frac{v_k^n - v_k^{n+1}}{\Delta t} + \theta[\mathcal{L}^H]_k^n[v] + (1-\theta)[\mathcal{L}^H]_k^{n+1}[v],$$

where

$$\begin{aligned}
[\mathcal{L}^H]_k^n[v] = &\left[\frac{\mu(t^n, z_k)}{\Delta z} - \frac{\sigma^2(t^n, z_k)}{2(\Delta z)^2}\right] v_{k-1}^n \\
&+ \left[-\frac{\mu(t^n, z_k)}{\Delta z} + \frac{\sigma^2(t^n, z_k)}{(\Delta z)^2} + \rho\right] v_k^n - \frac{\sigma^2(t^n, z_k)}{2(\Delta z)^2} v_{k+1}^n.
\end{aligned} \tag{2.16}$$

Note that the first inequality can be discretized as follows:

$$
\begin{aligned}
&-\Delta t\theta\frac{\sigma^2(t^n,z_k)}{2(\Delta z)^2}v_{k+1}^n+\left[1+\Delta t\theta\big[\rho-\frac{\mu(t^n,z_k)}{\Delta z}+\frac{\sigma^2(t^n,z_k)}{(\Delta z)^2}\big]\right]v_k^n\\
&+\Delta t\theta\left[\frac{\mu(t^n,z_k)}{\Delta z}-\frac{\sigma^2(t^n,z_k)}{2(\Delta z)^2}\right]v_{k-1}^n \quad\geq\quad \Delta t(1-\theta)\frac{\sigma^2(t^{n+1},z_k)}{2(\Delta z)^2}v_{k+1}^{n+1}\\
&+\left[1+\Delta t(1-\theta)\big[\frac{\mu(t^{n+1},z_k)}{\Delta z}-\frac{\sigma^2(t^{n+1},z_k)}{(\Delta z)^2}-\rho\big]\right]v_k^{n+1}\\
&+\Delta t(1-\theta)\left[-\frac{\mu(t^{n+1},z_k)}{\Delta z}+\frac{\sigma^2(t^{n+1},z_k)}{2(\Delta z)^2}\right]v_{k-1}^{n+1}+\pi_k^\theta,
\end{aligned}
$$

Additionally, the final and boundary conditions (2.14) are approximated by:

$$
\begin{aligned}
&v_k^{N_t}=v_T(z_k),\qquad \theta v_0^\theta=s^\theta, \qquad\qquad (2.17)\\
&\theta\frac{2v_{N_z}^n-5v_{N_z-1}^n+4v_{N_z-2}^n-v_{N_z-3}^n}{(\Delta z)^2}+(1-\theta)\frac{2v_{N_z}^{n+1}-5v_{N_z-1}^{n+1}+4v_{N_z-2}^{n+1}-v_{N_z-3}^{n+1}}{(\Delta z)^2}=0.
\end{aligned}
$$

Therefore, the previous discretization leads to the sequence of discrete complementarity problems:

$$
A^nV^n\geq f^{n+1},\quad V^n\geq S^n,\quad (A^nV^n-f^{n+1})^t\cdot(V^n-S^n)=0, \qquad (2.18)
$$

which are sequentially solved for $n=N_t-1,N_t-2,\ldots,1,0$. Note that the components of vector V^n are the value function at the productivity nodes for time t^n, the matrix A^n only depends on n when the functions μ and σ depend on time, $S^n=S(t^n)$ for a time-dependent scrap value, and f^{n+1} depends on the previously computed vector V^{n+1}.

For the numerical solution of problem (2.18) we also propose the use of the ALAS algorithm previously described for the steady-state problem.

2.2.1.2 Problem of evolutionary firm distribution

In this problem, we consider the computational domain $\Omega_Z=\mathcal{E}_Z\cup\mathcal{S}_Z$, where $\mathcal{E}_Z=[0,T]\times[0,\underline{z}(t)]$ and $\mathcal{S}_Z=[0,T]\times(\underline{z}(t),Z]$. Note that both subdomains depend on t, as the optimal exit productivity $\underline{z}(t)$ depends on t in the evolutive problem. Thus, we impose $g(t,z)=0$ on $\mathcal{E}_Z$ and pose equation (1.26) on $\mathcal{S}_Z$, jointly with the initial and boundary conditions:

$$g(0,z)=g_0(z) \quad \text{and} \quad g(t,Z)=0, \tag{2.19}$$

where $g_0(z)$ is the initial probability function, which is given in all examples by:

$$g_0(z)=\frac{1}{\nu\sqrt{2\pi}}\sum_{i=1}^{I} p_i\, e^{-\frac{(z-z_i^e)^2}{2\nu^2}}, \quad \text{with} \quad \sum_{i=1}^{I} p_i = 1. \tag{2.20}$$

Thus, the initial condition comes from a weighted sum of Gaussian random variables, each one with mean and variance equal to z_i^e and ν^2, respectively.

Let us denote by g_k^n the approximation to the solution at the point $(n\Delta t, k\Delta z)$, i.e. $g_k^n \approx g(t^n, z_k)$, and by $z_{\widetilde{k}}^n$ the approximation of the optimal exit productivity at time t^n, i.e. $z_{\widetilde{k}}^n \approx \underline{z}(t^n)$.

As for the backward in time HJB PDE, we consider the θ-method for the time discretization, so that for $\theta=1$ and $\theta=0$ we recover the implicit and explicit methods respectively, although in practice we use Crank-Nicolson ($\theta=0.5$). Thus, we discretize (1.26) at the grid point (t_θ^n, z_k), with $t_\theta^n=(1-\theta)t^n+\theta t^{n+1}$, for $k=\widetilde{k}+1,\ldots,N_z-1$ and $n=0,1,\ldots,N_t-1$, using the approximations:

$$\begin{aligned}\frac{\partial\big(\mu(t_\theta^n,z_k)g(t_\theta^n,z_k)\big)}{\partial z} &\approx (1-\theta)\frac{\partial[\mu g]_k^n}{\partial z}+\theta\frac{\partial[\mu g]_k^{n+1}}{\partial z},\\ \frac{\partial^2\left(\sigma^2(t_\theta^n,z_k)g(t_\theta^n,z_k)\right)}{\partial z^2} &\approx (1-\theta)\frac{\partial^2[\sigma^2 g]_k^n}{\partial z^2}+\theta\frac{\partial^2[\sigma^2 g]_k^{n+1}}{\partial z^2},\end{aligned} \tag{2.21}$$

where

$$\begin{aligned}\frac{\partial[\mu g]_k^n}{\partial z} &= \frac{[\mu(t^n,z_k)]^+g_k^n-[\mu(t^n,z_{k-1})]^+g_{k-1}^n}{\Delta z}+\frac{[\mu(t^n,z_{k+1})]^-g_{k+1}^n-[\mu(t^n,z_k)]^-g_k^n}{\Delta z},\\ \frac{\partial^2[\sigma^2 g]_k^n}{\partial z^2} &= \frac{\sigma^2(t^n,z_{k+1})g_{k+1}^n-2\sigma^2(t^n,z_k)g_k^n+\sigma^2(t^n,z_{k-1})g_{k-1}^n}{(\Delta z)^2}.\end{aligned}$$

Thus, replacing these approximations in (1.26) and after some reordering of terms, we obtain the expression:

$$\mathcal{L}_\theta^K[g]=\frac{\sigma^2(t^n,z_{\widetilde{k}}^n)}{2}\frac{\partial g}{\partial z}(t^n,z_{\widetilde{k}}^n)g^e(t^n,z_k), \tag{2.22}$$

such that

$$\mathcal{L}_\theta^K[g] = \frac{g_k^{n+1} - g_k^n}{\Delta t} + (1-\theta)[\mathcal{L}^K]_k^n + \theta[\mathcal{L}^K]_k^{n+1},$$

where

$$\begin{aligned}
[\mathcal{L}^K]_k^n[g] = &- \left[\frac{\sigma^2(t^n, z_{k-1})}{2\Delta z} + [\mu(t^n, z_{k-1})]^+\right] g_{k-1}^n \\
&+ \left[\frac{\sigma^2(t^n, z_k)}{\Delta z} + [\mu(t^n, z_k)]^+ - [\mu(t^n, z_k)]^-\right] g_k^n \\
&- \left[\frac{\sigma^2(t^n, z_{k+1})}{2\Delta z} - [\mu(t^n, z_{k+1})]^-\right] g_{k+1}^n.
\end{aligned} \tag{2.23}$$

Note that the previous equation can be discretized as follows:

$$\begin{aligned}
&\frac{\Delta t\theta}{\Delta z}\left[-\frac{\sigma^2(t^{n+1}, z_{k-1})}{2\Delta z} - [\mu(t^{n+1}, z_{k-1})]^+\right] g_{k-1}^{n+1} \\
&+ \left[1 + \frac{\Delta t\theta}{\Delta z}\left(\frac{\sigma^2(t^{n+1}, z_k)}{\Delta z} + [\mu(t^{n+1}, z_k)]^+ - [\mu(t^{n+1}, z_k)]^-\right)\right] g_k^{n+1} \\
&+ \frac{\Delta t\theta}{\Delta z}\left[-\frac{\sigma^2(t^{n+1}, z_{k+1})}{2\Delta z} + [\mu(t^{n+1}, z_{k+1})]^-\right] g_{k+1}^{n+1} \quad = \\
&\frac{\Delta t(1-\theta)}{\Delta z}\left[\frac{\sigma^2(t^n, z_{k-1})}{2\Delta z} + [\mu(t^n, z_{k-1})]^+\right] g_{k-1}^n \\
&+ \left[1 + \frac{\Delta t(1-\theta)}{\Delta z}\left(-\frac{\sigma^2(t^n, z_k)}{\Delta z} - [\mu(t^n, z_k)]^+ + [\mu(t^n, z_k)]^-\right)\right] g_k^n \\
&+ \frac{\Delta t(1-\theta)}{\Delta z}\left[\frac{\sigma^2(t^n, z_{k+1})}{2\Delta z} - [\mu(t^n, z_{k+1})]^-\right] g_{k+1}^n \\
&+ \frac{\sigma^2(t^n, z_{\widetilde{k}}^n)}{2}\frac{\partial g}{\partial z}(t^n, z_{\widetilde{k}}^n) g^e(t^n, z_k),
\end{aligned}$$

for $k = \widetilde{k}+1, \dots, N_z - 1$ and $n = 0, 1, \dots, N_t - 1$.

Previous equations are completed with equations $g_k^{n+1} = 0$, for $k = 0, \dots \widetilde{k}$.

Finally, the initial and boundary conditions (2.19) are approximated by

$$g_k^0 = g_0(z_k) \quad \text{and} \quad (1-\theta)g_{N_z}^n + \theta g_{N_z}^{n+1} = 0.$$

After the previous discretization, the fully discretized problem can be written in matrix form and the resulting linear system at each time step is solved.

2.2.1.3 Evolutionary equilibrium problem

In this section we describe the numerical algorithm to compute the evolutionary equilibrium for given specified functions $\mu(t,z)$, $\sigma(t,z)$ and $s(t)$, as well as given values for the parameters ρ, e and c_f. The algorithm is the natural generalization of the one used for the stationary equilibrium. Thus, we start with $\omega^0(t)$ given and for $m = 0, 1, 2, \ldots$ we follow:

1. Given the wages $\omega^m(t)$ at the mesh points in time, we solve the backward in time HJB PDE (1.25) with the method described in Section 2.1.1.1 using Crank-Nicolson ($\theta = 0.5$). Thus, we obtain the value function approximation v^m at the mesh points and the approximation of the optimal exit boundary $\underline{z}^m(t)$ at t^n, with $n = 0, 1, \ldots, N_t$.

2. Given the approximation of $\underline{z}^m(t)$, we solve the forward in time KFP PDE (1.26) with the method detailed in Section 2.1.1.2 for $\theta = 0.5$. Thus, we obtain the approximation of g^m at the mesh points.

3. Given the approximation of g^m, we compute the wages $\omega_1^m(t)$ by using (1.23).

4. Given the wages $\omega_1^m(t)$, we repeat Steps 1 to 4 for calculating $\omega_2^m(t)$ and then update the wages using (2.12).

When the difference between two consecutive approximations of $\omega^m(t)$ is below a prescribed tolerance, we consider $\omega^m(t)$, $\underline{z}\big(\omega^m(t)\big)$, $v\big(\omega^m(t)\big)$ and $g\big(\omega^m(t)\big)$ as the solution of the evolutionary equilibrium problem.

2.2.2 Numerical results

We present two examples related to the ones considered in the steady-state case. As the main objective is to illustrate the convergence of the solutions of the evolutionary equilibrium problem to corresponding ones of the steady-state, we assume that the productivity dynamics follows a geometric Brownian motion, with parameters μ and σ^2 given in Table 1.

2.2.2.1 Example 3: The time-dependent equilibrium with a prescribed entry productivity

In this example we consider the time-dependent equilibrium model associated with the particular steady-state one presented in Section 1.1.6, for which we could obtain a semianalytical solution and we also validated the proposed numerical solution with the examples in Section 2.1.2.2. Although we have addressed the tests with all the values of z_0^e considered in Section 2.1.2.2, we just report here the results for $z_0^e = 3$. We use the same parameters as in the steady-state case and the initial condition for the distribution of firms problem is given by the choice $I = 1$, $p_1 = 1$ and $\nu = 0.44$ in expression (2.20), so that firms initially distribute around z_0^e with a certain spread associated with the value of ν.

Table 2.10: Wages and optimal exit productivity for $z_0^e = 3$ in the time-dependent Example 3

t	$\omega(t)$	$\underline{z}(t)$
0	1.296225	1.379375
2.5	1.224418	1.316250
5	1.162491	1.266250
7.5	1.118295	1.233125
10	1.094643	1.216875
12.5	1.087246	1.213125
SS	1.087548	1.213594

Table 2.10 shows the computed equilibrium values of the wages and optimal exit productivity, for times $t = 0$, 2.5, 5, 7.5, 10 and 12.5, jointly with the values obtained for the steady-state (SS) equilibrium model in the last row.

Next, in Figures 2.6 and 2.7 we show the time evolution of the value function and the probability density function of firms, so that we can observe how the graphics

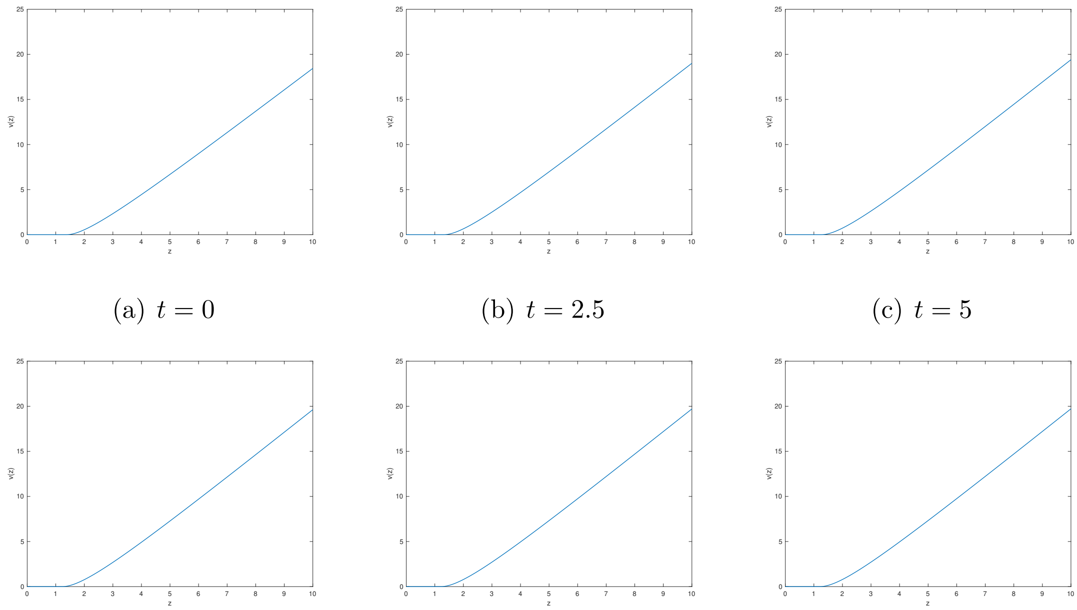

(a) $t = 0$ (b) $t = 2.5$ (c) $t = 5$

(d) $t = 7.5$ (e) $t = 10$ (f) $t = 12.5$

Figure 2.6: The time-dependent value function for $z_0^e = 3$ in Example 3

for $T = 12.5$ are in agreement with the computed ones in Section 2.1.2.1 with the semianalytical solution and in Section 2.1.2.2 with the numerical methods for the steady-state problem with $z_0^e = 3$.

2.2.2.2 Example 4: The time-dependent equilibrium with random entry productivities

For this example, we consider the time-dependent equilibrium model associated with the steady-state one posed in Section 2.1.2.3. Although we have addressed the tests with all values considered in Section 2.1.2.3, we just report here the results for the choice $\mathbf{z^e} = (2, 3, 4)$ and $\mathbf{p^e} = (0.25, 0.5, 0.25)$ for the entry productivities and probabilities. We use the same parameters as in the steady-state case. As initial distribution of firms we use $I = 3$, $p_1 = 0.25$, $p_2 = 0.5$, $p_3 = 0.25$ and $\nu = 0.13$ in expression (2.20), so that they initially distribute around the entry productivities following a weighted combination of Gaussian random variables.

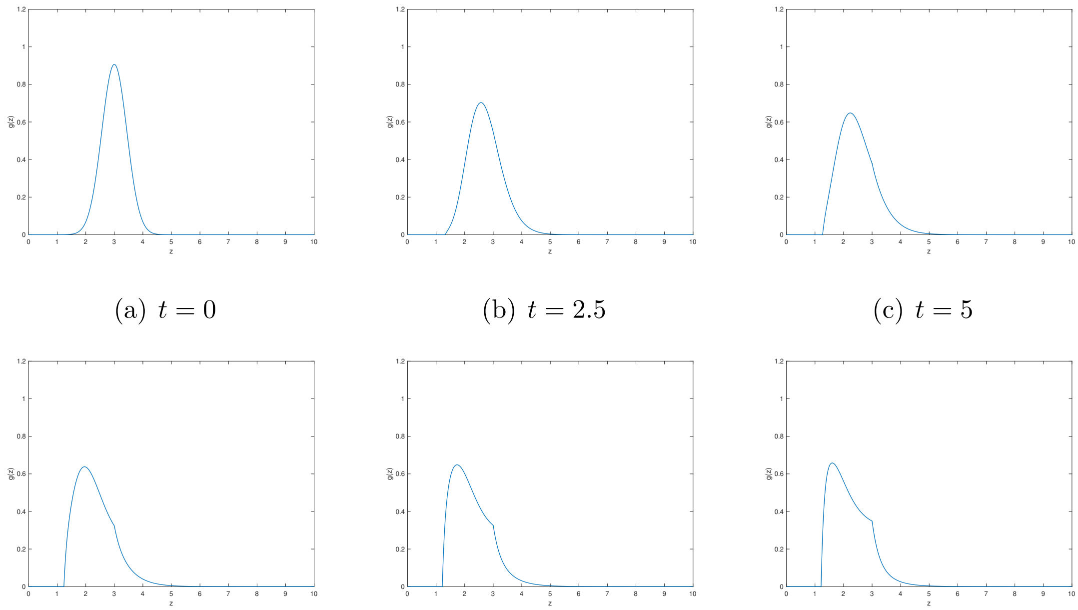

(a) $t = 0$ (b) $t = 2.5$ (c) $t = 5$

(d) $t = 7.5$ (e) $t = 10$ (f) $t = 12.5$

Figure 2.7: The time-dependent firm distribution for $z_0^e = 3$ in Example 3

Table 2.11: Wages and optimal exit productivity with $\mathbf{z^e} = (2, 3, 4)$ and $\mathbf{p^e} = (0.25, 0.5, 0.25)$ in the time-dependent Example 4

t	$\omega(t)$	$\underline{z}(t)$
0	1.296225	1.390625
2.5	1.231462	1.336875
5	1.186020	1.298125
7.5	1.150821	1.269375
10	1.127934	1.252500
12.5	1.116721	1.246250
SS	1.117000	1.246563

Table 2.11 shows the computed wages and optimal exit productivity for specific times $t = 0, 2.5, 5, 7.5, 10$ and 12.5, jointly with the values obtained for the

steady-state (SS) equilibrium model in the last row.

Next, in Figures 2.8 and 2.9 we show the time evolution of the value function and the probability density function of firms, so that we can observe how the graphics for $T = 12.5$ are in agreement with the ones in Section 2.1.2.3 which are obtained with the numerical methods for the steady-state problem. Note that in Figure 2.9 we use a different scale for $t = 0$.

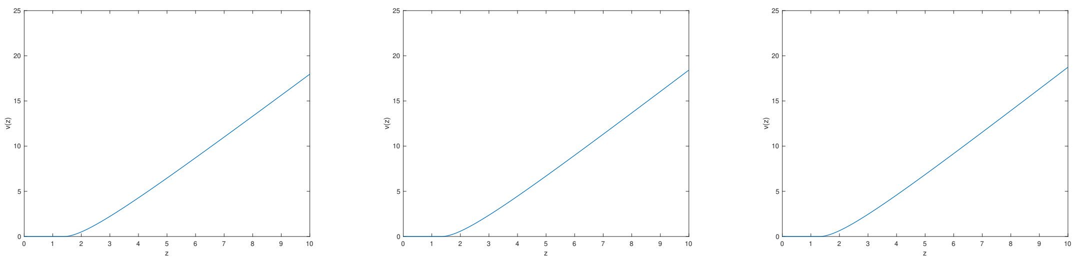

(a) $t = 0$ (b) $t = 2.5$ (c) $t = 5$

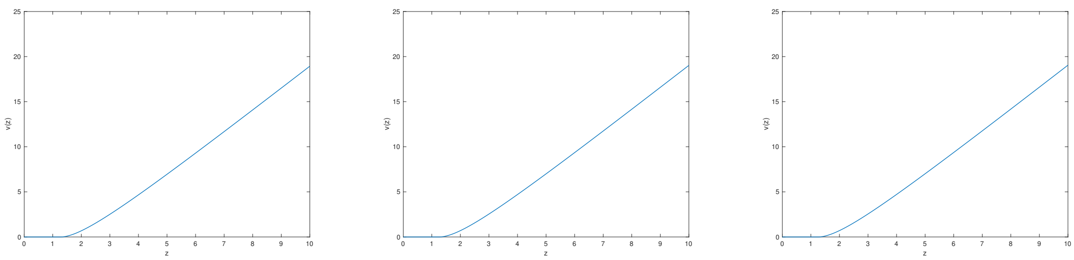

(d) $t = 7.5$ (e) $t = 10$ (f) $t = 12.5$

Figure 2.8: The time-dependent value function with $\mathbf{z^e} = (2, 3, 4)$ and $\mathbf{p^e} = (0.25, 0.5, 0.25)$ in Example 4

Remark 2.2.1. *All computations in Sections 2.1.2 and 2.2.2 are obtained with a MATLAB implementation of the algorithms. The numerical solution of the evolutionary equilibrium problem with* 16001×10001 *mesh takes around 400 seconds, while the stationary equilibrium problem with* 64001 *mesh points takes around 55 seconds on a MacBook Pro laptop. The CPU we use is a Apple M2 Chip with 8 GB RAM.*

The contents of Section 2.2 have been previously published in our article [46].

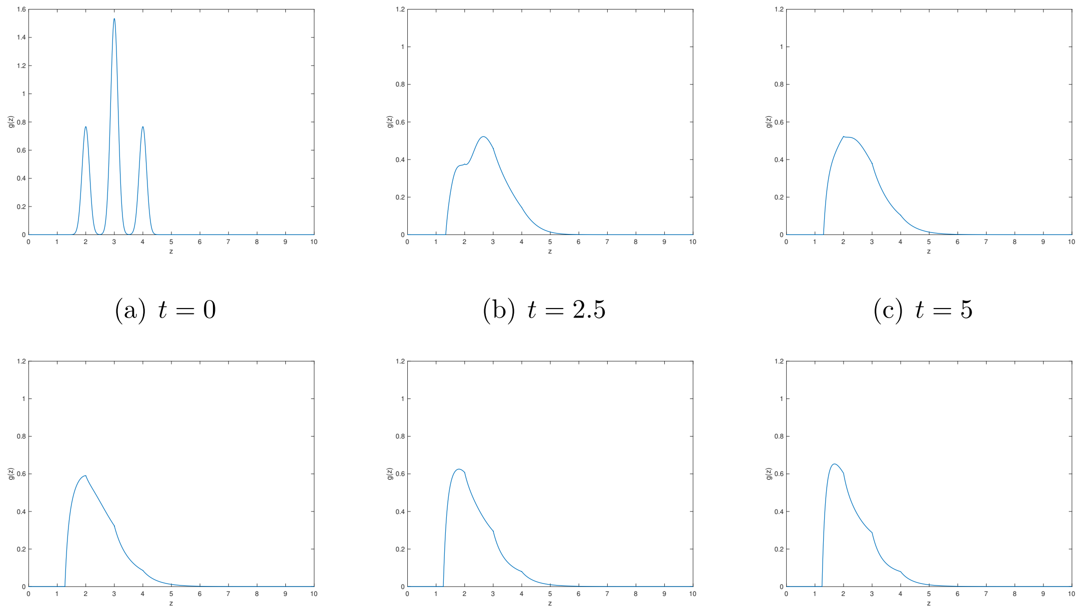

(a) $t = 0$ (b) $t = 2.5$ (c) $t = 5$

(d) $t = 7.5$ (e) $t = 10$ (f) $t = 12.5$

Figure 2.9: The time-dependent firm distribution with $\mathbf{z^e} = (2, 3, 4)$ and $\mathbf{p^e} = (0.25, 0.5, 0.25)$ in Example 4

2.3 Numerical solution for the steady-state PIDEs problem

This section is devoted to describe the numerical solution of the steady-state equilibrium problem, which is defined by the PIDEs represented as (1.57) and (1.58), jointly with equation (1.24). The proposed numerical method involves the use of a fixed-point iteration technique to derive the numerical solution for the problems outlined by these equations.

Firstly, we introduce the numerical methods utilized in this process. Next, we present various numerical examples to showcase the effectiveness and performance of the proposed methodology.

2.3.1 Numerical methods

Following the approach used in Section 2.1.1, we present a numerical strategy for solving the HJB and KFP equations. Our approach involves a combination of numerical techniques, which includes: a finite differences scheme for discretization in the productivity domain and the ALAS algorithm to address the nonlinearity inherent in inequality and complementarity conditions in the free boundary problem (1.57). Moreover, we incorporate the Adams-Bashforth (AB) method, as proposed in [48], to explicitly handle integral terms that arise in the PIDEs.

2.3.1.1 Problem of stationary incumbent firms

Regarding spatial discretization, we establish a uniform grid with the same notation we have used in Section 2.1.1.1, so that the approximation $v_k \approx v(z_k)$ represents the steady-state optimal firm value at the grid points. Moreover, in order to approximate the incumbent problem (1.57) at the grid point z_k, where $k = 1, \ldots, N_z - 1$, we employ expressions (2.2) to approximate the first and second-order derivatives.

After some reordering of terms, we obtain the following expressions for $k = 1, \ldots, N_z - 1$:

$$[\mathcal{L}_J^H]_k[v] \geq \pi_k, \quad v_k \geq s, \quad \big([\mathcal{L}_J^H]_k[v] - \pi_k\big) \cdot (v_k - s) = 0,$$

such that

$$[\mathcal{L}_J^H]_k[v] = \mathcal{L}_k^H[v] - \lambda \int_{-\infty}^{+\infty} F_k(v) f(x)\, \mathrm{d}x, \tag{2.24}$$

where the steady-state HJB PDE operator $\mathcal{L}_k^H[\cdot]$ is defined in (2.3) and $F_k(v) = v\big(z_k + \beta(z_k, x)\big) - v(z_k) - \beta(z_k, x)\dfrac{\partial v}{\partial z}(z_k)$.

To efficiently maintain the structure of the matrix, we approximate the integral term using the AB scheme. Consequently, the HJB PIDE operator (2.24) is replaced by:

$$[\mathcal{L}_J^H]_k[v] = \mathcal{L}_k^H[v] - \lambda \int_{x_{\min}}^{x_{\max}} \frac{3F_k^m(v) - F_k^{m-1}(v)}{2} f(x)\, dx,$$

where F^m and F^{m-1} come from previous fixed-point iterations. It is important to note that for the first iteration, the AB scheme simplifies to the explicit scheme proposed in [15].

Additionally, we approximate the boundary conditions of (1.57) by expressions (2.4).

These boundary conditions ensure consistency and stability in the numerical solution. Thus, the fully discretized linear complementarity problem can be represented in matrix form as in (2.5), considering the vector $f \in \mathbb{R}^{N_z+1}$, such that $f_0 = -c_f/\rho$ and $f_{N_z} = 0$, while

$$f_k = \pi_k + \lambda \int_{x_{\min}}^{x_{\max}} \frac{3F_k^m(v) - F_k^{m-1}(v)}{2} f(x)\, dx, \qquad k = 1, \ldots, N_z - 1.$$

Therefore, the matrix A is defined as in Section 2.1.1.1. This matrix formulation represents the discretized problem and the coefficients associated with the discretization scheme, allowing for an efficient numerical solution to the linear complementarity problem. For this aim, the ALAS algorithm previously described for the PDEs problem is used.

2.3.1.2 Problem of stationary firm distribution

For the numerical solution of the steady-state firm distribution problem, we set $g(z) = 0$ on the exit boundary $\hat{\mathcal{E}}$ and pose equation (1.58) on the stay region $\hat{\mathcal{S}}$. For this aim, we establish the same notation we have used in Section 2.1.1.2, so that the approximations $g_k \approx g(z_k)$ and $z_{\widetilde{k}}$ represent the steady-state firm density function at the grid points and the optimal exit productivity, which is derived from the numerical solution of the incumbent problem.

Subsequently, we discretize equation (1.58) at the grid points z_k, where $k = \widetilde{k} + 1, \ldots, N_z - 1$. This is achieved by introducing expressions (2.6) to calculate the first and second-order derivatives.

Thus, for $k = \widetilde{k} + 1, \ldots, N_z - 1$, we have the equation:

$$[\mathcal{L}_J^K]_k[g] = \frac{\sigma^2(z_{\widetilde{k}})}{2} \frac{\partial g}{\partial z}(z_{\widetilde{k}}) g^e(z_k),$$

such that for the steady-state KFP operator $\mathcal{L}_k^K[\cdot]$ defined in (2.8), we have:

$$[\mathcal{L}_J^K]_k[g] = \mathcal{L}_k^K[g] - \lambda \int_{-\infty}^{+\infty} H_k(g) f(x)\,\mathrm{d}x. \tag{2.25}$$

where $H_k(g) = g\big(z_k - \beta(z_k, x)\big) - g(z_k)$.

Moreover, to maintain matrix structures for an efficient solution of tridiagonal systems, a fixed-point iteration is applied to the term involving $\frac{\partial g}{\partial z}(z_{\widetilde{k}})$ and the integral term is approximated using the AB scheme.

Thus, the previous KFP equation is replaced by:

$$[\mathcal{L}_J^K]_k[g] = \frac{\sigma^2(z_{\widetilde{k}})}{2}\frac{\partial g^m}{\partial z}(z_{\widetilde{k}}) g^e(z_k),$$

where

$$[\mathcal{L}_J^K]_k[g] = \mathcal{L}_k^K[g] - \lambda \int_{x_{\min}}^{x_{\max}} \frac{3H_k^m(g) - H_k^{m-1}(g)}{2} f(x)\,\mathrm{d}x,$$

which is completed with $g_k = 0$, for $k = 0, \dots, \widetilde{k}$ and $g_{N_z} = 0$. It is important to note that g^m, H^m and H^{m-1} come from previous fixed-point iterations. Moreover, the AB scheme is also reduced to the explicit scheme for the first iteration.

Therefore, the discretized problem can be written as in (2.9), considering $b_k = 0$, $k = 0, \dots, \widetilde{k}$ and $b_{N_z} = 0$, while for $k = \widetilde{k} + 1, \dots, N_z - 1$,

$$b_k = \frac{\sigma^2(z_{\widetilde{k}})}{2}\frac{\partial g^m}{\partial z}(z_{\widetilde{k}}) g^e(z_k) + \lambda \int_{x_{\min}}^{x_{\max}} \frac{3H_k^m(g) - H_k^{m-1}(g)}{2} f(x)\,\mathrm{d}x.$$

Furthermore, to ensure $g_k = 0$ for $k = 0, \dots, \widetilde{k}$, the matrix B is defined as in Section 2.1.1.2 and the resulting linear system is solved.

2.3.1.3 Stationary equilibrium problem

In this section, we outline the procedure for calculating the steady-state jump-diffusion equilibrium with specified functions $\mu(z)$, $\sigma(z)$ and $\beta(z)$, along with known parameter values s, ρ, e, c_f and λ. To enhance the convergence of fixed-point algorithms with linear convergence, we introduce a Steffensen method, as detailed in Section 2.1.1.3. We start with an initial guess ω^0 and set $m = 0$. The process proceeds as follows:

1. Using the current wages ω^m, solve the stationary HJB PIDE (1.57) to obtain v^m and $\underline{z}^m$. This step follows the methods outlined in Section 2.3.1.1.
2. Given $\underline{z}^m$, solve the stationary KFP PIDE (1.58) for $g^m(z)$ using the approach described in Section 2.3.1.2.
3. Calculate the wages ω_1^m based on g^m using the implicit formula from (1.24).
4. Repeat Steps 1 to 4 to compute ω_2^m, and then generate a new guess using the Steffensen formula (2.12).

Repeat the process until convergence is achieved or the desired accuracy is attained.

2.3.2 Numerical results

In this section, we consider the examples derived from Section 2.1.2. Therefore, the productivity follows a geometric Brownian motion with jumps. As a result, we have the following relationships for the functions involved: $\mu(z_t) = \mu z_t$, $\sigma(z_t) = \sigma z_t$ and $\beta(z_t) = \beta z_t$. Note that β is the magnitude of the random jumps.

Thus, we can rewrite the steady-state HJB and KFP PIDEs (1.57) and (1.58) by introducing the following differential operators:

$$\mathcal{L}_J^H[v] = -\frac{\sigma^2 z^2}{2}\frac{\partial^2 v}{\partial z^2} - (\mu - \lambda\overline{\kappa})z\frac{\partial v}{\partial z} + (\rho + \lambda)v - \lambda\int_{-\infty}^{+\infty} v(z + xz)f(x)\,\mathrm{d}x,$$
$$\mathcal{L}_J^K[g] = -\frac{\sigma^2 z^2}{2}\frac{\partial^2 g}{\partial z^2} + \overline{\mu}z\frac{\partial g}{\partial z} + \overline{\lambda}g - \lambda\int_{-\infty}^{+\infty} g(z - xz)f(x)\,\mathrm{d}x,$$

where $\overline{\mu} = \mu - 2\sigma^2$ and $\overline{\lambda} = \mu - \sigma^2 + \lambda$. The probability density function f and its expectation $\overline{\kappa}$ are defined according to the expressions (1.44)–(1.46), taking into account either the Merton model or the Kou model.

Moreover, all tests use the macroeconomic data in Table 2.12 and the upper limit $Z = 10$ in the productivity interval. The notation as in Section 2.1.2 has been used.

Most parameters used in this study have been adopted from Table 2.1. However, due to the introduction of jumps, we incorporate the Poisson process parameter $\lambda =$

Table 2.12: Macroeconomic parameters for one productive sector jump-diffusion models

Symbol	Value	Description
e	1.53	Utility parameter
ρ	0.05	Discount rate
μ	-0.04	Productivity drift
σ^2	0.01	Productivity volatility
s	0	Scrap value
c_f	0.31	Fixed cost
λ	0.01	Poisson process parameter
ν_m	-0.1	Mean jump size (Merton)
γ_m	0.45	Standard deviation of jump size (Merton)
q	0.3445	Probability of upward jump (Kou)
α_1	3.0775	Parameter (Kou)
α_2	3.0465	Parameter (Kou)

0.01. Additionally, specific values are assigned to the parameters for the Merton and Kou models: the mean jump size (ν_m) $= -0.1$ and the standard deviation of the jump size (γ_m) $= 0.45$ are taken from Calvo and Vázquez [14], while the probability of an upward jump (q) $= 0.3445$, and parameters $\alpha_1 = 3.0775$ and $\alpha_2 = 3.0465$ are set from Almendral and Oosterlee [5] and d'Halluin, Forsyth and Vetzal [20].

2.3.2.1 Example 5: The steady-state equilibrium with a entry productivity

In this example, we assume that all new establishments enter the industry with a predetermined productivity level z_0^e. To account for this, we introduce the term $g^e(z) = \delta(z - z_0^e)$ in equation (1.58).

We begin by presenting the numerical solution for the case where $z_0^e = 3$. The results are shown for different mesh steps to illustrate the behavior of the proposed numerical approach. Tables 2.13 and 2.14 display the numerical solutions, considering both the Merton and the Kou models. It is worth noting that as the mesh step becomes smaller, the values of ω and $\underline{z}$ tend to converge towards each other.

Table 2.13: Equilibrium wages and optimal exit productivities for $z_0^e = 3$ in the Merton model's Example 5

N_z	ω	$\underline{z}$
8001	1.159863	1.293750
16001	1.160135	1.294375
32001	1.160205	1.294375
64001	1.160240	1.294375

Table 2.14: Equilibrium wages and optimal exit productivities for $z_0^e = 3$ in the Kou model's Example 5

N_z	ω	$\underline{z}$
8001	1.148947	1.281250
16001	1.149220	1.281875
32001	1.149290	1.281875
64001	1.149357	1.282031

Subsequently, we select three distinct values of z_0^e to show the solution's behavior concerning the productivity level at which new firms enter the industry. For both Merton and Kou models, we observe how the values of ω and $\underline{z}$ increase in response to variations in z_0^e, as presented in Tables 2.15 and 2.16. Furthermore, it is noteworthy that, for the selected parameters, the computed values obtained for the Merton model are slightly higher than those for the Kou model.

Table 2.15: Entry productivity, wages and optimal exit productivity with the Merton model's Example 5

z_0^e	ω	$\underline{z}$
2	1.009460	1.126250
3	1.160240	1.294375
4	1.286796	1.435625

Table 2.16: Entry productivity, wages and optimal exit productivity with the Kou model's Example 5

z_0^e	ω	$\underline{z}$
2	0.995646	1.110625
3	1.149357	1.282031
4	1.279090	1.426719

Figures 2.10 and 2.11 show the value function and the firm density function for the aforementioned values of z_0^e. As noted in the steady-state PDEs problem, the empirical regularity in the distribution of firms experiences a singular behaviour at the entry productivity z_0^e, displaying a kink-like behavior at that point. On the right tail ($z > z_0^e$), we observe an expected power law distribution. When the value of z_0^e is increased, the probability density function spreads across a wider range of productivities, resulting in a lower maximum. Indeed, the kink phenomenon becomes more pronounced as z_0^e assumes higher values.

Additionally, when compared with a analogous example with $z_0 = 3$ in the PDEs model associated to an Ito process that excludes jumps ($\lambda = 0$) represented in Figure 2.2 we observe a lower value function in the PIDEs models. Nevertheless, the computed wages and free boundaries appear higher in the PIDEs models (see Table 2.7). This outcome aligns with expectations, as the presence of jumps increases

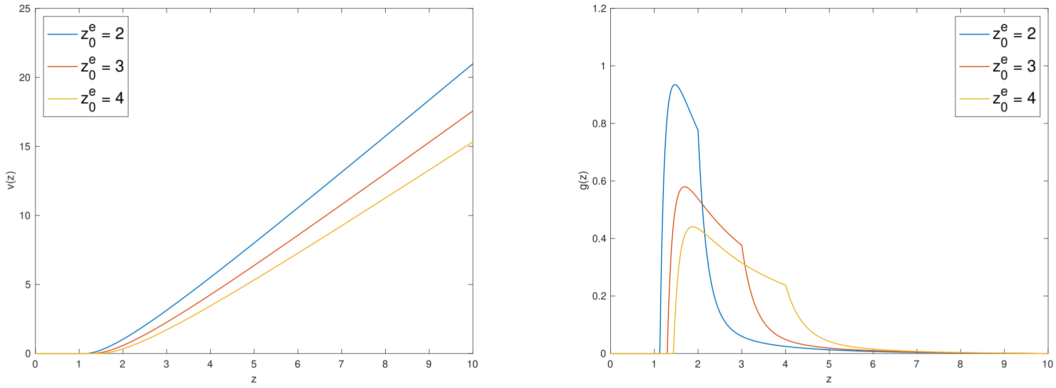

Figure 2.10: The value function (left) and the firm distribution (right) with the Merton model's Example 5

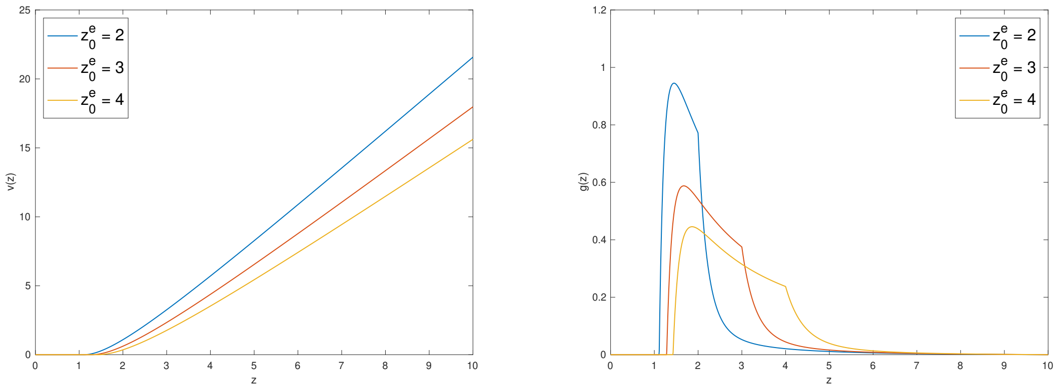

Figure 2.11: The value function (left) and the firm distribution (right) with the Kou model's Example 5

uncertainty in productivity. Therefore, it is evident that both Merton and Kou models influence the firm distribution, as shown in Figure 2.2. With the inclusion of jumps, the probability density function spreads more smoothly across a wider range of productivities, resulting in a decreased maximum. Consequently, the significance of the kink phenomenon diminishes.

2.3.2.2 Example 6: The steady-state equilibrium with random entry productivities

In this example, we introduce randomness into the entry productivity in the steady-state KFP problem (1.58). This randomness is achieved by utilizing a discrete random variable to model the entry productivity. Specifically, we consider a probability distribution for new establishments defined by the expression (1.19) with $I = 3$.

In this context, we will explore various combinations of entry productivities (z_i^e) and their associated probabilities (p_i^e).

As our initial dataset, we consider $\mathbf{z^e} = (2,\ 3,\ 4)$ and $\mathbf{p^e} = (0.25,\ 0.5,\ 0.25)$. Moreover, we have included the results for $\mathbf{p^e} = (0.1,\ 0.8,\ 0.1)$ and $\mathbf{p^e} = (0.1,\ 0.1,\ 0.8)$ as in the steady-state PDEs model. These choices help us illustrate how the numerical strategy behaves in terms of the entry productivities and their associated probabilities for the Merton model. In Tables 2.17–2.19, we can observe that as the mesh size becomes finer, the values of ω and $\underline{z}$ tend to converge. Although it has not been explicitly showcased, a similar behavior has been attained for the Kou model.

Table 2.17: Equilibrium wages and optimal exit productivities for $\mathbf{z_0^e} = (2,\ 3,\ 4)$ and $\mathbf{p^e} = (0.25,\ 0.5,\ 0.25)$ in the Merton model's Example 6

N_z	ω	$\underline{z}$
8001	1.184903	1.321250
16001	1.185183	1.321875
32001	1.185396	1.322500
64001	1.185430	1.322500

Next, we take the finest mesh and present the previous results for the Merton model in Table 2.20. Similarly, we provide numerical results for the Kou model in Table 2.21. As the previous example, note that the values ω and $\underline{z}$ are smaller in the

Table 2.18: Equilibrium wages and optimal exit productivities for $\mathbf{z_0^e} = (2, 3, 4)$ and $\mathbf{p^e} = (0.1, 0.8, 0.1)$ in the Merton model's Example 6

N_z	ω	$\underline{z}$
8001	1.169356	1.303750
16001	1.169770	1.305000
32001	1.169838	1.305000
64001	1.169909	1.305156

Table 2.19: Computed wages and optimal exit productivity for $\mathbf{z_0^e} = (2, 3, 4)$ and $\mathbf{p^e} = (0.1, 0.1, 0.8)$ in the Merton model's Example 6

N_z	ω	$\underline{z}$
8001	1.266332	1.412500
16001	1.266592	1.413125
32001	1.266653	1.413125
64001	1.266683	1.413125

case of the Kou model. Moreover, if we compare with the case without jumps, the absence of jumps provides lower values of both magnitudes (see Table 2.9).

Table 2.20: Probabilities, wages and optimal exit productivity for $\mathbf{z_0^e} = (2, 3, 4)$ in the Merton model's Example 6

$\mathbf{p^e}$	ω	$\underline{z}$
$(0.25, 0.5, 0.25)$	1.185430	1.322500
$(0.1, 0.8, 0.1)$	1.169909	1.305156
$(0.1, 0.1, 0.8)$	1.266683	1.413125

Table 2.21: Probabilities, wages and optimal exit productivity for $\mathbf{z_0^e} = (2, 3, 4)$ in the Kou model's Example 6

$\mathbf{p^e}$	ω	$\underline{z}$
$(0.25, 0.5, 0.25)$	1.175140	1.310781
$(0.1, 0.8, 0.1)$	1.159274	1.293125
$(0.1, 0.1, 0.8)$	1.258481	1.403750

In Figures 2.12 and 2.13, we present the computed value function and firm density function for both the Merton model and the Kou model. Similar to the analogous PDEs example, for the selected parameters, we can observe a distinct kink at each possible entry productivity in the probability density function of firms, resulting in a total of three kinks. The kink is more pronounced at the productivity with the highest probability.

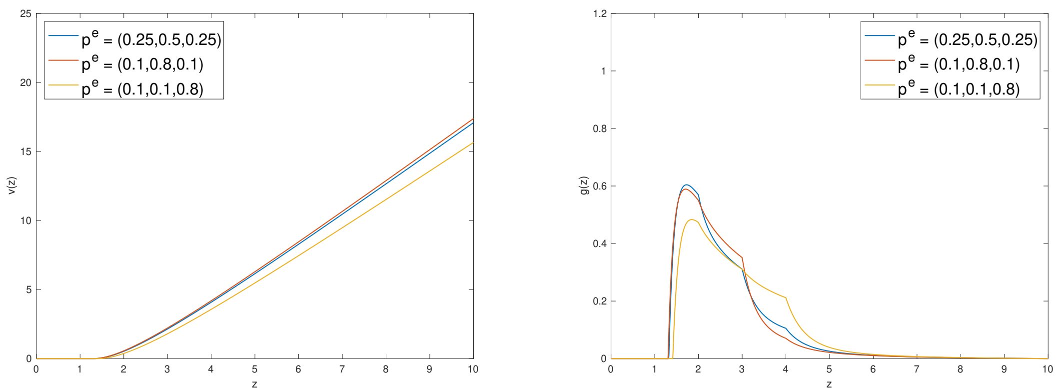

Figure 2.12: The value function (left) and the firm distribution (right) for $\mathbf{z^e} = (2, 3, 4)$ in the Merton model's Example 6

Moreover, it is evident that the portions of the density function on the right tails of the different entry productivities (z_i^e) exhibit a power-law behavior, with each case having a different exponent. Additionally, at each entry productivity, the

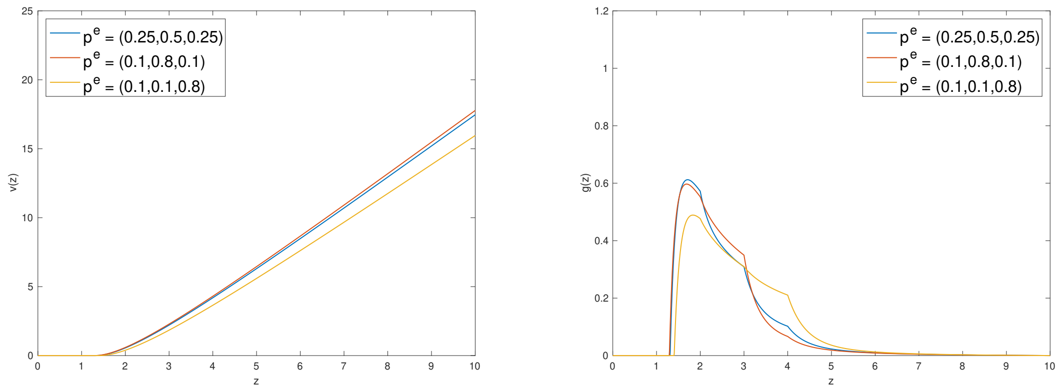

Figure 2.13: The value function (left) and the firm distribution (right) for $\mathbf{z^e} = (2, 3, 4)$ in the Kou model's Example 6

density function becomes singular, a consequence of employing combinations of delta functions in the source term g^e.

It is worth noting that examples presented in Figure 2.10 for the Merton model and Figure 2.11 for the Kou model can be associated with the cases where $\mathbf{p^e} = (1, 0, 0)$ (blue line), $\mathbf{p^e} = (0, 1, 0)$ (red line) and $\mathbf{p^e} = (0, 0, 1)$ (yellow line).

The contents of Section 2.3 are included in our article [47].

2.4 Numerical solution for the time-dependent PIDEs problem

In this section, we present a numerical solution for the time-dependent equilibrium problem, mainly defined by PIDEs (1.55) and (1.56), and (1.23). As the steady-state problem, we employ a fixed-point iteration approach between the numerical solutions of the involved problems.

Our objective is to prove the convergence of the solution for the time-dependent problem to the solution for the corresponding steady-state one. For the final condition in (1.55), we utilize the solution obtained from the steady-state problem. Concerning the initial condition to complete (1.56), we consider it to be linked to the productivities at which new establishments enter the industry.

First, we describe the additional numerical methods integrated into the time-dependent problems, and subsequently, we present numerical examples to demonstrate the efficacy of the proposed methodology.

2.4.1 Numerical methods

As Section 2.2.1, we propose a Crank-Nicolson scheme for the time discretization, which will be combined with the finite difference methods we used for the spatial discretization in the steady-state problems. During each time step, the fully discretized problems will be solved using the same techniques as those used for the discretized steady-state problems in Section 2.3.1. Note that we use the same notation as Section 2.2.1.

2.4.1.1 Problem of evolutionary incumbent firms

In this section, we propose a numerical methodology to solve the time-dependent PIDEs problem defined by (1.55). To approximate problem (1.55) at the point (t_θ^n, z_k), where $k = 1, \ldots, N_z - 1$ and $n = 0, 1, \ldots, N_t - 1$, we introduce the θ-method ($0 \leq \theta \leq 1$). Notably, the Crank-Nicolson method ($\theta = 0.5$) and the AB scheme will be used in practice.

After some reordering of terms, we get for (t_θ^n, z_k), with $k = 1, \ldots, N_z - 1$ and $n = 0, 1, \ldots, N_t - 1$, the expressions

$$[\mathcal{L}_J^H]_\theta[v] \geq \pi_k^\theta, \quad v_k^\theta \geq s^\theta, \quad \big([\mathcal{L}_J^H]_\theta[v] - \pi_k^\theta\big) \cdot (v_k^\theta - s^\theta) = 0,$$

such that v_k^θ, π_k^θ and s^θ are defined in Section 2.2.1.1 and for the HJB PDE operator $\mathcal{L}_\theta^H[\cdot]$ given by (2.16), we have:

$$[\mathcal{L}_J^H]_\theta[v] = \mathcal{L}_\theta^H[v] - \lambda \int_{x_{\min}}^{x_{\max}} \frac{3F_k^{n+1}(v) - F_k^{n+2}(v)}{2} f(x)\,\mathrm{d}x, \tag{2.26}$$

where $F_k^n(v) = v\big(t^n, z_k + \beta(t^n, z_k, x)\big) - v(t^n, z_k) - \beta(t^n, z_k, x)\dfrac{\partial v}{\partial z}(t^n, z_k)$. For the first time step, the AB scheme is reduced to the explicit scheme.

The final and boundary conditions for (1.55) are approximated by (2.14). Thus, a fully discritized linear complementarity problem is represented as in (2.5).

Once the discretization of the time-dependent HJB PIDEs formulation is done, we propose the use of the ALAS algorithm for each time step as in Section 2.2.1.1.

2.4.1.2 Problem of evolutionary firm distribution

For the time-dependent firm distribution problem, we impose $g(t, z) = 0$ on the set $\mathcal{E}_Z$ and pose the PIDE (1.56) on the set $\mathcal{S}_Z$. The initial condition for (1.56) is defined as $g^0(z)$ using a weighted sum of Gaussian random variables as in (2.20).

Similar to Section 2.2.1.2, for approximating problem (1.56), we utilize the θ-method. In practice, we use Crank-Nicolson ($\theta = 0.5$) and the AB method as done for solving the backward-in-time HJB PIDEs problem.

After rearranging terms, we obtain a system of equations for (t_θ^n, z_k) which are solved sequentially for $n = 0, 1, \ldots, N_t - 1$:

$$[\mathcal{L}_J^K]_\theta[g] = \frac{\sigma^2(t^n, z_{\widetilde{k}}^n)^2}{2}\frac{\partial g}{\partial z}(t^n, z_{\widetilde{k}}^n)\delta(z_k - z_{\widetilde{k}}^n), \qquad k = \widetilde{k} + 1, \ldots, N_z - 1, \tag{2.27}$$

such that for the KFP PDE operator $\mathcal{L}_\theta^K[\cdot]$ given by (2.23), we have

$$[\mathcal{L}_J^K]_\theta[g] = \mathcal{L}_\theta^K[g] - \lambda \int_{x_{\min}}^{x_{\max}} \frac{3H_k^n(g) - H_k^{n-1}(g)}{2} f(x)\, \mathrm{d}x, \tag{2.28}$$

where $H_k^n(g) = g\big(t^n, z_k - \beta(t^n, z_k, x)\big) - g(t^n, z_k)$.

Moreover, equation (2.27) is completed with $g_k^{n+1} = 0$, for $k = 0, \ldots \widetilde{k}$ and the initial condition is approximated by $g_k^0 = g^0(z_k)$.

The fully discretized problems can be written in a matrix form as in Section 2.3.1.2 and the resulting linear systems are solved for each time step.

2.4.1.3 Evolutionary equilibrium problem

In this section, we describe the numerical algorithm for computing the evolutionary equilibrium, considering given functions $\mu(t,z)$, $\sigma(t,z)$, $\beta(t,z)$ and $s(t)$, along with fixed parameters ρ, e, c_f and λ. The algorithm is similar to the one used in Section 2.2.1.3. We start with $\omega^0(t)$ given and for $m = 0, 1, 2, \ldots$ we follow:

1. Given the wages $\omega^m(t)$, solve the backward-in-time HJB PIDE (1.55) with the method described in Section 2.4.1.1 using the Crank-Nicolson method ($\theta = 0.5$). This will yield the value function approximation v^m at the mesh points and the approximation of the optimal exit boundary $\underline{z}^m(t)$ at t^n for $n = 0, 1, \ldots, N_t$.

2. Given $\underline{z}^m(t)$, solve the forward-in-time KFP PIDE (1.56) with the method detailed in Section 2.4.1.2 for $\theta = 0.5$. This will provide an approximation of g^m at the mesh points.

3. Compute the wages $\omega_1^m(t)$ by employing the implicit formula from (1.23).

4. Given the wages $\omega_1^m(t)$, we repeat Steps 1 to 4 for computing $\omega_2^m(t)$ and then update the wages using (2.12).

2.4.2 Numerical results

This section discusses the time-dependent jump-diffusion equilibrium model and provides validation for the proposed numerical solution. The main objective is to demonstrate the convergence of solutions from the evolutionary equilibrium problem to those of the corresponding steady-state. For this aim, we present similar tests to Section 2.2.2.

2.4.2.1 Example 7: The time-dependent equilibrium with random entry productivities

In this example, the same parameters as those used in the steady-state case are employed, and the initial condition for the distribution of firms is set to $I = 3$ with

$\nu_0 = 0.44$ in expression (2.20).

Regarding $\mathbf{z^e} = (2, 3, 4)$, the computed wages and optimal exit productivities using the Merton model at specific times ($t = 0, 2.5, 5, 7.5, 10, 12.5$ and 15) are detailed in Tables 2.22 for $\mathbf{p^e} = (0.25, 0.5, 0.25)$, while Table 2.23 shows results for $\mathbf{p^e} = (0.1, 0.1, 0.8)$. The values obtained for the steady-state (SS) equilibrium model are included in the last row for comparison.

Table 2.22: Wages and the optimal exit productivity for $\mathbf{z^e} = (2, 3, 4)$ and $\mathbf{p^e} = (0.25, 0.5, 0.25)$ in the time-dependent Merton model's Example 7

t	$\omega(t)$	$\underline{z}(t)$
0	1.296229	1.421250
2.5	1.265437	1.383750
5	1.229971	1.355000
7.5	1.205470	1.355000
10	1.191773	1.326250
12.5	1.186142	1.322500
15	1.185087	1.321875
SS	1.185430	1.322500

Additionally, Figure 2.14 illustrates the time evolution of the value function and the probability density function of firms for the Merton model with $\mathbf{p^e} = (0.25, 0.5, 0.25)$, while Figure 2.15 showcases the same for $\mathbf{p^e} = (0.1, 0.1, 0.8)$. These figures provide a visual comparison between the graphics at $T = 15$ and those presented in Section 2.3.2.2, which were obtained using numerical methods for the steady-state problem.

In Tables 2.24 and 2.25, the computed wages and optimal exit productivities are outlined for each $\mathbf{p^e}$ in the Kou model. Similar to the Merton model, a strong alignment is noticeable between $T = 15$ and the steady-state case.

Furthermore, Figures 2.16 and 2.17 depict the time evolution of the value function

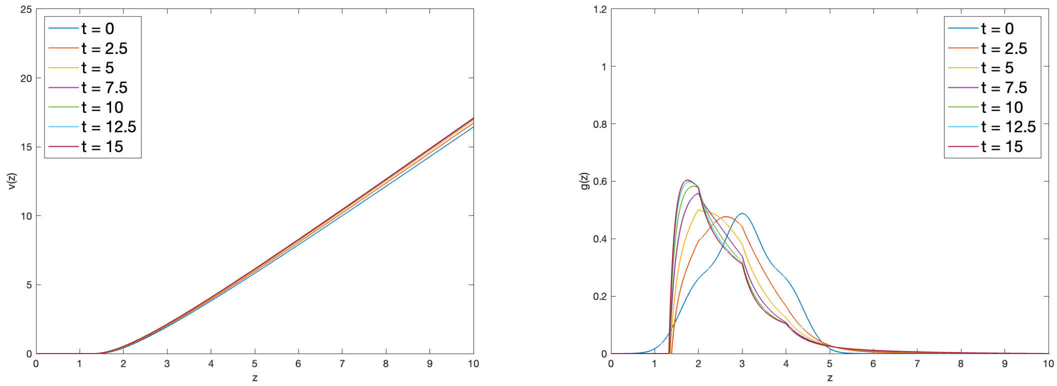

Figure 2.14: The time-dependent value function (left) and firm distribution (right) for $\mathbf{z^e} = (2, 3, 4)$ and $\mathbf{p^e} = (0.25, 0.5, 0.25)$ in the Merton model's Example 7

Table 2.23: Wages and the optimal exit productivity for $\mathbf{z^e} = (2, 3, 4)$ and $\mathbf{p^e} = (0.1, 0.1, 0.8)$ in the time-dependent Merton model's Example 7

t	$\omega(t)$	$\underline{z}(t)$
0	1.461956	1.575625
2.5	1.413061	1.523125
5	1.357171	1.475625
7.5	1.310676	1.439375
10	1.279196	1.416875
12.5	1.269870	1.414063
15	1.266733	1.414063
SS	1.266683	1.413125

and the probability density function of firms for each $\mathbf{p^e}$ in the Kou model. As in the Merton model, a notable consistency is observed between the graphs at $T = 15$ and those illustrating the steady-state cases outlined in Section 2.3.2.2.

In Figure 2.18, the temporal evolution of the free boundaries for the Merton (left), Kou (middle), and PDEs (right) models is showcased. This visualization allows us to

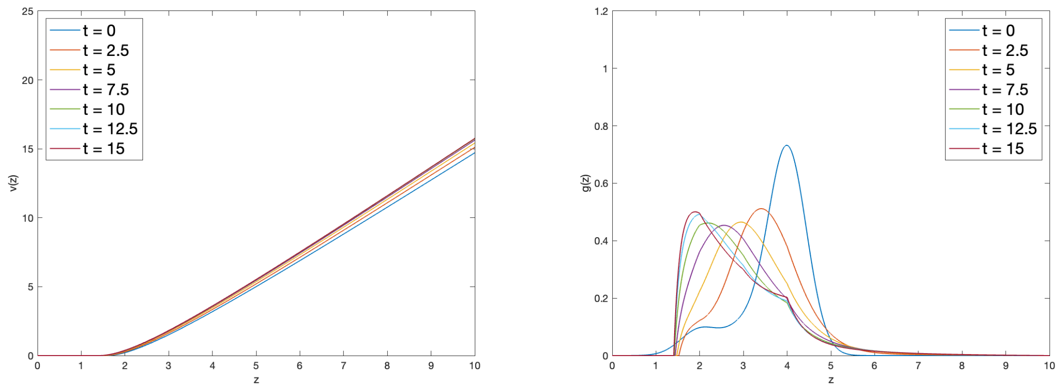

Figure 2.15: The time-dependent value function (left) and firm distribution (right) for $\mathbf{z^e} = (2,\, 3,\, 4)$ and $\mathbf{p^e} = (0.1,\, 0.1,\, 0.8)$ in the Merton model's Example 7

Table 2.24: Wages and optimal exit productivity for $\mathbf{z^e} = (2,\, 3,\, 4)$ and and $\mathbf{p^e} = (0.25,\, 0.5,\, 0.25)$ in the time-dependent Kou model's Example 7

t	$\omega(t)$	$\underline{z}(t)$
0	1.296229	1.418125
2.5	1.262867	1.378750
5	1.225191	1.347500
7.5	1.198668	1.326875
10	1.183272	1.315625
12.5	1.176464	1.311250
15	1.174715	1.310000
SS	1.175140	1.310781

observe the convergence of $\underline{z}(t)$ towards the steady-state case, as numerically detailed in Table 2.22, Table 2.24, and Table 2.11. Notably, the free boundaries in the three different modelling approaches exhibit a decreasing behaviour with respect to time until the corresponding curves transition into a straight line associated to the free boundary value of the associated steady state model. Note that exit regions are

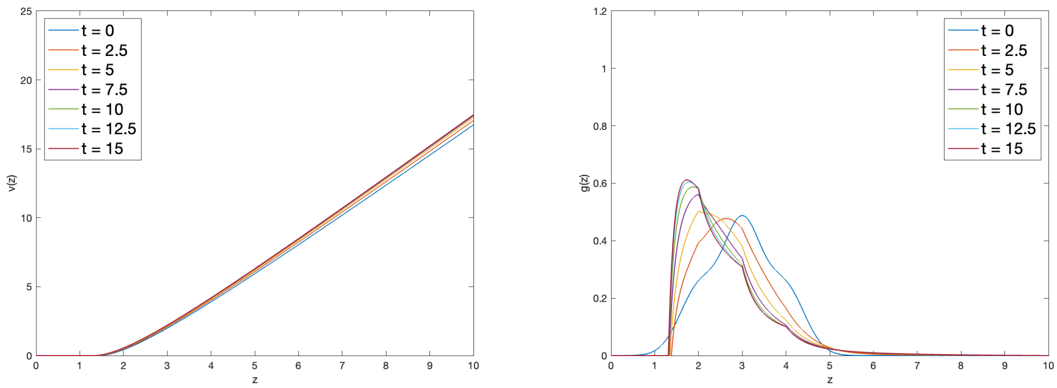

Figure 2.16: The time-dependent value function (left) and firm distribution (right) for the data $\mathbf{z^e} = (2, 3, 4)$ and $\mathbf{p^e} = (0.25, 0.5, 0.25)$ in the Kou model's Example 7

Table 2.25: Wages and optimal exit productivity for $\mathbf{z^e} = (2, 3, 4)$ and and $\mathbf{p^e} = (0.1, 0.1, 0.8)$ in the time-dependent Kou model's Example 7

t	$\omega(t)$	$\underline{z}(t)$
0	1.461956	1.572500
2.5	1.411043	1.518750
5	1.353413	1.470000
7.5	1.305151	1.431250
10	1.271900	1.407500
12.5	1.265100	1.404531
15	1.261084	1.404531
SS	1.258481	1.403750

depicted in black, while stay regions are illustrated in white for each model.

Remark 2.4.1. *All computations in Sections 4.3.2 and 4.4.2 are obtained with a MATLAB implementation of the algorithms. The numerical solution of the evolutionary equilibrium problem with* 16001×12001 *mesh takes around 8000 seconds,*

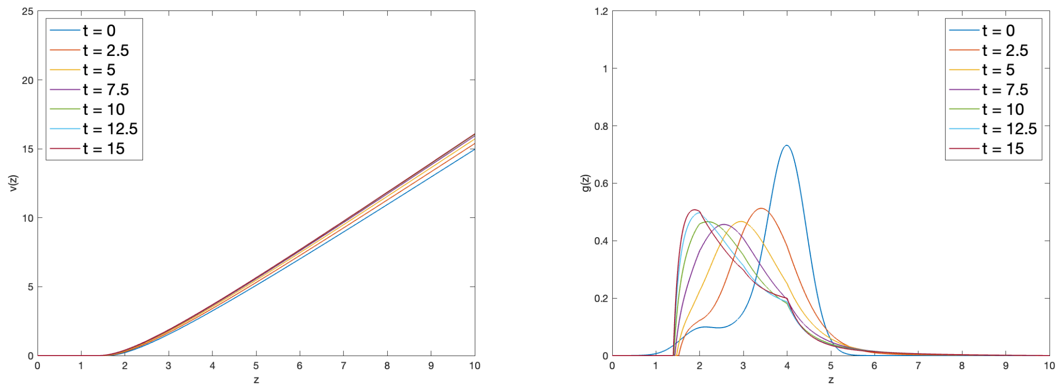

Figure 2.17: The time-dependent value function (left) and firm distribution (right) for the data $\mathbf{z^e} = (2, 3, 4)$ and $\mathbf{p^e} = (0.1, 0.1, 0.8)$ in the Kou model's Example 7

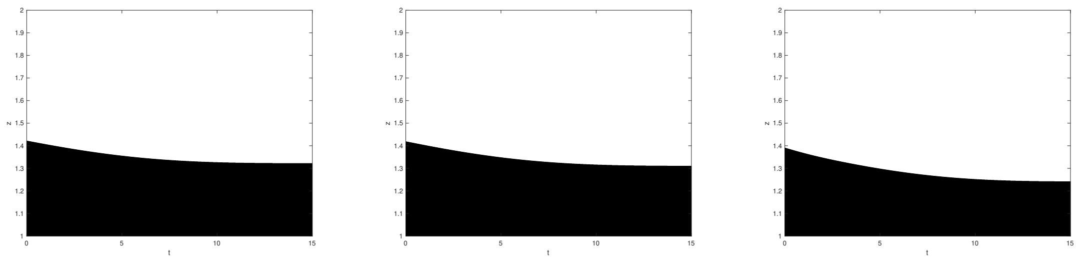

Figure 2.18: Approximated exit region (in black) and stay region (in white) with Merton (left), Kou (middle) and PDEs (right) models for the data $\mathbf{z^e} = (2, 3, 4)$ and $\mathbf{p^e} = (0.25, 0.5, 0.25)$

while the stationary equilibrium problem with 64001 *mesh points takes around 110 seconds on a MacBook Pro laptop. The CPU we use is a Apple M2 Chip with 8 GB RAM.*

The contents of Section 2.4 are included in our article [46].

Chapter 3

Mathematical models for two productive sectors

In this chapter, we propose a new mathematical model associated to the equilibrium problem that considers the interaction of two different sectors of the economy. More precisely, we assume that a company belonging to one of the sectors, namely the second one, has the option to move to the first sector after assuming the conversion costs associated to the change of sector. Additionally, the companies of the first sector have the option to change to the second sector facing the corresponding conversion costs or exit the sector by charging a subsidy and leaving the economy.

Although there are many examples along time, many of them related to the appearance of new disruptive technologies, the recent Covid-19 pandemia has led to specific crisis in certain sectors and the adaption of the affected companies to new opportunities by adapting their teams and tools to the production of different highly demanded goods, such as protection masks or medical products to face the critical situation.

In order to model the evolution of the two economic sectors, we consider the same general equilibrium framework than in previous models related to one sector. As a departure point, we also assume the existence of heterogeneous agents and rational expectations. However, we need to adapt and extend the modelling approach. Thus, we assume a continuous time formulation with heterogeneous agents in each one of the two referred sectors with idiosyncratic shocks and incomplete markets, following [30].

Therefore, as in the case of one sector, the productivity is the unique stochastic underlying factor. For the productivity dynamics, we initially consider a general Itô process, which provides a system of PDEs for the different problems. More precisely, we will have one HJB and one KFP PDE per sector.

Specifically, the HJB PDEs are different for the first and second sector. This is due to the fact that for a company in the first sector corresponding to small establishments, the are two options to leave the sector, thus giving rise to a HJB equation that admits a formulation in terms of a double obstacle problem. On the other hand, a company in the second sector related to large establisments can only leave the sector by moving to the first sector, so that a formulation in terms of one obstacle problem can be obtained for the associated HJB PDE.

In the second part of this chapter, in order to incorporate the possibility of jumps in the dynamics of the productivity, we consider that it follows a more general Lévy process. Under this alternative assumption, the different PDEs turn into PIDEs.

Note that we mainly adapt and extend the notation followed in the case of one productive sector.

3.1 The coupled PDEs problems

In order to pose the coupled PDEs problems in the case on two sectors, we are not going to repeat all common arguments used in the case of one sector, just highlight the main points.

In this section, we assume that the productivity is a stochastic process that satisfies the SDE (1.1). Again, although time-dependent drift and volatility fall inside the proposed modelling and numerical methodology, the consideration of time independent drift and volatility (as stated by (1.2)) facilitates the study of numerical convergence of the time-dependent problems to the steady-state ones. In this context, the productivity variable is governed by different SDEs based on establishment size. For small establishments, the productivity evolution z_t^1 is described by:

$$dz_t^1 = \mu_1(t, z_t)dt + \sigma_1(t, z_t)dW_t. \tag{3.1}$$

Nevertheless, for large establishments, z_t^2 satisfies the following equation:

$$dz_t^2 = \mu_2(t, z_t)dt + \sigma_2(t, z_t)dW_t. \tag{3.2}$$

Note that μ_1 and μ_2 denote the drift, while σ_1 and σ_2 represent the volatility of productivity for small and large establishments, respectively.

Additionally, the steady-state version of SDEs (3.1) and (3.2) is given by:

$$dz_t^1 = \mu_1(z_t)dt + \sigma_1(z_t)dW_t, \qquad dz_t^2 = \mu_2(z_t)dt + \sigma_2(z_t)dW_t. \tag{3.3}$$

3.1.1 Problems of incumbent firms

Let $T > 0$ and $\Omega = [0, T] \times \mathbb{R}^+$, following analogous arguments to Chapter 1 for the case of one sector, the problems of incumbent firms can be written in terms of linear complementarity problems, where $v_1(t, z)$ and $v_2(t, z)$ are the optimal firm values for the productivity z and time t for small and large establishments, respectively.

More precisely, given the optimal profits:

$$\pi_1(t, z) = \frac{z}{4\omega_1(t)} - c_f, \quad \pi_2(t, z) = \frac{z}{4\omega_2(t)} - c_f, \tag{3.4}$$

the incumbent firm problems aim to find v_1 and v_2, such that

$$\begin{cases} \mathcal{L}^{H,1}[v_1] \geq \pi_1, \ s \leq v_1 \leq s_1^2, \ \left(\mathcal{L}^{H,1}[v_1] - \pi_1\right) \cdot (v_1 - s) \cdot (s_1^2 - v_1) = 0, & \forall (t, z) \in \Omega, \\ v_1(t, 0) = -c_f/\rho, \qquad \lim_{z \to \infty} \dfrac{\partial^2 v_1}{\partial z^2}(t, z) = 0, & \forall t \in [0, T], \\ v_1(T, z) = v_1^T(z), & \forall z \in \mathbb{R}^+, \end{cases} \tag{3.5}$$

$$\begin{cases} \mathcal{L}^{H,2}[v_2] \geq \pi_2, \quad v_2 \geq s_2^1, \quad \left(\mathcal{L}^{H,2}[v_2] - \pi_2\right) \cdot (v_2 - s_2^1) = 0, & \forall (t,z) \in \Omega, \\ v_2(t,0) = -c_f/\rho, \qquad \lim_{z\to\infty} \dfrac{\partial^2 v_2}{\partial z^2}(t,z) = 0, & \forall t \in [0,T], \\ v_2(T,z) = v_2^T(z), & \forall z \in \mathbb{R}^+, \end{cases} \tag{3.6}$$

where v_1^T and v_2^T are the final conditions of the respective HJB problems and $\mathcal{L}^{H,i}[\cdot]$ is the parabolic differential operator of second order in the space variable z defined by:

$$\mathcal{L}^{H,i}[v_i] = -\frac{\partial v_i}{\partial t} - \mu_i(t,z)\frac{\partial v_i}{\partial z} - \frac{1}{2}\sigma_i^2(t,z)\frac{\partial^2 v_i}{\partial z^2} + \rho v_i, \qquad i = 1,2. \tag{3.7}$$

Note that the complementarity problems (3.5) and (3.6) can also be formulated in terms of parabolic variational inequalities of obstacle type, [36]. Also they represent examples of free boundary problems.

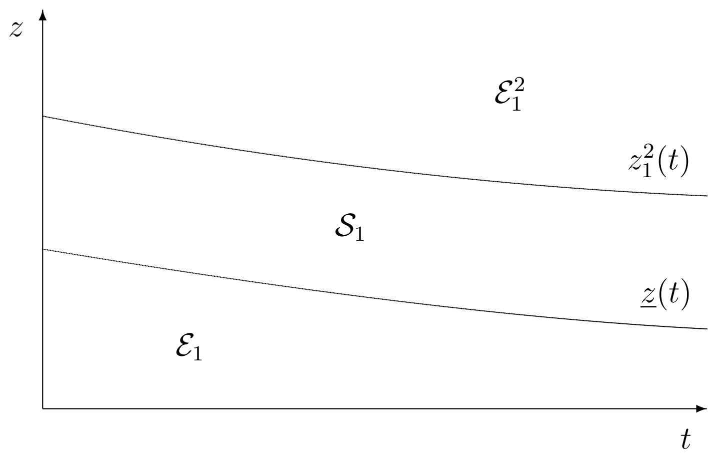

Figure 3.1: Exit regions ($\mathcal{E}_1$ and $\mathcal{E}_1^2$), stay region ($\mathcal{S}_1$) and free boundaries between them $\left(\underline{z}(t)\text{ and } z_1^2(t)\right)$

In particular, the double obstacle problem defined by (3.5) involves the presence of two unknown free boundaries that separate three unknown regions:

$$\begin{aligned}\mathcal{E}_1 &:= \{(t,z) \in [0,T] \times \Omega \,|\, v_1(t,z) = s(t)\},\\ \mathcal{S}_1 &:= \{(t,z) \in [0,T] \times \Omega \,|\, s(t) < v_1(t,z) < s_1^2(t)\},\\ \mathcal{E}_1^2 &:= \{(t,z) \in [0,T] \times \Omega \,|\, v_1(t,z) = s_1^2(t)\},\end{aligned} \tag{3.8}$$

In region $\mathcal{E}_1$, the solution coincides with the value of the lower obstacle s, so that the company in the sector of small establishments is in the exit region of the economy and receives the subsidy. In region $\mathcal{E}_1^2$, the solution coincides with the upper obstacle s_1^2, so that the company is in the region to exit to the large establishments sector. In region $\mathcal{S}_1$, the company remains in the sector of small establishments and this region is referred in free-boundary literature as non coincidence region.

Associated to the previous regions related to the double obstacle problem, we can identify the two free-boundaries that separate the stay region $\mathcal{S}_1$ from the two exit regions $\mathcal{E}_1$ and $\mathcal{E}_1^2$, respectively. More precisely, these free boundaries can be parameterized in the $t-z$ plane as follows:

$$\partial\mathcal{E}_1 \cap \partial\mathcal{S}_1 = \{(t, \underline{z}(t)),\, t \in [0,T]\}, \quad \partial\mathcal{E}_1^2 \cap \partial\mathcal{S}_1 = \{(t, z_1^2(t)),\, t \in [0,T]\}. \tag{3.9}$$

These two unknown free boundaries correspond to optimal exit boundaries from the sector of small establishments in the context of the incumbent firm problem. In Fig. 3.1, we can identify in the $t-z$ plane the exit and stay regions as well as the optimal exit boundaries.

Also note that in these optimal exit boundaries the following smooth pasting conditions are satisfied:

$$\begin{aligned} v_1(t,\underline{z}(t)) &= s(t), \qquad \frac{\partial v_1}{\partial z}(t,\underline{z}(t)) = 0,\\ v_1(t,z_1^2(t)) &= s_1^2(t), \qquad \frac{\partial v_1}{\partial z}(t,z_1^2(t)) = 0.\end{aligned} \tag{3.10}$$

An example of double obstacle problem appears in the valuation of optimal investment problems under transaction costs (see [18] or Arregui and Vázquez [7] and references therein, for example).

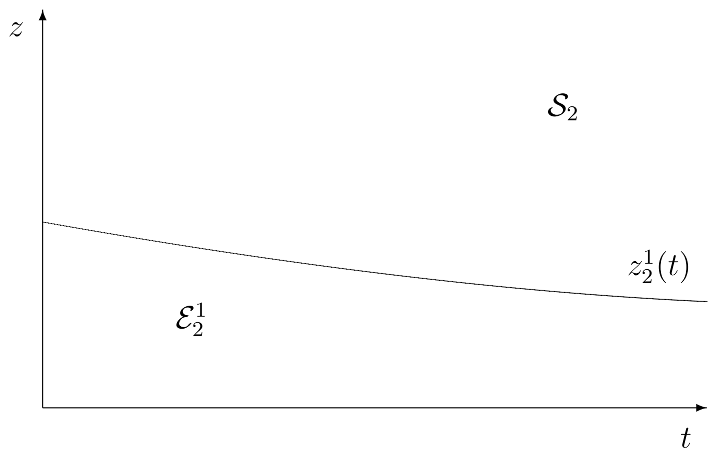

Figure 3.2: Exit region ($\mathcal{E}_2^1$), stay region ($\mathcal{S}_2$) and the free boundary between them $\big(z_2^1(t)\big)$

On the other hand, the single obstacle problem defined by (3.6) involves the presence of one unknown free boundary that separates the two unknown regions:

$$\begin{aligned} \mathcal{E}_2^1 &:= \{(t,z) \in [0,T] \times \Omega \,|\, v_2(t,z) = s_2^1(t)\}, \\ \mathcal{S}_2 &:= \{(t,z) \in [0,T] \times \Omega \,|\, v_2(t,z) > s_2^1(t)\}. \end{aligned} \tag{3.11}$$

The region $\mathcal{E}_2^1$ represents the exit region for the company in the sector of large establishments, while $\mathcal{S}_2$ represents the stay region for this company. Thus, the unknown free boundary the separates both regions can be parameterized in the $t - z$ plane as follows:

$$\partial\mathcal{E}_2^1 \cap \partial\mathcal{S}_2 = \{(t, z_2^1(t)),\, t \in [0,T]\} \tag{3.12}$$

and represents the optimal exit boundary for the company in the sector of large establishments. In Fig. 3.2, we can identify in the $t - z$ plane the exit and stay regions as well as the optimal exit boundary.

At this free boundary, the following smooth pasting condition is satisfied:

$$v_2(t, z_2^1(t)) = s_2^1(t), \qquad \frac{\partial v_2}{\partial z}(t, z_2^1(t)) = 0. \tag{3.13}$$

Moreover, the value functions v_1 and v_2 satisfy the following equations:

$$\begin{aligned} &\mathcal{L}^{H,1}[v_1] = \pi_1 \quad \text{in } \mathcal{S}_1, \qquad v_1 = s \quad \text{in } \mathcal{E}_1, \qquad v_1 = s_1^2 \quad \text{in } \mathcal{E}_1^2, \\ &\mathcal{L}^{H,2}[v_2] = \pi_2 \quad \text{in } \mathcal{S}_2, \qquad v_2 = s_2^1 \quad \text{in } \mathcal{E}_2^1, \end{aligned}$$

jointly with the smooth pasting conditions (3.10) and (3.13), respectively.

Additionally, we can write the steady-state version of equations (3.5) and (3.6) as follows:

$$\begin{cases} \hat{\mathcal{L}}^{H,1}[v_1] \geq \pi_1, \quad s \leq v_1 \leq s_1^2, \quad \left(\hat{\mathcal{L}}^{H,1}[v_1] - \pi_1\right) \cdot (v_1 - s) \cdot (s_1^2 - v_1) = 0, \quad \forall z \in \mathbb{R}^+, \\ v_1(0) = -c_f/\rho, \qquad \lim_{z\to\infty} \dfrac{\partial^2 v_1}{\partial z^2}(z) = 0. \end{cases} \tag{3.14}$$

$$\begin{cases} \hat{\mathcal{L}}^{H,2}[v_2] \geq \pi_2, \quad v_2 \geq s_2^1, \quad \left(\hat{\mathcal{L}}^{H,2}[v_2] - \pi_2\right) \cdot (v_2 - s_2^1) = 0, \quad \forall z \in \mathbb{R}^+, \\ v_2(0) = -c_f/\rho, \qquad \lim_{z\to\infty} \dfrac{\partial^2 v_2}{\partial z^2}(z) = 0, \end{cases} \tag{3.15}$$

with the involved differential operator given by:

$$\hat{\mathcal{L}}^{H,i}[v_i] = -\mu_i(z)\frac{\partial v_i}{\partial z} - \frac{1}{2}\sigma_i^2(z)\frac{\partial^2 v_i}{\partial z^2} + \rho v_i, \qquad i = 1, 2. \tag{3.16}$$

Note that the free boundaries of the steady-state problems correspond to fixed values of productivity. They represent unknown points in the z-line, dividing intervals of productivity values that correspond to different unknown regions. In the case of (3.14), there are two free boundary points, whereas in the case of (3.15), there is one free boundary point.

3.1.2 Problems of the dynamics of firm distribution

As companies of the first sector corresponding to small establishments decide to leave the industry when their low productivity cannot compensate the costs, the productivity process has a reflecting barrier at the optimal exit productivity boundary. As Section 1.1, they are replaced by the entry of new firms. Moreover, companies in both the first and second sectors have the option of abandoning it to enter in the other sector, by facing the corresponding costs of conversion.

Therefore, the problem of the dynamics of firm distribution can be written as a couple of KFP equations.

Let $g_1(t,z)$ and $g_2(t,z)$ be the probability distributions of firms for the productivity z and time t for small and large establishments, respectively. Given the new establishment entry rates $\alpha_1(t)$ and $\alpha_2(t)$ and the probability function of new small establishments $g^e(z,t)$, find g_1 and g_2 such that

$$\begin{cases} \mathcal{L}^{K,1}[g_1] = \alpha_1(t) g^e(t,z), & & \forall (t,z) \in \mathcal{S}_1, \\ g_1(t,\underline{z}(t)) = 0, & g_1(t, z_1^2(t)) = 0, & \forall t \in [0,T], \\ g_1(0,z) = g_1^0(z), & & \forall z \in [\underline{z}(0), z_1^2(0)], \end{cases} \tag{3.17}$$

$$\begin{cases} \mathcal{L}^{K,2}[g_2] = \alpha_2(t) \delta(z - z_1^2), & & \forall (t,z) \in \mathcal{S}_2, \\ g_2(t, z_2^1(t)) = 0, & g_2(t, Z) = 0, & \forall t \in [0,T], \\ g_2(0,z) = g_2^0(z), & & \forall z \in [z_2^1(0), +\infty), \end{cases} \tag{3.18}$$

where g_1^0 and g_2^0 are the initial conditions of the respective KFP problems and $\mathcal{L}^{K,i}[\cdot]$ is the involved differential operator of second order in the space variable z given by:

$$\mathcal{L}^{K,i}[g] = \frac{\partial g_i}{\partial t} + \frac{\partial\big(\mu_i(t,z) g_i\big)}{\partial z} - \frac{1}{2}\frac{\partial^2\big(\sigma_i^2(t,z) g_i\big)}{\partial z^2}, \qquad i = 1,2. \tag{3.19}$$

In this particular problem, we assume that the support of $g^e(t,\cdot)$ is contained in $(\underline{z}(t), z_1^2(t))$ to be consistent with the solution of the incumbent problem.

By integrating the PDE of (3.17) between $\underline{z}$ and z_1^2, and the PDE of (3.18) between z_2^1 and $+\infty$, applying their boundary conditions, respectively, and using the Leibniz integral rule, we obtain:

$$\alpha_1(t) = \frac{1}{2}\sigma_1^2(t,\underline{z})\frac{\partial g_1}{\partial z}(t,\underline{z}), \qquad \alpha_2(t) = \frac{1}{2}\sigma_2^2(t,z_2^1)\frac{\partial g_2}{\partial z}(t,z_2^1),$$

which state that the entry rate $\alpha_1(t)$ is equal to the exit rate at point $z = \underline{z}(t)$ and $\alpha_2(t)$ is equal to the exit rate at point $z = z_2^1(t)$, so that entry rates are endogenous.

Moreover, we can write the steady-state version of equations (3.17) and (3.18) as follows:

$$\begin{cases} \hat{\mathcal{L}}^{K,1}[g_1] = \alpha_1 g^e(z), & \forall z \in (\underline{z}, z_1^2), \\ g_1(\underline{z}) = 0, \qquad g_1(z_1^2) = 0, & \end{cases} \tag{3.20}$$

$$\begin{cases} \hat{\mathcal{L}}^{K,2}[g_2] = \alpha_2 \delta(z - z_1^2), & \forall z \in (z_2^1, \infty), \\ g_2(z_2^1) = 0, \qquad \lim_{z\to\infty} g_2(z) = 0, & \end{cases} \tag{3.21}$$

where the differential operator $\hat{\mathcal{L}}^{K,i}[\cdot]$ is defined by:

$$\hat{\mathcal{L}}^{K,i}[g_i] = \frac{\partial\big(\mu_i(z) g_i\big)}{\partial z} - \frac{1}{2}\frac{\partial^2\big(\sigma_i^2(z) g_i\big)}{\partial z^2}, \qquad i = 1, 2. \tag{3.22}$$

3.1.3 Equilibrium model

In order to close the equilibrium problem, we need to consider the household problem and the feasibility conditions as in Section 1.1. Given HJB and KFP equations (3.5–3.6 and 3.17–3.18) and the implicit equation (1.23), find $\underline{z}(t)$, $z_1^2(t)$, $z_2^1(t)$, $v_1(t,z)$, $v_2(t,z)$, $g_1(t,z)$, $g_2(t,z)$, $\omega_1(t)$ and $\omega_2(t)$ such that

$$\begin{cases} \mathcal{L}^{H,1}[v_1] \geq \pi_1,\; s \leq v_1 \leq s_1^2,\; \big(\mathcal{L}^{H,1}[v_1] - \pi_1\big)\cdot(v_1 - s)\cdot(s_1^2 - v_1) = 0, & \forall (t,z) \in \Omega, \\ \mathcal{L}^{H,2}[v_2] \geq \pi_2, \quad v_2 \geq s_2^1, \quad \big(\mathcal{L}^{H,2}[v_2] - \pi_2\big)\cdot(v_1 - s_2^1) = 0, & \forall (t,z) \in \Omega, \\ \mathcal{L}^{K,1}[g_1] = \frac{1}{2}\sigma^2(t,\underline{z})\frac{\partial g_1}{\partial z}(t,\underline{z}) g^e(t,z), & \forall (t,z) \in \mathcal{S}_1, \\ \mathcal{L}^{K,2}[g_2] = \frac{1}{2}\sigma^2(t,z_2^1)\frac{\partial g_2}{\partial z}(t,z_2^1)\delta(z - z_1^2), & \forall (t,z) \in \mathcal{S}_2, \\ \omega_1(t) = e\left(\int_{\underline{z}(t)}^{z_1^2(t)} \frac{z}{2\omega_1(t)} g_1(t,z)\,\mathrm{d}z - c_f\right), & \forall t \in [0,T], \\ \omega_2(t) = e\left(\int_{z_2^1(t)}^{+\infty} \frac{z}{2\omega_2(t)} g_2(t,z)\,\mathrm{d}z - c_f\right), & \forall t \in [0,T]. \end{cases} \tag{3.23}$$

A stationary equilibrium is represented by the time independent solution $\underline{z}$, z_1^2, z_2^1, $v_1(z)$, $v_2(z)$, $g_1(z)$, $g_2(z)$, ω_1 and ω_2 to the corresponding steady-state HJB and

KFP PDEs (3.14–3.15 and 3.20–3.21), jointly with (1.24):

$$\begin{cases} \hat{\mathcal{L}}^{H,1}[v_1] \geq \pi_1, \ s \leq v_1 \leq s_1^2, \ \left(\hat{\mathcal{L}}^{H,1}[v_1] - \pi_1\right) \cdot (v_1 - s) \cdot (s_1^2 - v_1) = 0, & \forall z \in \mathbb{R}^+, \\ \hat{\mathcal{L}}^{H,2}[v_2] \geq \pi_2, \quad v_2 \geq s_2^1, \quad \left(\hat{\mathcal{L}}^{H,2}[v_2] - \pi_2\right) \cdot (v_1 - s_2^1) = 0, & \forall z \in \mathbb{R}^+, \\ \hat{\mathcal{L}}^{K,1}[g_1] = \frac{1}{2}\sigma^2(\underline{z})\frac{\partial g_1}{\partial z}(\underline{z})g^e(z), & \forall z \in \hat{\mathcal{S}}_1, \\ \hat{\mathcal{L}}^{K,2}[g_2] = \frac{1}{2}\sigma^2(z_2^1)\frac{\partial g_2}{\partial z}(z_2^1)\delta(z - z_1^2), & \forall z \in \hat{\mathcal{S}}_2, \\ \omega_1 = e\left(\int_{\underline{z}}^{z_1^2} \frac{z}{2\omega_1} g_1(z)\,\mathrm{d}z - c_f\right), \\ \omega_2 = e\left(\int_{z_2^1}^{+\infty} \frac{z}{2\omega_2} g_2(z)\,\mathrm{d}z - c_f\right). \end{cases} \tag{3.24}$$

3.2 The coupled PIDEs problems

As in the case of one sector, the consideration of possible jumps in the dynamics of productivity can be addressed by means a stochastic Lévy process. The motivation of this modelling approach is justified as in the case of one sector and we will consider that the productivity satisfies the SDE (1.43). Moreover, the steady-state SDE (1.42) also fits the proposed modelling approach and numerical methods. In this context, we assume that the productivity variable z is governed by different SDEs based on establishment size. For small establishments, the productivity evolution z_t^1 satisfies the following equation:

$$dz_t^1 = \mu_1(t, z_t^1)dt + \sigma_1(t, z_t^1)dW_t + \beta(t, z_t^1)dN_t. \tag{3.25}$$

Nonetheless, for large establishments, z_t^2 is described by:

$$dz_t^2 = \mu_2(t, z_t^2)dt + \sigma_2(t, z_t^2)dW_t + \beta(t, z_t^2)dN_t. \tag{3.26}$$

Additionally, the steady-state version of SDEs (3.25) and (3.26) is defined by:

$$\begin{aligned} dz_t^1 &= \mu_1(z_t^1)dt + \sigma_1(z_t^1)dW_t + \beta(z_t^1)dN_t, \\ dz_t^2 &= \mu_2(z_t^2)dt + \sigma_2(z_t^2)dW_t + \beta(z_t^2)dN_t. \end{aligned} \tag{3.27}$$

Under this assumption on the dynamics of productivity, the PDEs posed in previous section turn into PIDEs. Specifically, the PIDEs system consists of four equations: an HJB PIDE for the incumbent problem and a KFP PIDE that describe the distribution of firms within each sector.

3.2.1 Problems of incumbent firms

Let $\Omega = [0,T] \times \mathbb{R}^+$, the problems of incumbent firms can be written as linear complementarity problems. Given the optimal profits π_1 and π_2 defined by (3.4), if we denote by $v_1(t,z)$ and $v_2(t,z)$ the optimal firm value for the productivity z and time t for small and large establishments, then standard techniques based on Itô formulas for jump-diffusion process prove that functions v_1 and v_2 satisfy the following PIDEs:

$$\begin{cases} \mathcal{L}_J^{H,1}[v_1] \geq \pi_1, \; s \leq v_1 \leq s_1^2, \; \Big(\mathcal{L}_J^{H,1}[v_1] - \pi_1\Big) \cdot (v_1 - s) \cdot (s_1^2 - v_1) = 0, & \forall (t,z) \in \Omega, \\ v_1(t,0) = -c_f/\rho, \qquad \lim_{z\to\infty} \dfrac{\partial^2 v_1}{\partial z^2}(t,z) = 0, & \forall t \in [0,T], \\ v_1(T,z) = v_1^T(z), & \forall z \in \mathbb{R}^+, \end{cases} \tag{3.28}$$

$$\begin{cases} \mathcal{L}_J^{H,2}[v_2] \geq \pi_2, \quad v_2 \geq s_2^1, \quad \Big(\mathcal{L}_J^{H,2}[v_2] - \pi_2\Big) \cdot (v_2 - s_2^1) = 0, & \forall (t,z) \in \Omega, \\ v_2(t,0) = -c_f/\rho, \qquad \lim_{z\to\infty} \dfrac{\partial^2 v_2}{\partial z^2}(t,z) = 0, & \forall t \in [0,T], \\ v_2(T,z) = v_2^T(z), & \forall z \in \mathbb{R}^+, \end{cases} \tag{3.29}$$

where v_1^T and v_2^T are the final conditions of the respective HJB problems. Additionally, the parabolic integro-differential operator is given by:

$$\mathcal{L}_J^{H,i}[v_i] = \mathcal{L}^{H,i}[v_i] - \lambda \int_{-\infty}^{+\infty} \left[v_i\big(t, z + \beta(t,z,x)\big) - v_i(t,z) - \beta(t,z,x)\frac{\partial v_i}{\partial z}\right] f(x)\,\mathrm{d}x, \tag{3.30}$$

such that the HJB PDE operator $\mathcal{L}^{H,i}[\cdot]$ satisfies (3.7), for $i = 1, 2$.

Note that (3.28) and (3.29) can also be formulated as parabolic variational inequalities of obstacle type, [36]. In this way, we can identify the exit and stay regions for small establishments defined by (3.8), and for large establishments defined by (3.11). Thus, $\partial\mathcal{E}_1 \cap \partial\mathcal{S}_1$, $\partial\mathcal{E}_1^2 \cap \partial\mathcal{S}_1$ and $\partial\mathcal{E}_2^1 \cap \partial\mathcal{S}_2$ can be understood as optimal exit boundaries and can be parameterized in the (t, z)-plane as in Section 3.1.1 such that smooth pasting conditions (3.10) and (3.13) are satisfied.

Therefore, the value functions v_1 and v_2 satisfy the following equations:

$$\begin{aligned} &\mathcal{L}_J^{H,1}[v_1] = \pi_1 \quad \text{in } \mathcal{S}_1, \qquad v_1 = s \quad \text{in } \mathcal{E}_1, \qquad v_1 = s_1^2 \quad \text{in } \mathcal{E}_1^2, \\ &\mathcal{L}_J^{H,2}[v_2] = \pi_2 \quad \text{in } \mathcal{S}_2, \qquad v_2 = s_2^1 \quad \text{in } \mathcal{E}_2^1, \end{aligned}$$

jointly with the smooth pasting conditions (3.10) and (3.13), respectively.

Moreover, we can write the steady-state version of equations (3.28) and (3.29) as follows:

$$\begin{cases} \hat{\mathcal{L}}_J^{H,1}[v_1] \geq \pi_1, \quad s \leq v_1 \leq s_1^2, \quad \left(\hat{\mathcal{L}}_J^{H,1}[v_1] - \pi_1\right) \cdot (v_1 - s) \cdot (s_1^2 - v_1) = 0, \quad \forall z \in \mathbb{R}^+, \\ v_1(0) = -c_f/\rho, \qquad \lim_{z \to \infty} \dfrac{\partial^2 v_1}{\partial z^2}(z) = 0. \end{cases} \tag{3.31}$$

$$\begin{cases} \hat{\mathcal{L}}_J^{H,2}[v_2] \geq \pi_2, \quad v_2 \geq s_2^1, \quad \left(\hat{\mathcal{L}}_J^{H,2}[v_2] - \pi_2\right) \cdot (v_2 - s_2^1) = 0, \quad \forall z \in \mathbb{R}^+, \\ v_2(0) = -c_f/\rho, \qquad \lim_{z \to \infty} \dfrac{\partial^2 v_2}{\partial z^2}(z) = 0, \end{cases} \tag{3.32}$$

where the involved differential operator is defined by:

$$\hat{\mathcal{L}}_J^{H,i}[v_i] = \hat{\mathcal{L}}^{H,i}[v_i] - \lambda \int_{-\infty}^{+\infty} \left[v_i(z + \beta(z,x)) - v_i(z) - \beta(z,x) \frac{\partial v_i}{\partial z} \right] f(x)\,\mathrm{d}x, \quad i = 1, 2, \tag{3.33}$$

such that the steady-state HJB PDE operator $\hat{\mathcal{L}}^{H,i}[\cdot]$ satisfies (3.16).

3.2.2 Problems of the dynamics of firm distribution

When companies determine that their low productivity can no longer offset the costs, they opt to exit the industry. Consequently, the productivity process features a reflecting barrier at the optimal productivity boundary. Following the methodology presented in Section 3.1.2, these departing companies are promptly replaced by new entrants. Therefore, the dynamics of firm distribution per each sector can be mathematically formulated as a KFP equation with a source term.

Let $g_1(t,z)$ and $g_2(t,z)$ represent the probability distribution of firms concerning productivity z at time t for small and large establishments. With knowledge of the entry rates of new establishments $\alpha_1(t)$ and $\alpha_2(t)$, and the probability function governing new establishment entries for the small establishments $g^e(t,z)$, the objective is to determine distributions g_1 and g_2 that satisfy the following equations:

$$\begin{cases} \mathcal{L}_J^{K,1}[g_1] = \alpha_1(t) g^e(t,z), & & \forall (t,z) \in \mathcal{S}_1, \\ g_1(t,\underline{z}(t)) = 0, & g_1(t, z_1^2(t)) = 0, & \forall t \in [0,T], \\ g_1(0,z) = g_1^0(z), & & \forall z \in \mathbb{R}^+, \end{cases} \tag{3.34}$$

$$\begin{cases} \mathcal{L}_J^{K,2}[g_2] = \alpha_2(t) \delta(z - z_1^2), & & \forall (t,z) \in \mathcal{S}_2, \\ g_2(t, z_2^1(t)) = 0, & \lim\limits_{z\to\infty} g_2(t,z) = 0, & \forall t \in [0,T], \\ g_2(0,z) = g_2^0(z), & & \forall z \in \mathbb{R}^+, \end{cases} \tag{3.35}$$

where g_1^0 and g_2^0 are the initial conditions of the corresponding KFP problems. Additionally, the involved integro-differential operator is defined by:

$$\mathcal{L}_J^{K,i}[g_i] = \mathcal{L}^{K,i}[g_i] - \lambda \int_{-\infty}^{+\infty} \big[g_i(t, z - \beta(t,z,x)) - g_i(t,z) \big] f(x) \, \mathrm{d}x, \quad i = 1,2, \tag{3.36}$$

such that the KFP PDE operator $\mathcal{L}^{K,i}[\cdot]$ satisfies (1.52). Note that the range of $g^e(t,\cdot)$ falls within the interval $(\underline{z}(t), z_1^2(t))$, aligning with the solution for the incumbent firms.

By integrating the PIDE of (3.34) between $\underline{z}$ and z_1^2, and the PIDE of (3.35) between z_2^1 and $+\infty$, applying their boundary conditions, and using the Leibniz integral rule, we obtain

$$\alpha_1(t) = \frac{1}{2}\sigma_1^2(t,\underline{z}) \frac{\partial g_1}{\partial z}(t,\underline{z}), \qquad \alpha_2(t) = \frac{1}{2}\sigma_2^2(t, z_2^1) \frac{\partial g_2}{\partial z}(t, z_2^1),$$

which state that the entry rate $\alpha_1(t)$ is equal to the exit rate at point $z = \underline{z}(t)$ and $\alpha_2(t)$ is equal to the exit rate at point $z = z_2^1(t)$, so that entry rates are endogenous.

Moreover, we can write the steady-state version of equations (3.34) and (3.35) as follows:

$$\begin{cases} \hat{\mathcal{L}}_J^{K,1}[g_1] = \alpha_1 g^e(z), & \forall z \in \mathcal{S}_1, \\ \\ g_1(\underline{z}) = 0, \qquad g_1(z_1^2) = 0, \end{cases} \tag{3.37}$$

$$\begin{cases} \hat{\mathcal{L}}_J^{K,2}[g_2] = \alpha_2 \delta(z - z_1^2), & \forall z \in \mathcal{S}_2, \\ \\ g_2(z_2^1) = 0, \qquad \lim_{z\to\infty} g_2(z) = 0, \end{cases} \tag{3.38}$$

where the involved differential operator is defined by:

$$\hat{\mathcal{L}}_J^{K,i}[g_i] = \hat{\mathcal{L}}^{K,i}[g_i] - \lambda \int_{-\infty}^{+\infty} \big[g_i(z - \beta(z,x)) - g_i(z)\big] f(x)\,\mathrm{d}x, \quad i = 1, 2, \tag{3.39}$$

such that the steady-state KFP operator $\hat{\mathcal{L}}^{K,i}[\cdot]$ satisfies (3.22).

3.2.3 Equilibrium model

Given HJB and KFP equations (3.28–3.29 and 3.34–3.35) and the implicit equation (1.23), find $\underline{z}(t)$, $z_1^2(t)$, $z_2^1(t)$, $v_1(t,z)$, $v_2(t,z)$, $g_1(t,z)$, $g_2(t,z)$, $\omega_1(t)$ and $\omega_2(t)$ such that

$$\begin{cases} \mathcal{L}_J^{H,1}[v_1] \geq \pi_1,\ s \leq v_1 \leq s_1^2,\ \left(\mathcal{L}_J^{H,1}[v_1] - \pi_1\right) \cdot (v_1 - s) \cdot (s_1^2 - v_1) = 0, & \forall (t,z) \in \Omega, \\ \mathcal{L}_J^{H,2}[v_2] \geq \pi_2, \quad v_2 \geq s_2^1, \quad \left(\mathcal{L}_J^{H,2}[v_2] - \pi_2\right) \cdot (v_1 - s_2^1) = 0, & \forall (t,z) \in \Omega, \\ \mathcal{L}_J^{K,1}[g_1] = \dfrac{1}{2}\sigma^2(t,\underline{z}) \dfrac{\partial g_1}{\partial z}(t,\underline{z}) g^e(t,z), & \forall (t,z) \in \mathcal{S}_1, \\ \mathcal{L}_J^{K,2}[g_2] = \dfrac{1}{2}\sigma^2(t,z_2^1) \dfrac{\partial g_2}{\partial z}(t,z_2^1) \delta(z - z_1^2), & \forall (t,z) \in \mathcal{S}_2, \\ \omega_1(t) = e\left(\displaystyle\int_{\underline{z}(t)}^{z_1^2(t)} \frac{z}{2\omega_1(t)} g_1(t,z)\,\mathrm{d}z - c_f\right), & \forall t \in [0,T], \\ \omega_2(t) = e\left(\displaystyle\int_{z_2^1(t)}^{+\infty} \frac{z}{2\omega_2(t)} g_2(t,z)\,\mathrm{d}z - c_f\right), & \forall t \in [0,T]. \end{cases} \tag{3.40}$$

A stationary equilibrium is represented by the time independent solution $\underline{z}$, z_1^2, z_2^1, $v_1(z)$, $v_2(z)$, $g_1(z)$, $g_2(z)$, ω_1 and ω_2 to the corresponding steady-state HJB and KFP PIDEs (3.31–3.32 and 3.37–3.38), jointly with (1.24):

$$\begin{cases} \hat{\mathcal{L}}_J^{H,1}[v_1] \geq \pi_1,\ s \leq v_1 \leq s_1^2,\ \left(\hat{\mathcal{L}}_J^{H,1}[v_1] - \pi_1\right) \cdot (v_1 - s) \cdot (s_1^2 - v_1) = 0, & \forall z \in \mathbb{R}^+, \\ \hat{\mathcal{L}}_J^{H,2}[v_2] \geq \pi_2, \quad v_2 \geq s_2^1, \quad \left(\hat{\mathcal{L}}_J^{H,2}[v_2] - \pi_2\right) \cdot (v_1 - s_2^1) = 0, & \forall z \in \mathbb{R}^+, \\ \hat{\mathcal{L}}_J^{K,1}[g_1] = \dfrac{1}{2}\sigma^2(\underline{z})\dfrac{\partial g_1}{\partial z}(\underline{z}) g^e(z), & \forall z \in \hat{\mathcal{S}}_1, \\ \hat{\mathcal{L}}_J^{K,2}[g_2] = \dfrac{1}{2}\sigma^2(z_2^1)\dfrac{\partial g_2}{\partial z}(z_2^1)\delta(z - z_1^2), & \forall z \in \hat{\mathcal{S}}_2, \\ \omega_1 = e\left(\displaystyle\int_{\underline{z}}^{z_1^2} \frac{z}{2\omega_1} g_1(z)\,\mathrm{d}z - c_f\right), & \\ \omega_2 = e\left(\displaystyle\int_{z_2^1}^{+\infty} \frac{z}{2\omega_2} g_2(z)\,\mathrm{d}z - c_f\right). & \end{cases} \tag{3.41}$$

Chapter 4

Numerical simulation for two productive sectors

This chapter mainly focuses on explaining the methodologies proposed to treat both the steady-state and time-dependent equilibrium problems involved in the two productive sector problem. Additionally, it aims to show a set of results that serve to prove the efficacy and robustness of the suggested numerical approaches, following analogous arguments to Chapter 2 for the case of one sector.

The first part of the chapter is dedicated to the presentation of the numerical methodologies and tests for both the steady-state and time-dependent PDE problems. Additionally, numerical techniques to solve the steady-state and time-dependent PIDE problems and different examples are presented. Note that numerical strategies developed in Chapter 2 have been extended.

4.1 Numerical methods for the steady-state PDE problem

This section focuses on solving the steady-state equilibrium problem, mainly characterized by the PDEs denoted as (3.14) and (3.20) for small establishments, and (3.15) and (3.21) for large establishments, along with equation (1.24). Our approach involves a fixed-point iteration technique to compute the numerical solution for problems defined by these equations.

Firstly, we present the numerical methods employed in this process. Subsequently, we show different numerical examples to prove the effectiveness and performance of the proposed methodology.

4.1.1 Numerical methods

Since the equilibrium problem with two sectors lacks a known semianalytical solution, in this section we propose a set of numerical techniques to approximate the solution. The main point is the numerical discretization of the HJB and KFP equations governing the incumbent and firm distribution problems.

4.1.1.1 Problem of stationary incumbent firms

Similar to Section 2.1.1.1, we use a uniform grid, so that we denote $[v_1]_k \approx v_1(z_k)$ and $[v_2]_k \approx v_2(z_k)$ as the approximations of the solutions.

Next, in order to approximate problems (3.14) and (3.15) at the grid point z_k, $k = 1, \ldots, N_z - 1$, we consider (2.2) to approximate the first and second order derivatives. Therefore, after some reordering of terms, we get for $k = 1, \ldots, N_z - 1$ the expressions:

$$\begin{aligned} &\mathcal{L}_k^{H,1}[v_1] \geq \pi_1^k, \quad s \leq v_k^1 \leq s_1^2, \quad \left(\mathcal{L}_k^{H,1}[v_1] - \pi_1^k\right) \cdot (v_k^1 - s) \cdot (s_1^2 - v_k^1) = 0, \\ &\mathcal{L}_k^{H,2}[v_2] \geq \pi_2^k, \quad v_k^2 \geq s_2^1, \quad \left(\mathcal{L}_k^{H,2}[v_2] - \pi_2^k\right) \cdot (v_k^2 - s_2^1) = 0, \end{aligned}$$

where

$$\begin{aligned} \mathcal{L}_k^{H,i}[v_i] = \left[\frac{\mu_i(z_k)}{\Delta z} - \frac{\sigma_i^2(z_k)}{2(\Delta z)^2}\right][v_i]_{k-1} + \left[\rho - \frac{\mu_i(z_k)}{\Delta z} + \frac{\sigma_i^2(z_k)}{(\Delta z)^2}\right][v_i]_k \\ - \frac{\sigma_i^2(z_k)}{2(\Delta z)^2}[v_i]_{k+1}, \quad i = 1, 2. \quad (4.1) \end{aligned}$$

Additionally, the boundary conditions of (3.14) and (3.15) are approximated by:

$$
\begin{aligned}
&[v_1]_0 = -c_f/\rho \quad \text{and} \quad \frac{2[v_1]_{N_z} - 5[v_1]_{N_z-1} + 4[v_1]_{N_z-2} - [v_1]_{N_z-3}}{(\Delta z)^2} = 0., \\
&[v_2]_0 = -c_f/\rho \quad \text{and} \quad \frac{2[v_2]_{N_z} - 5[v_2]_{N_z-1} + 4[v_2]_{N_z-2} - [v_2]_{N_z-3}}{(\Delta z)^2} = 0.
\end{aligned}
\tag{4.2}
$$

Thus, the fully discretized linear complementarity problem can be written in a matrix formulation as follows:

$$A_1V_1 \geq f^1,\ S \leq V_1 \leq S_1^2,\ \big((A_1V_1-f^1)^t\cdot(V_1-S)\big)\cdot\big((A_1V_1-f^1)^t\cdot(S_1^2-V_1)\big) = 0, \tag{4.3}$$

$$A_2V_2 \geq f^2, \quad V_2 \geq S_2^1, \quad (A_2V_2 - f^2)^t \cdot (V_2 - S_2^1) = 0, \tag{4.4}$$

where $V_i = ([v_i]_0, \dots, [v_i]_{N_z})^t$ is the unknown vector of nodal values of v_i; $S, S_1^2, S_2^1 \in \mathbb{R}^{N_z+1}$ are vectors with all components equal to s, s_1^2 and s_2^1, respectively; and vectors $f^1, f^2 \in \mathbb{R}^{N_z+1}$, such that $f_0^i = -c_f/\rho$, $f_{N_z}^i = 0$, while $f_k^i = [\pi_i]_k$, for $i = 1, 2$ and $k = 1, \dots, N_z - 1$. Therefore, matrix A_i is given by:

$$
A_i = \begin{pmatrix}
1 & 0 & 0 & 0 & \cdots & \cdots & 0 & 0 & 0 & 0 \\
a_1^i & b_1^i & c_1^i & 0 & \cdots & \cdots & 0 & 0 & 0 & 0 \\
0 & a_2^i & b_2^i & c_2^i & \ddots & & 0 & 0 & 0 & 0 \\
\vdots & \vdots & \ddots & \ddots & \ddots & \ddots & \vdots & \vdots & \vdots & \vdots \\
\vdots & \vdots & \vdots & \ddots & \ddots & \ddots & 0 & 0 & 0 & 0 \\
\vdots & \vdots & \vdots & \vdots & \ddots & \ddots & c_{N_z-4}^i & 0 & 0 & 0 \\
\vdots & \vdots & \vdots & \vdots & & \ddots & b_{N_z-3}^i & c_{N_z-3}^i & 0 & 0 \\
0 & 0 & 0 & 0 & \cdots & \cdots & a_{N_z-2}^i & b_{N_z-2}^i & c_{N_z-2}^i & 0 \\
0 & 0 & 0 & 0 & \cdots & \cdots & 0 & a_{N_z-1}^i & b_{N_z-1}^i & c_{N_z-1}^i \\
0 & 0 & 0 & 0 & \cdots & \cdots & e_{N_z} & d_{N_z} & a_{N_z} & b_{N_z}
\end{pmatrix}
$$

such that

$$a_k^i = \frac{\sigma_i^2(z_k)}{2(\Delta z)^2} - \frac{\mu_i(z_k)}{\Delta z}, \quad b_k^i = -\frac{\sigma_i^2(z_k)}{(\Delta z)^2} + \frac{\mu_i(z_k)}{\Delta z} - \rho, \quad c_k^i = \frac{\sigma_i^2(z_k)}{2(\Delta z)^2},$$

for $k = 1, \dots, N_z - 1$, and,

$$a_{N_z} = \frac{-5}{(\Delta z)^2},\ b_{N_z} = \frac{2}{(\Delta z)^2},\ d_{N_z} = \frac{4}{(\Delta z)^2},\ e_{N_z} = \frac{-1}{(\Delta z)^2}.$$

In this study, we opt to employ the ALAS algorithm, as developed in [35], for addressing both the bilateral obstacle problem (4.3) and the unilateral obstacle problem (4.4). Section 2.1.1.1 provides a detailed exposition of the numerical solution methodology applied to the unilateral obstacle problem. For the bilateral obstacle problem, we propose utilizing the primal-dual active set strategy outlined in Algorithm 2, which is included in the Appendix. To achieve this objective, it is vital to consider the following statements.

The formulation (4.3) can be written with the equivalent matrix form:

$$A_1 V_1 + P = f^1,$$

where P denotes the vector of the multiplier values associated with the inequality constraint.

For any decomposition of nodes $\overline{\mathcal{N}} = \overline{\mathcal{I}} \cup \overline{\mathcal{J}}$, where $\overline{\mathcal{N}} = \{0, 1, 2, \ldots, N_z\}$, the ALAS algorithm for bilateral obstacle problems computes not only V_1 and $\overline{P}$, but also updates the decomposition $\overline{\mathcal{N}} = \overline{\mathcal{I}} \cup \overline{\mathcal{J}}$, where $\overline{\mathcal{J}} = \mathcal{J}_S \cup \mathcal{J}_{S_1^2}$, and such that

$$\begin{aligned}
&A_1 V_1 + \overline{P} = f^1, && \\
&\overline{P}_j + \hat{\beta}([V_1]_j - S_j) \leq 0, && \text{for all } j \in \mathcal{J}_S, \\
&\overline{P}_j + \hat{\beta}([V_1]_j - [S_1^2]_j) \geq 0, && \text{for all } j \in \mathcal{J}_{S_1^2}, \\
&\overline{P}_i = 0, && \text{for all } i \in \mathcal{I},
\end{aligned}$$

where $\overline{\mathcal{I}}$ and $\overline{\mathcal{J}}$ are the inactive and the active sets, for a given positive constant $\hat{\beta}$.

Note that (A.2) reduces to solving

$$\begin{aligned}
[A_1]_{\overline{\mathcal{I}\mathcal{I}}}[V_1]_{\overline{\mathcal{I}}} &= [f^1]_{\overline{\mathcal{I}}} - [A_1]_{\overline{\mathcal{I}}\mathcal{J}_S}[S]_{\mathcal{J}_S} - [A_1]_{\overline{\mathcal{I}}\mathcal{J}_{S_1^2}}[S_1^2]_{\mathcal{J}_{S_1^2}}, \\
[V_1]_{\mathcal{J}_S} &= [S]_{\mathcal{J}_S}, \\
[V_1]_{\mathcal{J}_{S_1^2}} &= [S_1^2]_{\mathcal{J}_{S_1^2}}, \\
\overline{P} &= f^1 - A_1 V^1,
\end{aligned}$$

where $[A_1]_{\overline{\mathcal{I}\mathcal{I}}}$ denotes the main diagonal block of matrix A_1 indexed by $\overline{\mathcal{I}}$ and $[A_1]_{\overline{\mathcal{I}}\mathcal{J}_S}$ and $[A_1]_{\overline{\mathcal{I}}\mathcal{J}_{S_1^2}}$ denote the codiagonal blocks indexed by $\overline{\mathcal{I}}$ and $\mathcal{J}_S$, and $\overline{\mathcal{I}}$ and $\mathcal{J}_{S_1^2}$, respectively.

4.1.1.2 Problem of stationary firm distribution

In this problem, the computational domain for small establishments will be:

$$\hat{\Omega}_Z = [\hat{E}_1]_Z \cup [\hat{S}_1]_Z \cup [\hat{E}_1^2]_Z,$$

where $[\hat{E}_1]_Z = [0, \underline{z}]$, $[\hat{S}_1]_Z = (\underline{z}, z_1^2)$ and $[\hat{E}_1^2]_Z = [z_1^2, Z]$. Similarly, for large establishments:

$$\hat{\Omega}_Z = [\hat{E}_2^1]_Z \cup [\hat{S}_2]_Z,$$

where $[\hat{E}_1^2]_Z = [0, z_2^1]$ and $[\hat{S}_2]_Z = (z_2^1, Z]$.

Therefore, for small establishments, we consider $g_1(z) = 0$ on $[\hat{E}_1]_Z$ and $[\hat{E}_1^2]_Z$, and formulate the PDE of (3.20) on $[\hat{S}_1]_Z$. Meanwhile, for large establishments, we set $g_2(z) = 0$ on $[\hat{E}_2^1]_Z$ and solve the PDE of (3.21) on $[\hat{S}_2]_Z$.

Let us denote by $[g_1]_k \approx g_1(z_k)$ and $[g_2]_k \approx g_2(z_k)$ approximations obtained from KFP problems (3.20) and (3.21). Let $z_{\widetilde{k}}$, $z_{k_1^2}$ and $z_{k_2^1}$ be approximations of optimal exit productivities, where $\widetilde{k} = \max\{j : j \in \mathcal{J}_S\}$, $k_1^2 = \min\{j : j \in \mathcal{J}_{S_1^2}\}$ and $k_2^1 = \max\{j : j \in \mathcal{J}_{S_2^1}\}$ are obtained in terms of the sets defined in the numerical solution of incumbent problems. Note that the set $\mathcal{J}_{S_1^2}$ is the active set obtained from the unilateral problem (4.4).

In order to approximate KFP problems (3.20) and (3.21) at the grid points z_k, we introduce (2.6) to approximate the first and second order derivatives. Thus, we get equations:

$$\begin{aligned} \mathcal{L}_k^{K,1}[g_1] &= \frac{\sigma^2(z_{\widetilde{k}})}{2}\frac{\partial g_1}{\partial z}(z_{\widetilde{k}})g^e(z_k), & k &= \widetilde{k}+1,\ldots,k_1^2-1, \\ \mathcal{L}_k^{K,2}[g_2] &= \frac{\sigma^2(z_{k_2^1})}{2}\frac{\partial g_2}{\partial z}(z_{k_2^1})\delta(z_k - z_1^2), & k &= k_2^1+1,\ldots,N_z-1, \end{aligned} \tag{4.5}$$

where

$$\begin{aligned} \mathcal{L}_k^{K,i}[g_i] = &-\frac{1}{\Delta z}\left[\frac{\sigma_i^2(z_{k-1})}{2\Delta z} + [\mu_i(z_{k-1})]^+\right][g_i]_{k-1} \\ &+\frac{1}{\Delta z}\left[\frac{\sigma_i^2(z_k)}{\Delta z} + [\mu_i(z_k)]^+ - [\mu_i(z_k)]^-\right][g_i]_k \\ &-\frac{1}{\Delta z}\left[\frac{\sigma_i^2(z_{k+1})}{2\Delta z} - [\mu_i(z_{k+1})]^-\right][g_i]_{k+1}. \end{aligned} \tag{4.6}$$

The numerical strategy to solve problem (3.21) was detailed in Section 2.2.1.2, while the methodology for problem (3.20) needs adapting. For this aim, the following statements need to be considered.

The discretized problem for large establishments can be written as the linear system:

$$B_1 G_1 = b^1, \tag{4.7}$$

where $G_1 = ([g_1]_0, [g_1]_1, \ldots, [g_1]_{N_z})^t$ is the solution vector and $b^1 \in \mathbb{R}^{N_z+1}$, such that $b^1_k = 0$, $k = 0, \ldots, \widetilde{k}, k_1^2, \ldots, N_z$, while

$$b^1_k = \frac{\sigma_1^2(z_{\widetilde{k}})}{2} \frac{\partial g_1^p}{\partial z}(z_{\widetilde{k}}) g^e(z_k), \qquad k = \widetilde{k}+1, \ldots, k_1^2 - 1,$$

where g_1^p comes from the previous fixed point iteration in order to mantain the structure of matrices to make an efficient solution of tridiagonal systems.

In order to impose that $g_k = 0$ for $k = 0, \ldots, \widetilde{k}, k_1^2, \ldots, N_z$, the matrix B_1 is given by

$$B_1 = \begin{pmatrix}
1 & 0 & 0 & 0 & 0 & \cdots & 0 & 0 & 0 & 0 & 0 \\
\vdots & \ddots & \vdots & \vdots & \vdots & \cdots & 0 & 0 & 0 & 0 & 0 \\
0 & 0 & 1 & 0 & 0 & \cdots & 0 & 0 & 0 & 0 & 0 \\
\vdots & \vdots & \hat{a}^1_{\widetilde{k}+1} & \hat{b}^1_{\widetilde{k}+1} & \hat{c}^1_{\widetilde{k}+1} & & \vdots & \vdots & \vdots & \vdots & \vdots \\
\vdots & \vdots & \vdots & \ddots & \ddots & \ddots & \vdots & \vdots & \vdots & \vdots & \vdots \\
\vdots & \vdots & \vdots & \vdots & \ddots & \ddots & \ddots & \vdots & \vdots & \vdots & \vdots \\
\vdots & \vdots & \vdots & \vdots & & \ddots & \ddots & \ddots & \vdots & \vdots & \vdots \\
\vdots & \vdots & \vdots & \vdots & \vdots & & \hat{a}^1_{k_1^2-1} & \hat{b}^1_{k_1^2-1} & \hat{c}^1_{k_1^2-1} & \vdots & \vdots \\
0 & 0 & 0 & 0 & 0 & \cdots & 0 & 0 & 1 & 0 & 0 \\
0 & 0 & 0 & 0 & 0 & \cdots & \vdots & \vdots & \vdots & \ddots & \vdots \\
0 & 0 & 0 & 0 & 0 & \cdots & 0 & 0 & 0 & 0 & 1
\end{pmatrix},$$

where for $k = \widetilde{k}+1, \ldots, k_1^2 - 1$, we have

$$\hat{a}^1_k = -\frac{\sigma_1^2(z_{k-1})}{2(\Delta z)^2} - \frac{[\mu_1(z_{k-1})]^+}{\Delta z}, \qquad \hat{b}^1_k = \frac{\sigma_1^2(z_k)}{(\Delta z)^2} + \frac{[\mu_1(z_k)]^+}{\Delta z} - \frac{[\mu_1(z_k)]^-}{\Delta z},$$

$$\hat{c}^1_k = -\frac{\sigma_1^2(z_{k+1})}{2(\Delta z)^2} + \frac{[\mu_1(z_{k+1})]^-}{\Delta z}.$$

It is worth noting that since g_i represents a probability density function, its integral must equal one, so that the equation (2.10) is satisfied.

4.1.1.3 Stationary equilibrium problem

In this section, we briefly describe how we calculate the stationary equilibrium given specified functions $\mu_1(z)$, $\mu_2(z)$, $\sigma_1(z)$ and $\sigma_2(z)$; and values for the parameters s, s_1^2, s_2^1, ρ, e and c_f.

Following a similar approach to the one sector case, we propose employing the Steffensen method. In Fig. 4.1, we see as the proposed methodology is the generalization for two sectors of that used to compute the equilibrium in Section 2.1.1.3. Therefore, we start with ω_1^0 and ω_2^0 given and for $m = 0, 1, 2, \ldots$ we follow:

1. Given wages ω_1^m and ω_2^m, solve stationary HJB equations (3.14) and (3.15) to obtain $\underline{z}^m$, $[z_1^2]^m$, $[z_2^1]^m$, v_1^m and v_2^m with methods described in Section 4.1.1.1.

2. Given $\underline{z}^m$, $[z_1^2]^m$ and $[z_2^1]^m$ solve stationary KFP equations (3.20) and (3.21) for g_1^m and g_2^m using methods detailed in Section 4.1.1.2.

3. Given g_1^m and g_2^m, we compute wages $[\omega_1^m]_1$ and $[\omega_2^m]_1$ by using implicit formulas from (3.24).

4. Given wages $[\omega_1^m]_1$ and $[\omega_2^m]_1$, we repeat Steps 1 to 4 for calculating $[\omega_1^m]_2$ and $[\omega_2^m]_2$, and generate a new guess using the Steffensen formula:

$$\omega_i^{m+1} = \omega_i^m - \frac{([\omega_i^m]_1 - \omega_i^m)^2}{[\omega_i^m]_2 - 2[\omega_i^m]_1 + \omega_i^m}, \qquad i = 1, 2. \tag{4.8}$$

4.1.2 Numerical results

In this section, we assume that the productivity follows a geometric Brownian motion, so that equations of (3.3) with $\mu_1(z_t) = \mu_1 z_t$, $\mu_2(z_t) = \mu_2 z_t$, $\sigma_1(z_t) = \sigma_1 z_t$ and $\sigma_2(z_t) = \sigma_2 z_t$ are satisfied, where constants $\mu_1, \mu_2 < 0$, σ_1 and σ_2 are the expected growth rate and the per-unit time volatility for small and large establishments, respectively.

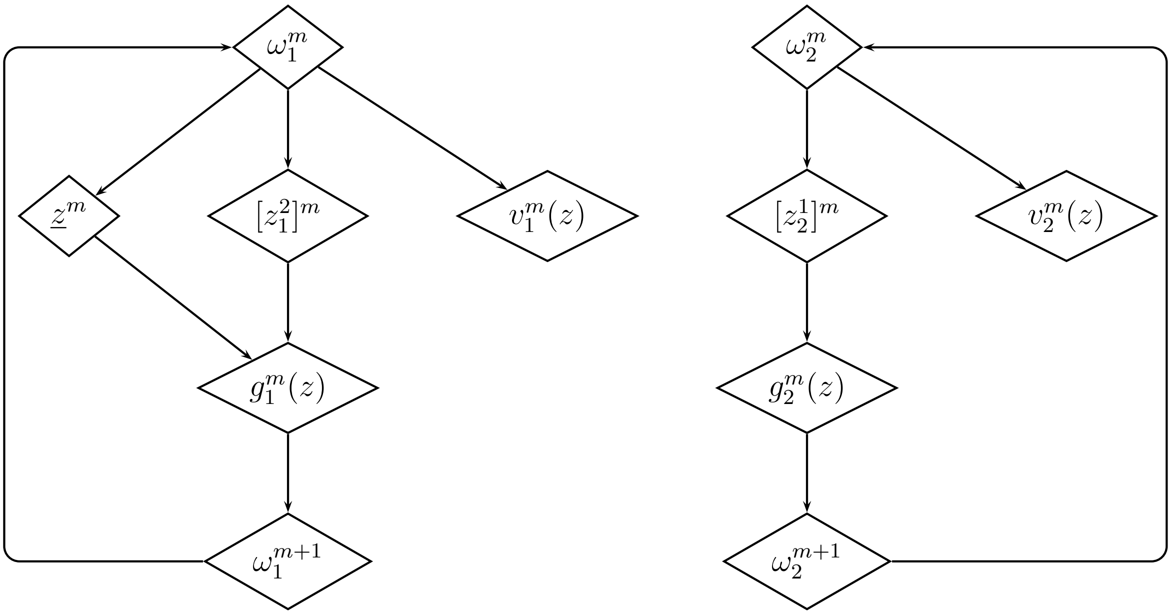

Figure 4.1: Sketch of the algorithm to compute the equilibrium solution in the two sector problem

Table 4.1: Macroeconomic parameters for two productive sectors

Symbol	Value	Description
e	1.53	Utility parameter
ρ	0.05	Discount rate
μ_1	-0.08	Small establishment productivity drift
σ_1^2	0.02	Small establishment productivity volatility
μ_2	-0.04	Large establishment productivity drift
σ_2^2	0.01	Large establishment productivity volatility
s	0	Scrap value
s_2^1	3	Large-to-small establishment policy
s_1^2	7	Small-to-large establishment policy
c_f	0.31	Fixed cost

All examples use the economic data in Table 4.1 and the upper limit $Z = 15$ in the productivity interval. Most parameters have been considered as in Section 2.1.2, while the large to small establishment policy $s_2^1 = 3$ and the small to large establishment policy $s_1^2 = 7$ are considered.

4.1.2.1 Example 8: The steady-state equilibrium with a prescribed entry productivity

In this example, we consider that new establishments for the first sector enter with a given productivity $\underline{z} < z_0^e < z_1^2$, so that $g^e(z) = \delta(z - z_0^e)$.

In Table 4.2, we show the obtained wages and the free boundary points separating the different regions that we obtain for three values of z_0^e. Notably, all values demonstrate an increase concerning z_0^e.

Table 4.2: Equilibrium wages and optimal exit productivities for different entry productivities in Example 8

z_0^e	ω_1	ω_2	$\underline{z}$	z_2^1	z_1^2
2	0.902241	1.679102	1.001250	2.780625	6.044375
3	1.085086	1.812918	1.204063	3.002188	7.269375
4	1.234449	1.911103	1.370000	3.164688	8.270000

Figure 4.2 illustrates the value function and firm density corresponding to $z_0^e = 3$. The blue line represents the value function for small establishments. Notably, for lower productivity values in this sector ($z \leq \underline{z}$), companies exit the economy and receive subsidies. Between specific productivity levels ($\underline{z} < z < z_1^2$), firms remain within the sector, transitioning to the sector of large establishments only when productivity reaches a sufficiently high threshold (z_1^2). The smooth pasting condition is evident at the two free boundaries that separate these distinct regions. On the other hand, the red line represents the value function for firms in the sector of large establishments.

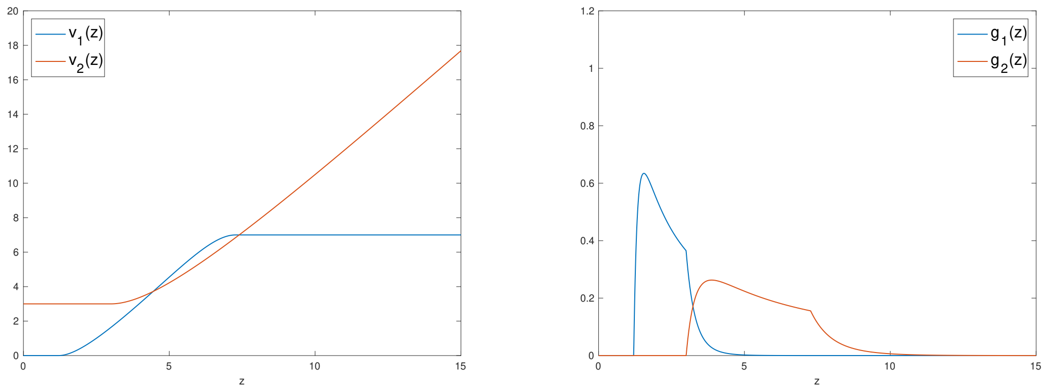

Figure 4.2: The value function (left) and the firm distribution (right) for $z_0^e = 3$ in Example 8

Here, companies either exit the economy for lower productivity values ($z \leq z_2^1$) or persist within the sector above a certain productivity threshold (z_2^1).

Additionally, Figure 4.2 represents the firm distribution in each sector. It is worth noting that for each sector, the kink in the firm distribution occurs at the productivity level at which companies enter the respective sector.

4.1.2.2 Example 9: The steady-state equilibrium with random entry productivities

In this example, we incorporate to the model the randomness in the entry productivity for the first sector by means of a discrete random variable. For this purpose, we consider a probability function of new establishments given by expression (1.19) with $I = 3$. In this case, we can rewrite the KFP PDE of (3.20) as follows:

$$\overline{\mu}_1 z \frac{\partial g_1}{\partial z}(z) - \frac{\sigma_1^2 z^2}{2} \frac{\partial^2 g_1}{\partial z^2}(z) + \overline{\lambda} g_1(z) = \frac{\sigma_1^2 \underline{z}}{2} \frac{\partial g_1}{\partial z}(\underline{z}) \sum_{i=1}^{3} p_i^e \delta(z - z_i^e), \qquad \forall z \in \hat{\mathcal{S}}_1, \quad (4.9)$$

where $\overline{\mu}_1 = \mu_1 - 2\sigma_1^2$ and $\overline{\lambda}_1 = \mu_1 - \sigma_1^2$.

In this setting, we will consider different choices for the productivities z_i^e and the associated probabilities p_i^e.

Table 4.3: Probabilities, wages and optimal exit productivities for $\mathbf{z^e} = (2,\ 3,\ 4)$ in Example 9

$\mathbf{p^e}$	ω_1	ω_2	$\underline{z}$	z_2^1	z_1^2
$(0.25, 0.5, 0.25)$	1.113406	1.832239	1.235625	3.034063	7.459063
$(0.1, 0.8, 0.1)$	1.095976	1.820359	1.216250	3.014375	7.342188
$(0.8, 0.1, 0.1)$	0.992964	1.747481	1.101875	2.893750	6.652188

As a first data set, we use $\mathbf{z^e} = (2,\ 3,\ 4)$ and $\mathbf{p^e} = (0.25,\ 0.5,\ 0.25)$. Next, we have chosen two additional data sets for $\mathbf{p^e}$ to illustrate the behaviour of the equilibrium solution in terms of the productivity at which entry of firms takes place and their associated probabilities. These computations allow us to obtain the equilibrium values of ω_1, ω_2, $\underline{z}$, z_2^1 and z_1^2 for these sets of parameters. In Table 4.3 these equilibrium values are shown.

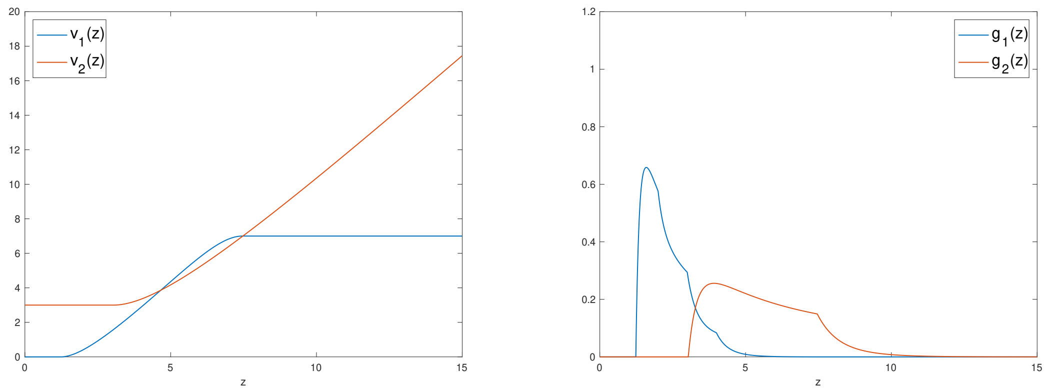

Figure 4.3: The value function (left) and the firm distribution (right) with $\mathbf{z^e} = (2,\ 3,\ 4)$ and $\mathbf{p^e} = (0.25,\ 0.5,\ 0.25)$ in Example 9

Next, in Figures 4.3, 4.4 and 4.5 we show the corresponding value functions and probability densities of firms for the different sets $\mathbf{p^e}$ that appear in Table 4.3. We notice kinks in the probability densities of firms, with three kinks present in the

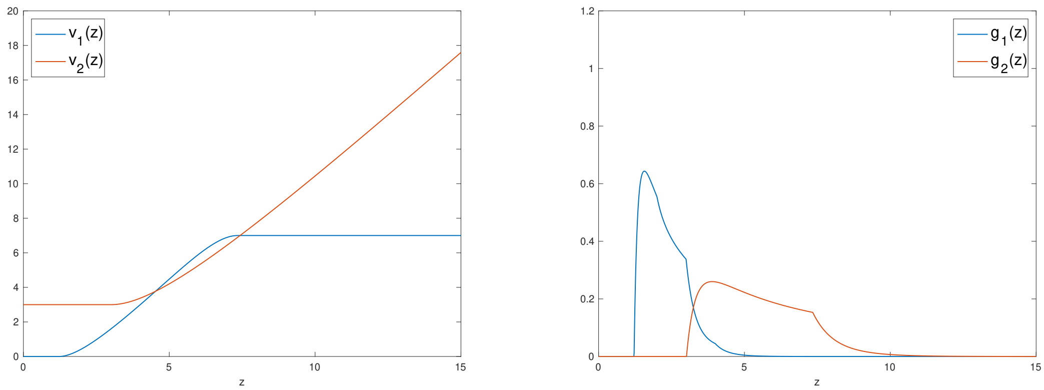

Figure 4.4: The value function (left) and the firm distribution (right) with $\mathbf{z^e} = (2, 3, 4)$ and $\mathbf{p^e} = (0.1, 0.8, 0.1)$ in Example 9

first sector –particularly, the kink associated with the highest probability is more pronounced– and one kink in the second sector. This results in a total of four kinks. Furthermore, the density functions exhibit singularity at z_i^e and z_1^2, attributed to the presence of delta functions.

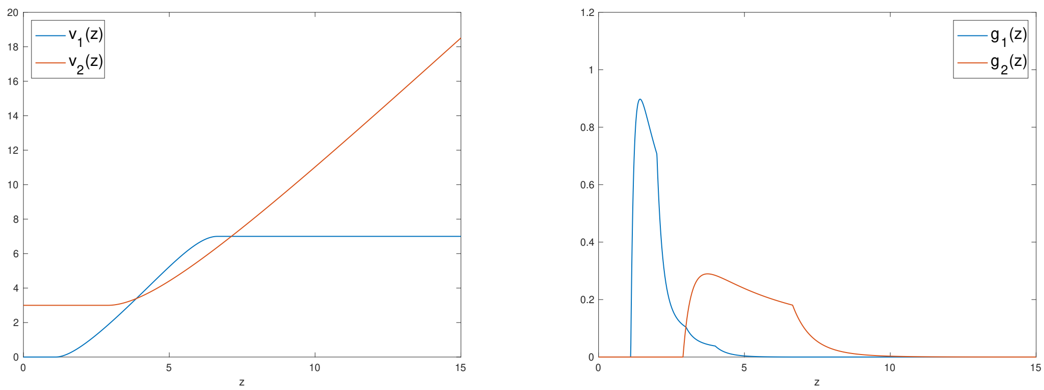

Figure 4.5: The value function (left) and the firm distribution (right) with $\mathbf{z^e} = (2, 3, 4)$ and $\mathbf{p^e} = (0.8, 0.1, 0.1)$ in Example 9

4.2 Numerical solution for the time-dependent PDEs problem

In this section we address the numerical solution of the time-dependent equilibrium problem, which is mainly defined by equations (3.5) and (3.17) for small establishments, and (3.6) and (3.18) for large establishments. Similar to the steady-state problem, in the time-dependent equilibrium, we utilize a fixed point iteration between the numerical solution of the involved problems.

As we aim to show the convergence of the solution of the time-dependent problem to the solution of the corresponding steady-state one, we consider as final conditions for (3.5) and (3.6) their solutions of their steady-state problem. Concerning the initial conditions to complete equations (3.17) and (3.18), we assume that they are related to the productivities at which establishments enter each sector.

We first describe the additional numerical methods we incorporate in the time-dependent problems and secondly we show some numerical examples to illustrate the performance of the proposed methodology.

4.2.1 Numerical methods

For the numerical solution of problems defined by equations (3.5), (3.6), (3.17) and (3.18), we propose a Crank-Nicolson scheme for the time discretization, which will be combined with the finite difference methods we used for the spatial discretization in the steady-state problems. For this aim, we propose a similar numerical strategy to Section 2.1.1.

4.2.1.1 Problem of evolutionary incumbent firms

As in Section 2.2.1.1, we propose utilizing a uniform mesh for spatial and time discretizations, so that we define $[v_1]_k^n$ and $[v_2]_k^n$ as the approximation of the solution of problems (3.5) and (3.6) at $\big(n\Delta t, k\Delta z\big)$, i.e. $[v_1]_k^n \approx v_1(t^n, z_k)$ and $[v_2]_k^n \approx v_2(t^n, z_k)$.

In order to approximate problems (3.5) and (3.6), we present the θ-method ($0 \leq \theta \leq 1$). Nevertheless, the Crank-Nicolson scheme ($\theta = 0.5$) will be used in the practice.

After some reordering of terms, we get for (t_θ^n, z_k), with with $t_\theta^n = (1-\theta)t^n + \theta t^{n+1}$, $k = 1, \ldots, N_z - 1$ and $n = 0, 1, \ldots, N_t - 1$, the expressions:

$$\mathcal{L}_\theta^{H,1}[v_1] \geq [\pi_1]_k^\theta,\ s^\theta \leq [v_1]_k^\theta \leq [s_1^2]^\theta,\ \left(\mathcal{L}_\theta^{H,1}[v_1] - [\pi_1]_k^\theta\right) \cdot ([v_1]_k^\theta - s^\theta) \cdot ([s_1^2]^\theta - [v_1]^\theta) = 0,$$
$$\mathcal{L}_\theta^{H,2}[v_2] \geq [\pi_2]_k^\theta, \quad [v_2]_k^\theta \geq [s_2^1]^\theta, \quad \left(\mathcal{L}_\theta^{H,2}[v_2] - [\pi_2]_k^\theta\right) \cdot ([v_2]_k^\theta - [s_2^1]^\theta) = 0,$$

such that

$$[v_i]_k^\theta = \theta[v_i]_k^n + (1-\theta)[v_i]_k^{n+1}, \quad [\pi_i]_k^\theta = \theta[\pi_i]_k^n + (1-\theta)[\pi_i]_k^{n+1},$$
$$s^\theta = \theta s^n + (1+\theta)s^{n+1},\ [s_1^2]^\theta = \theta[s_1^2]^n + (1+\theta)[s_1^2]^{n+1},\ [s_2^1]^\theta = \theta[s_2^1]^n + (1+\theta)[s_2^1]^{n+1},$$

where $[\pi_i]_k^n = \pi(t^n, z_k)$, $s^n = s(t^n)$, $[s_1^2]^n = s_1^2(t^n)$ and $[s_2^1]^n = s_2^1(t^n)$. Moreover, the involved operator is defined by:

$$\mathcal{L}_\theta^{H,i}[v_i] = \frac{[v_i]_k^n - [v_i]_k^{n+1}}{\Delta t} + \theta[\mathcal{L}^{H,i}]_k^n[v_i] + (1-\theta)[\mathcal{L}^{H,i}]_k^{n+1}[v_i],$$

where

$$[\mathcal{L}^{H,i}]_k^n[v_i] = \left[\frac{\mu_i(t^n, z_k)}{\Delta z} - \frac{\sigma_i^2(t^n, z_k)}{2(\Delta z)^2}\right][v_i]_{k-1}^n + \left[\rho - \frac{\mu_i(t^n, z_k)}{\Delta z} + \frac{\sigma_i^2(t^n, z_k)}{(\Delta z)^2}\right][v_i]_k^n - \frac{\sigma_i^2(t^n, z_k)}{2(\Delta z)^2}[v_i]_{k+1}^n. \quad (4.10)$$

Moreover, the final and boundary conditions of (3.5) and (3.6) are approximated by:

$$[v_1]_k^{N_t} = v_T^1(z_k), \quad [v_1]_0^\theta = -c_f/\rho, \quad \theta\frac{\partial^2[v_1]_{N_z}^n}{\partial z^2} + (1-\theta)\frac{\partial^2[v_1]_{N_z}^{n+1}}{\partial z^2} = 0, \quad (4.11)$$

$$[v_2]_k^{N_t} = v_T^2(z_k), \quad [v_2]_0^\theta = -c_f/\rho, \quad \theta\frac{\partial^2[v_2]_{N_z}^n}{\partial z^2} + (1-\theta)\frac{\partial^2[v_2]_{N_z}^{n+1}}{\partial z^2} = 0, \quad (4.12)$$

where

$$\frac{\partial^2[v_i]_{N_z}^n}{\partial z^2} = \frac{2[v_i]_{N_z}^n - 5[v_i]_{N_z-1}^n + 4[v_i]_{N_z-2}^n - [v_i]_{N_z-3}^n}{(\Delta z)^2}, \quad i = 1, 2.$$

Therefore, previous discretizations lead to the sequence of discrete complementarity problems:

$$\begin{gathered} A_1^n V_1^n \geq f_1^{n+1}, \quad S^n \leq V_1^n \leq [S_1^2]^n, \\ \big((A_1^n V_1^n - f_1^{n+1})^t (V_1^n - S^n)\big) \cdot \big((A_1^n V_1^n - f_1^{n+1})^t ([S_1^2]^n - V_1^n)\big) = 0, \end{gathered} \tag{4.13}$$

$$A_2^n V_2^n \geq f_2^{n+1}, \quad V_2^n \geq [S_2^1]^n, \quad (A_2^n V_2^n - f_2^{n+1})^t ([S_2^1]^n - V_2^n) = 0, \tag{4.14}$$

which are sequentially solved for $n = N_t - 1, N_t - 2, \ldots, 1, 0$. Note that the components of vector V_i^n are the value function at the productivity nodes for time t^n, the matrix A_i^n only depends on n when the functions μ_i and σ_i depend on time, $S^n = S(t^n)$, $[S_2^1]^n = S_2^1(t^n)$ and $[S_1^2]^n = S_1^2(t^n)$, and f_i^{n+1} depends on the previously computed vector V_i^{n+1}, $i = 1, 2$.

In order to solve problems (4.13) and (4.14) we propose the use of the ALAS algorithm at each time step. Algorithm 1 is used to solve the PDE problem related to small establishments (4.13), while Algorithm 2 is implemented to obtain the numerical solution of the PDE problem for large establishments (4.14).

4.2.1.2 Problem of evolutionary firm distribution

In this problem, we consider the computational domain for small establishments:

$$\Omega_Z = [\mathcal{E}_1]_Z \cup [\mathcal{S}_1]_Z \cup [\mathcal{E}_1^2]_Z,$$

where $[\mathcal{E}_1]_Z = [0, T] \times [0, \underline{z}(t)]$, $[\mathcal{S}_1]_Z = [0, T] \times (\underline{z}(t), z_1^2(t))$ and $[\mathcal{E}_1^2]_Z = [0, T] \times [z_1^2(t), Z]$. Similarly, for large establishments:

$$\Omega_Z = [\mathcal{E}_2^1]_Z \cup [\mathcal{S}_2]_Z,$$

where $[\mathcal{E}_2^1]_Z = [0, T] \times [0, z_2^1(t)]$ and $[\mathcal{S}_2]_Z = [0, T] \times (z_2^1(t), Z]$.

Therefore, for small establishments, we impose $g_1(z, t) = 0$ on $[\mathcal{E}_1]_Z$ and $[\mathcal{E}_1^2]_Z$, and pose the PDE of (3.17) on $[\mathcal{S}_1]_Z$, while for large establishments we impose $g_2(z, t) = 0$ on $[\mathcal{E}_2^1]_Z$ and pose the PDE of (3.18) on $[\mathcal{S}_2]_Z$. Moreover, we assume $g_1^0(z)$ and $g_2^0(z)$

are the initial probability functions, which are given in all examples by:

$$
\begin{aligned}
g_1^0(z) &= \frac{1}{\nu\sqrt{2\pi}} \sum_{i=1}^{I} p_i \, e^{-\frac{(z-z_i^e)^2}{2\nu^2}}, \quad \text{with} \quad \sum_{i=1}^{I} p_i = 1, \\
g_2^0(z) &= \frac{1}{\nu\sqrt{2\pi}} e^{-\frac{(z-z_1^2)^2}{2\nu^2}}.
\end{aligned} \tag{4.15}
$$

Let us denote by $[g_1]_k^n$ and $[g_2]_k^n$ the approximation to the solution of problems (3.17) and (3.18) at the point $(n\Delta t, k\Delta z)$, i.e. $[g_k^n]^1 \approx g_1(t^n, z_k)$ and $[g_k^n]^2 \approx g_2(t^n, z_k)$. Let $z_{\widetilde{k}}^n$, $z_{k_1^2}^n$ and $z_{k_2^1}^n$ be approximations of optimal exit productivities, i.e. $z_{\widetilde{k}}^n \approx \underline{z}(t^n)$, $z_{k_1^2}^n \approx z_1^2(t^n)$ and $z_{k_2^1}^n \approx z_2^1(t^n)$.

Although we describe the θ-method for the time discretization, in practice we use Crank-Nicolson ($\theta = 0.5$). After some reordering of terms, we get for (t_θ^n, z_k), with $t_\theta^n = (1-\theta)t^n + \theta t^{n+1}$, $n = 0, 1, \ldots, N_t - 1$, the expressions:

$$
\mathcal{L}_\theta^{K,1}[g_1] = \frac{\sigma_1^2(t^n, z_{\hat{k}}^n)}{2} \frac{\partial g_1}{\partial z}(t^n, z_{\hat{k}}^n) g^e(t^n, z_k), \qquad k = \widetilde{k}+1, \ldots, k_1^2 - 1, \tag{4.16}
$$

$$
\mathcal{L}_\theta^{K,2}[g_2] = \frac{\sigma_2^2(t^n, z_{k_2^1}^n)^2}{2} \frac{\partial g_2}{\partial z}(t^n, z_{k_2^1}^n) \delta(z_k - z_{k_1^2}^n), \qquad k = k_2^1 + 1, \ldots, N_z - 1, \tag{4.17}
$$

such that

$$
\mathcal{L}_\theta^{K,i}[g_i] = \frac{[g_i]_k^{n+1} - [g_i]_k^n}{\Delta t} + (1-\theta)[\mathcal{L}^{K,i}]_k^n + \theta[\mathcal{L}^{K,i}]_k^{n+1}, \quad i = 1, 2,
$$

where

$$
\begin{aligned}
[\mathcal{L}^{K,i}]_k^n[g_i] = &- \left[\frac{\sigma_i^2(t^n, z_{k-1})}{2\Delta z} + [\mu_i(t^n, z_{k-1})]^+ \right] [g_i]_{k-1}^n \\
&+ \left[\frac{\sigma_i^2(t^n, z_k)}{\Delta z} + [\mu_i(t^n, z_k)]^+ - [\mu_i(t^n, z_k)]^- \right] [g_i]_k^n \\
&- \left[\frac{\sigma_i^2(t^n, z_{k+1})}{2\Delta z} - [\mu_i(t^n, z_{k+1})]^- \right] [g_i]_{k+1}^n, \qquad i = 1, 2.
\end{aligned} \tag{4.18}
$$

Equation (4.16) is completed with $[g_1]_k^{n+1} = 0$, for $k = 0, \ldots, \widetilde{k}, k_1^2, \ldots, N_Z$ and the initial condition is approximated by $[g_1]_k^0 = g_1^0(z_k)$, while equation (4.17) is completed with $[g_2]_k^{n+1} = 0$, for $k = 0, \ldots, k_2^1$ and the initial condition is approximated by $[g_2]_k^0 = g_2^0(z_k)$.

After the previous discretizations, the fully discretized problems can be written in a matrix form and the resulting linear systems at each time step are solved.

4.2.1.3 Evolutionary equilibrium problem

Given functions $\mu_1(t,z)$, $\mu_2(t,z)$, $\sigma_1(t,z)$, $\sigma_2(t,z)$, $s(t)$, $s_1^2(t)$ and $s_2^1(t)$, as well as the values for the parameters ρ, e and c_f. The Steffensen algorithm is proposed. This method is the natural generalization of the one used for the steady-state equilibrium. Thus, we start with $\omega_1^0(t)$ and $\omega_2^0(t)$ given and for $m = 0, 1, 2, \ldots$ we follow:

1. Given the wages $\omega_1^m(t)$ and $\omega_2^m(t)$ at the mesh points in time, we solve the backward in time HJB equations (3.5) and (3.6) with methods described in Section 4.2.1.1 using Crank-Nicolson ($\theta = 0.5$). Thus, we obtain the value function approximations v_1^m and v_2^m at the mesh points and the approximation of the optimal exit boundaries $\underline{z}^m(t)$, $[z_1^2]^m(t)$ and $[z_2^1]^m(t)$ at t^n, with $n = 0, 1, \ldots, N_t$.

2. Given $\underline{z}^m(t)$, $[z_1^2]^m(t)$ and $[z_2^1]^m(t)$, we solve the forward in time KFP problems (3.17) and (3.18) with methods detailed in Section 4.2.1.2 for $\theta = 0.5$. Thus, we obtain approximations of g_1^m and g_2^m at the mesh points.

3. Given g_1^m and g_2^m, we compute the wages $[\omega_1^m(t)]^1$ and $[\omega_2^m(t)]^1$ by using the implicit formulas from (3.23).

4. Given the wages $[\omega_1^m(t)]_1$ and $[\omega_2^m(t)]_1$, we repeat Steps 1 to 4 for calculating $[\omega_1^m(t)]_2$ and $[\omega_2^m(t)]_2$, and then update the wages by using the formula (4.8).

When the difference between two consecutive approximations of $\omega_1^m(t)$ and $\omega_2^m(t)$ is below a prescribed tolerance, we consider $\omega_1^m(t)$, $\omega_2^m(t)$, $\underline{z}\big(\omega_1^m(t)\big)$, $z_1^2\big(\omega_1^m(t)\big)$, $z_2^1\big(\omega_2^m(t)\big)$, $v_1\big(\omega_1^m(t)\big)$, $v_2\big(\omega_2^m(t)\big)$, $g_1\big(\omega_1^m(t)\big)$ and $g_2\big(\omega_2^m(t)\big)$ as the solution of the time-dependent equilibrium problem for two productive sectors.

4.2.2 Numerical results

We present two examples related to the ones considered in the steady-state case. As the main objective is to illustrate the convergence of the solutions of the evolutionary equilibrium problem to corresponding ones of the steady-state, we assume that the productivity dynamics follows a geometric Brownian motion, with parameters μ_1, μ_2, σ_1^2 and σ_2^2 given in Table 4.1.

4.2.2.1 Example 10: The time-dependent equilibrium with a prescribed entry productivity

In this example, we consider the time-dependent equilibrium model for two sectors and validate the proposed numerical solution with examples in Section 4.1.2.1. Although we have addressed the tests with all the values of z_0^e considered in Section 4.1.2.1, we just report here the results for $z_0^e = 3$. We use the same parameters as in the steady-state case and the initial condition for the distribution of firms problem is given by the choice $I = 1$, $p_1 = 1$ and $\nu = 0.44$ in expression (4.15).

Table 4.4: Wages and optimal exit productivities for $z_0^e = 3$ in the time-dependent Example 10

t	$\omega_1(t)$	$\omega_2(t)$	$\underline{z}(t)$	$z_2^1(t)$	$z_1^2(t)$
0	1.296225	2.208003	1.365000	3.481250	7.741875
3	1.141608	2.067062	1.241250	3.290000	7.358125
6	1.085398	1.940869	1.204375	3.135625	7.275000
9	1.087646	1.854473	1.206875	3.040000	7.279375
12	1.086915	1.817207	1.205625	3.003750	7.273750
15	1.085326	1.814473	1.204375	3.002813	7.271250
SS	1.085086	1.812918	1.204063	3.002188	7.269375

Table 4.4 shows the computed equilibrium values of the wages ω_1 and ω_2, and optimal exit productivities $\underline{z}$, z_2^1 and z_1^2, for times $t = 0$, 3, 6, 9, 12 and 15, jointly with the values obtained for the steady-state (SS) equilibrium model in the last row. The results in this table illustrate the convergence of the values corresponding to the time dependent case to those ones of the steady state solution.

Analogous convergences have been observed for the different choices of z_0^e.

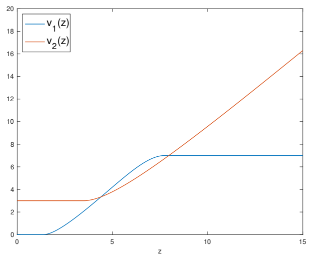

(a) $t = 0$

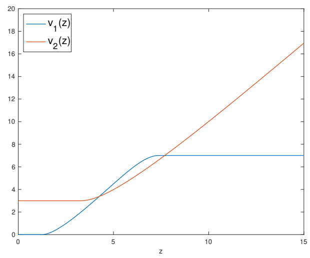

(b) $t = 3$

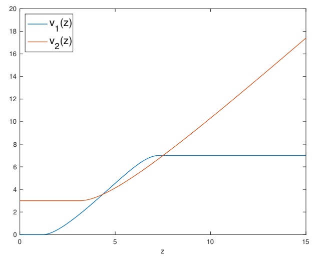

(c) $t = 6$

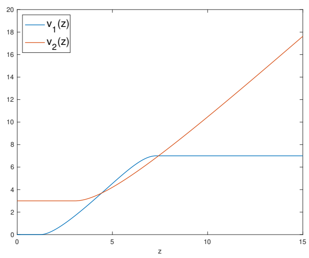

(d) $t = 9$

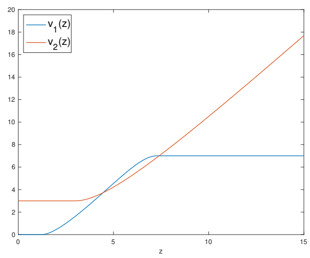

(e) $t = 12$

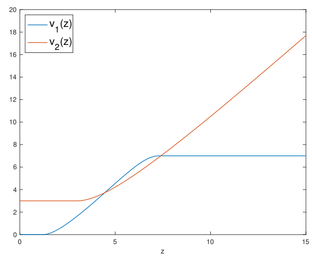

(f) $t = 15$

Figure 4.6: The time-dependent value function for $z_0^e = 3$ in Example 10

Next, in Figures 4.6 and 4.7 we show the time evolution of the value function and the probability density function of firms for small and large establishments, so that we can observe how the graphics for $T = 15$ are in agreement with the computed steady-state ones (see Figure 4.2).

4.2.2.2 Example 11: The time-dependent equilibrium with random entry productivities

We consider the time-dependent equilibrium model associated with the steady-state one posed in Section 4.1.2.2. Although we have addressed tests with all values considered in Section 4.1.2.1, we just report here the results for the choice $\mathbf{z^e} = (2, 3, 4)$ and $\mathbf{p^e} = (0.25, 0.5, 0.25)$. For this aim, we use the same parameters as in the steady-state case and the initial distribution of firms considering $I = 3$, $p_1 = 0.25$, $p_2 = 0.5$, $p_3 = 0.25$ and $\nu = 0.44$ in expression (4.15).

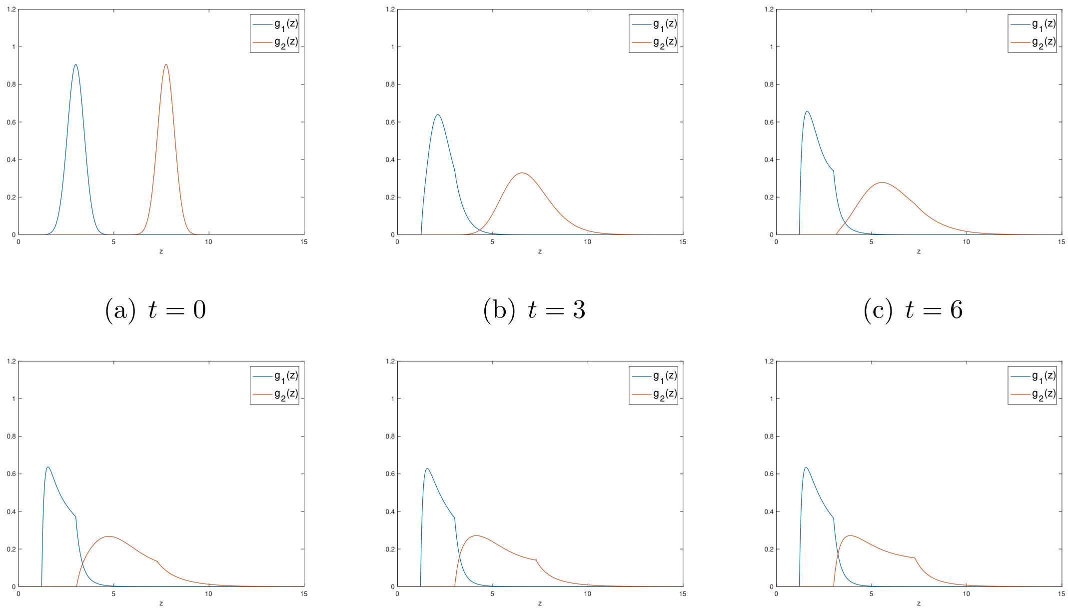

(a) $t = 0$ (b) $t = 3$ (c) $t = 6$

(d) $t = 9$ (e) $t = 12$ (f) $t = 15$

Figure 4.7: The time-dependent firm distribution for $z_0^e = 3$ in Example 10

Table 4.5: Wages and optimal exit productivities with $\mathbf{z^e} = (2, 3, 4)$ and $\mathbf{p^e} = (0.25, 0.5, 0.25)$ in the time-dependent Example 11

t	$\omega_1(t)$	$\omega_2(t)$	$\underline{z}(t)$	$z_2^1(t)$	$z_1^2(t)$
0	1.296226	2.237837	1.390625	3.525000	7.933750
3	1.181676	2.095116	1.285000	3.331875	7.586250
6	1.122137	1.966319	1.240625	3.173125	7.467500
9	1.112114	1.875731	1.234375	3.072500	7.456875
12	1.113379	1.835113	1.235625	3.033125	7.460000
15	1.113571	1.828637	1.235625	3.028125	7.460000
SS	1.113406	1.832239	1.235625	3.034063	7.459063

Table 4.5 shows the computed wages and optimal exit productivities for specific times $t = 0$, 3, 6, 9, 12 and 15, jointly with the values obtained for the steady-state

equilibrium model in the last row for comparison.

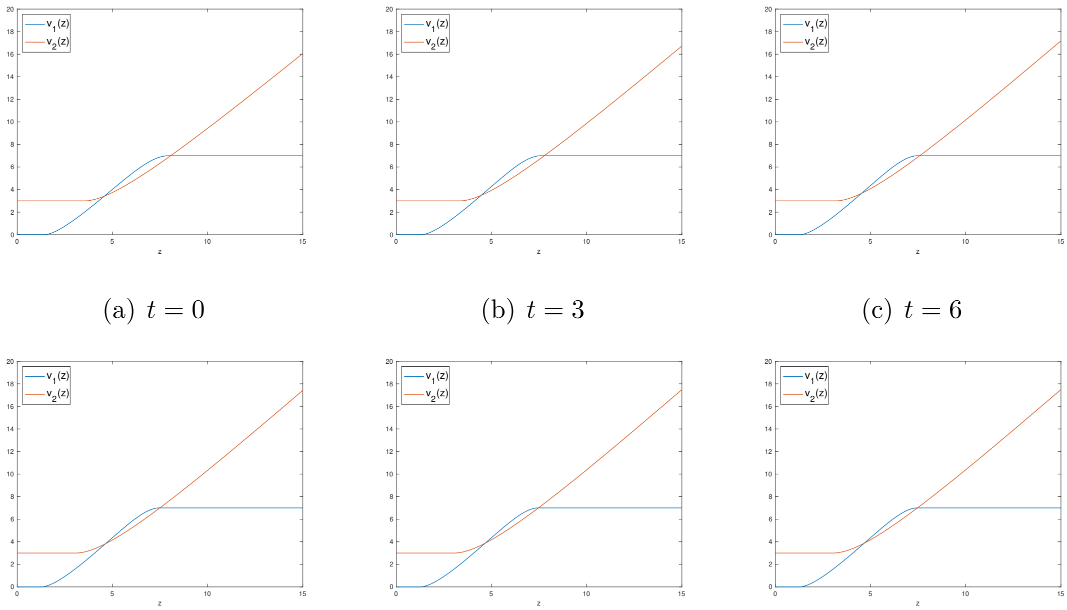

(a) $t = 0$ (b) $t = 3$ (c) $t = 6$

(d) $t = 9$ (e) $t = 12$ (f) $t = 15$

Figure 4.8: The time-dependent value function with $\mathbf{z^e} = (2, 3, 4)$ and $\mathbf{p^e} = (0.25, 0.5, 0.25)$ in Example 11

Next, in Figures 4.8 and 4.9 we show the time evolution of the value function and the probability density function of firms for small and large establishments. Similar to the previous example, a strong alignment is noticeable between $T = 15$ and the steady-state case (see Figure 4.3).

Remark 4.2.1. *All computations in Sections 4.1.2 and 4.2.2 are obtained with a MATLAB implementation of the algorithms. The numerical solution of the evolutionary equilibrium problem with* 24001×12001 *mesh takes around 8000 seconds, while the stationary equilibrium problem with* 48001 *mesh points takes around 70 seconds on a MacBook Pro laptop. The CPU we use is a Apple M2 Chip with 8 GB RAM.*

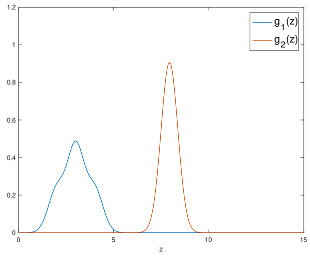

(a) $t = 0$

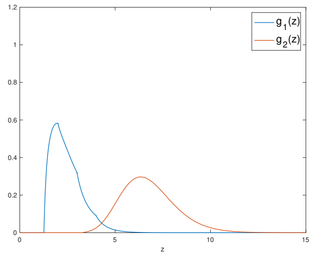

(b) $t = 3$

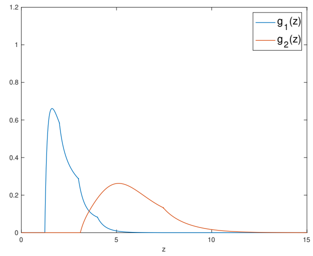

(c) $t = 6$

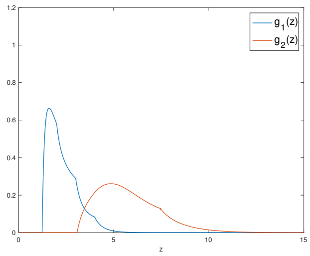

(d) $t = 9$

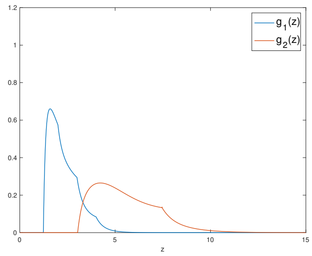

(e) $t = 12$

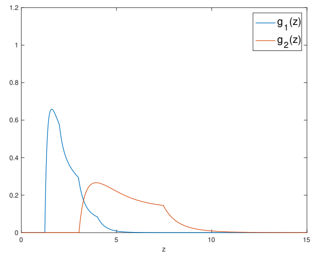

(f) $t = 15$

Figure 4.9: The time-dependent firm distribution with $\mathbf{z^e} = (2, 3, 4)$ and $\mathbf{p^e} = (0.25, 0.5, 0.25)$ in Example 11

4.3 Numerical solution for the steady-state PIDEs problem

This section is devoted to describe the numerical solution of the steady-state equilibrium problem, which is defined by the PIDEs represented as (3.31) and (3.37) for the first sector, and (3.32) and (3.38) for the second sector, jointly with the implicit equations given in (3.41). As previous sections, the use of a fixed-point iteration technique is considered to obtain the numerical solution for the problems outlined by these equations.

Firstly, we introduce the numerical methods utilized in this process. Next, we present various numerical examples to show the effectiveness and performance of the proposed methodology.

4.3.1 Numerical methods

Following the approach used in Section 4.1.1, we focus on the numerical strategy for solving the HJB and KFP PIDEs. Our approach includes: a finite differences scheme for discretization in the productivity domain and the ALAS algorithm to address the free boundary problems (3.31) and (3.32). Moreover, the AB scheme has been incorporated.

4.3.1.1 Problem of stationary incumbent firms

For the numerical solution, we propose the ALAS algorithm to solve the bilateral obstacle problem (3.31) and the unilateral obstacle problem (3.32), with a finite difference scheme for discretization in the productivity domain. Moreover, the AB method has been incorporated to explicitly handle integral terms that arise in the PIDEs.

As Section 4.1.1.1, we propose a uniform grid for the spatial discretization, so that $[v^1]_k \approx v_1(z_k)$ and $[v^2]_k \approx v_2(z_k)$ represent the steady-state optimal firm values for small and large establishments at the grid points, respectively.

In order to approximate the incumbent problems (3.31) and (3.32) at the grid point z_k, where $k = 1, \dots, N_z - 1$, we employ (2.2) to approximate the first and second-order derivatives. After some reordering of terms, we obtain the following expressions for $k = 1, \dots, N_z - 1$:

$$
\begin{aligned}
&[\mathcal{L}_J^{H,1}]_k[v_1] \geq \pi_1^k, \quad s \leq v_k^1 \leq s_1^2, \quad \Big([\mathcal{L}_J^{H,1}]_k[v_1] - \pi_1^k\Big) \cdot (v_k^1 - s) \cdot (s_1^2 - v_k^1) = 0, \\
&[\mathcal{L}_J^{H,2}]_k[v_2] \geq \pi_2^k, \quad v_k^2 \geq s_2^1, \quad \Big([\mathcal{L}_J^{H,2}]_k[v_2] - \pi_2^k\Big) \cdot (v_k^2 - s_2^1) = 0,
\end{aligned}
$$

such that

$$
[\mathcal{L}_J^{H,i}]_k[v_i] = \mathcal{L}_k^{H,i}[v_i] - \lambda \int_{x_{\min}}^{x_{\max}} \frac{3F_k^m(v_i) - F_k^{m-1}(v_i)}{2} f(x)\, \mathrm{d}x, \quad i = 1, 2,
$$

where the involved operator $\mathcal{L}_k^{H,i}[\cdot]$ is defined in (4.1) and $F_k(v_i) = v_i\big(z_k + \beta(z_k, x)\big) - v_i(z_k) - \beta(z_k, x)\dfrac{\partial v_i}{\partial z}(z_k)$.

It is worth noting that the integral term is approximated using the AB scheme. Moreover, F^m and F^{m-1} come from previous fixed-point iterations. For the first iteration, the AB scheme simplifies to the explicit scheme.

Additionally, we approximate the boundary conditions of (3.31) and (3.32) by (4.2). Therefore, the fully discretized linear complementarity problem can be represented in matrix form as (4.3) and (4.4), considering

$$f_k^i = [\pi_i]_k + \lambda \int_{x_{\min}}^{x_{\max}} \frac{3F_k^m(v_i) - F_k^{m-1}(v_i)}{2} f(x)\,\mathrm{d}x, \qquad k = 1, \ldots, N_z - 1.$$

These matrix formulations represent the discretized problems, enabling efficient numerical solutions for each linear complementarity problem. To achieve this, we utilize the ALAS algorithms previously mentioned for addressing the PDEs problems.

4.3.1.2 Problem of stationary firm distribution

For the numerical solution of the steady-state firm distribution problems, we set $g_1(z) = 0$ on $[\hat{\mathcal{E}}_1]_Z$ and $[\hat{\mathcal{E}}_1^2]_Z$, and pose equation (3.37) on $[\hat{\mathcal{S}}_1]_Z$. Moreover, we set $g_2(z) = 0$ on $[\hat{\mathcal{E}}_2^1]_Z$ and pose equation (3.38) on $[\hat{\mathcal{S}}_2]_Z$.

As in Section 4.1.1.2, we discretize equations (3.37) and (3.38) at the grid points z_k, where $k = \widetilde{k}+1, \ldots, N_z - 1$. This is achieved by introducing (2.6). Thus, we have equations:

$$\begin{aligned}
[\mathcal{L}_J^{K,1}]_k[g_1] &= \frac{\sigma_1^2(z_{\widetilde{k}})}{2} \frac{\partial g_1^p}{\partial z}(z_{\widetilde{k}}) g^e(z_k), \qquad & k &= \widetilde{k} + 1, \ldots, k_1^2 - 1, \\
[\mathcal{L}_J^{K,1}]_k[g_2] &= \frac{\sigma_2^2(z_{k_2^1})}{2} \frac{\partial g_2^p}{\partial z}(z_{k_2^1}) \delta(z_k - z_1^2), & k &= k_2^1 + 1, \ldots, N_z - 1,
\end{aligned} \tag{4.19}$$

such that for the involved operator $\mathcal{L}_k^{K,i}[\cdot]$ defined in (3.22), we have:

$$[\mathcal{L}_J^{K,i}]_k[g_i] = \mathcal{L}_k^{K,i}[g_i] - \lambda \int_{x_{\min}}^{x_{\max}} \frac{3H_k^m(g_i) - H_k^{m-1}(g_i)}{2} f(x)\,\mathrm{d}x,$$

where $H_k(g_i) = g_i\big(z_k - \beta(z_k, x)\big) - g_i(z_k)$. Notably, the AB scheme is used to approximate the integral term and H^m comes from previous fixed-point iterations.

Additionally, previous equations are completed with $g_k^1 = 0$, for $k = 0, \ldots, \widetilde{k}, k_1^2, \ldots, N_z$, and $g_k^2 = 0$, for $k = 0, \ldots, k_2^1, N_z$.

The numerical strategy to solve the KFP PIDE problem for the first sector (3.37) has been detailed in Section 4.1.1.2, while the methodology for KFP PIDE problem for the second sector (3.38) was presented in Section 2.1.1.2. Therefore, the discretized problem for the first sector can be written as (4.7), considering $b^1_k = 0$, $k = 0, \dots, \widetilde{k}, N_z$, while for $k = \widetilde{k} + 1, \dots, k^2_1 - 1$

$$b^1_k = \frac{\sigma^2(z_{\widetilde{k}})}{2} \frac{\partial g^m_1}{\partial z}(z_{\widetilde{k}}) g^e(z_k) + \lambda \int_{x_{\min}}^{x_{\max}} \frac{3H^m_k(g_1) - H^{m-1}_k(g_1)}{2} f(x)\,\mathrm{d}x.$$

These formulations allows for efficient numerical solutions to each firm distribution problem.

4.3.1.3 Stationary equilibrium problem

Given the steady-state equilibrium with specified functions $\mu_1(z)$, $\mu_2(z)$, $\sigma_1(z)$, $\sigma_2(z)$ and $\beta(z)$, along with known parameter values s, s^2_1, s^1_2, ρ, e, c_f and λ, a Steffensen method is considered. As Section 4.1.1.3, we start with ω^0_1 and ω^0_2 given and for $m = 0, 1, 2, \dots$ the process proceeds as follows:

1. Using the current wages ω^m_1 and ω^m_2, solve the stationary HJB PIDEs (3.31) and (3.32) to obtain $\underline{z}^m$, $[z^2_1]^m$, $[z^1_2]^m$, v^m_1 and v^m_2. This step follows the methods outlined in Section 4.3.1.1.

2. Given $\underline{z}^m$, $[z^2_1]^m$ and $[z^1_2]^m$, solve the stationary KFP PIDEs (3.37) and (3.38) for g^m_1 and g^m_2 using the approach described in Section 4.3.1.2.

3. Calculate the wages $[\omega^m_1]_1$ and $[\omega^m_2]_1$ based on g^m_1 and g^m_2 using implicit formulas from (3.41).

4. Repeat Steps 1 to 4 to compute $[\omega^m_1]_2$ and $[\omega^m_2]_2$, and generate a new guess using the Steffensen formula given by (2.12).

Repeat the process until convergence is achieved or the desired accuracy is attained.

4.3.2 Numerical results

In this section, we consider that productivity follows a geometric Brownian motion with jumps. As a result, we have the following relationships for the functions involved: $\mu_1(z_t) = \mu_1 z_t$, $\mu_2(z_t) = \mu_2 z_t$, $\sigma_1(z_t) = \sigma_1 z_t$, $\sigma_2(z_t) = \sigma_2 z_t$ and $\beta(z_t) = \beta z_t$.

With these relationships, we can rewrite the steady-state versions of the HJB problems (3.31) and (3.32), and the KFP problems (3.37) and (3.38) by introducing the following operators:

$$\mathcal{L}_J^{H,i}[v_i] = \frac{\sigma_i^2 z^2}{2}\frac{\partial^2 v_i}{\partial z^2} + (\mu_i - \lambda\overline{\kappa}) z \frac{\partial v_i}{\partial z} - (\rho + \lambda) v_i + \lambda \int_{-\infty}^{+\infty} v_i(z + xz) f(x)\,\mathrm{d}x,$$
$$\mathcal{L}_J^{K,i}[g_i] = -\frac{\sigma^2 z^2}{2}\frac{\partial^2 g_i}{\partial z^2} + \overline{\mu}_i z \frac{\partial g_i}{\partial z} + \overline{\lambda}_i g_i - \lambda \int_{-\infty}^{+\infty} g_i(z - xz) f(x)\,\mathrm{d}x,$$

where $\overline{\mu}_i = \mu_i - 2\sigma_i^2$ and $\overline{\lambda}_i = \mu_i - \sigma_i^2 + \lambda$, $i = 1, 2$. The probability density function f and its expectation $\overline{\kappa}$ are defined according to the expressions (1.44)–(1.46), taking into account either the Merton model or the Kou model.

In this context, we provide numerical results for two examples. These tests are conducted using the parameters listed in Table 4.6 and the upper limit $Z = 15$ in the productivity interval is considered. All parameters used in this Section have been adopted from Table 2.12 and Table 4.1.

4.3.2.1 Example 12: The steady-state equilibrium with a entry productivity

In this example, we assume that new establishments enter to the first productive sector with a predetermined productivity level denoted as z_0^e, such that $\underline{z} < z_0^e < z_1^2$. Therefore, we introduce the term $g^e(z) = \delta(z - z_0^e)$ in equation (3.37).

We begin by presenting the numerical solution for the case where $z_0^e = 3$. Tables 4.7 and 4.8 illustrate the numerical solutions, considering both the Merton and the Kou models. Note that as the mesh step becomes smaller, the values of ω_1, ω_2, $\underline{z}$, z_2^1 and z_1^2 tend to converge towards each other.

Table 4.6: Macroeconomic parameters for two productive sector jump-diffusion models

Symbol	Value	Description
e	1.53	Utility parameter
ρ	0.05	Discount rate
μ_1	-0.08	Small establishment productivity drift
σ_1^2	0.02	Small establishment productivity volatility
μ_2	-0.04	Large establishment productivity drift
σ_2^2	0.01	Large establishment productivity volatility
s	0	Scrap value
c_f	0.31	Fixed cost
λ	0.04	Poisson process parameter
ν_m	0.01	Mean of jump size (Merton)
γ_m	0.05	Standard desviation of jump size (Merton)
p	0.66	Probability of downward jump (Kou)
α_1	30.8	Parameter (Kou)
α_2	30.5	Parameter (Kou)

Table 4.7: Equilibrium wages and optimal exit productivities for $z_0^e = 3$ in the Merton model's Example 12

N_z	ω_1	ω_2	$\underline{z}$	z_2^1	z_1^2
6001	1.106551	1.874294	1.227500	3.102500	7.510000
12001	1.106831	1.874543	1.227500	3.102500	7.511250
24001	1.107257	1.874969	1.228750	3.103750	7.513750
48001	1.107329	1.875096	1.228750	3.104063	7.514375

Table 4.8: Equilibrium wages and optimal exit productivities for $z_0^e = 3$ in the Kou model's Example 12

N_z	ω_1	ω_2	$\underline{z}$	z_2^1	z_1^2
6001	1.102405	1.862784	1.222500	3.082500	7.450000
12001	1.102973	1.863387	1.223750	3.083750	7.453750
24001	1.103115	1.863645	1.223750	3.084375	7.455000
48001	1.103257	1.863840	1.224063	3.085000	7.455938

Moreover, we select three distinct values of z_0^e to show the solution's behavior concerning the productivity level at which new firms enter to the first sector. For both the Merton and Kou models, we observe how the values of ω_1, ω_2, $\underline{z}$, z_2^1 and z_1^2 increase in response to variations in z_0^e, as presented in Tables 4.9 and 4.10. Moreover, it is worth noting that, for the chosen parameters, the computed values obtained for the Merton model are slightly higher than those for the Kou model.

Table 4.9: Entry productivity, wages and optimal exit productivities in the Merton model's Example 12

z_0^e	ω_1	ω_2	$\underline{z}$	z_2^1	z_1^2
2	0.930077	1.762831	1.031875	2.918438	6.311563
3	1.107329	1.875096	1.228750	3.104063	7.514375
4	1.251783	1.959009	1.389063	3.243125	8.494688

Figures 4.10 and 4.11 show the value functions and the firm distributions for the aforementioned values of z_0^e. As observed in the PDEs case, the empirical regularity in the distribution of firms experiences a singular behaviour at the entry productivities z_0^e and z_1^2, displaying a kink-like behavior at that point. On the right tail ($z > z_0^e$ or $z > z_1^2$, for small and large establishments, respectively), we observe

an expected power law distribution. Moreover, when the value of z_0^e is increased, the probability density function for small establishments spreads across a wider range of productivities, resulting in a lower maximum. Indeed, the kink phenomenon becomes more pronounced as z_0^e assumes higher values.

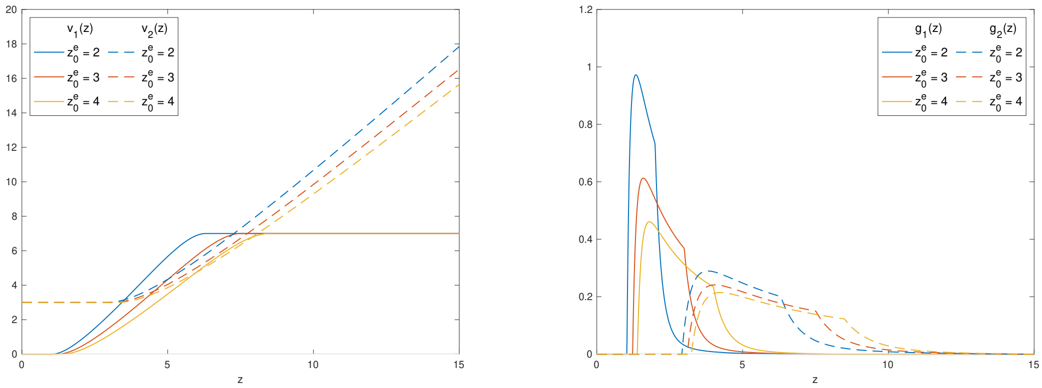

Figure 4.10: The value function (left) and the firm distribution (right) with the Merton model's Example 12

Table 4.10: Entry productivity, wages and optimal exit productivities in the Kou model's Example 12

z_0^e	ω_1	ω_2	$\underline{z}$	z_2^1	z_1^2
2	0.925003	1.748065	1.026250	2.893438	6.251250
3	1.103257	1.863840	1.224063	3.085000	7.455938
4	1.248626	1.950014	1.385313	3.227500	8.438437

Moreover, in comparison to a similar example with $z_0 = 3$ in the PDEs model associated with an Ito process that excludes jumps ($\lambda = 0$) illustrated in Figure 4.2, we observe a slightly lower value function in the PIDEs model. However, the computed wages and free boundaries are slightly higher in the PIDEs models (refer to Table 4.2). This outcome aligns with expectations since the presence of jumps

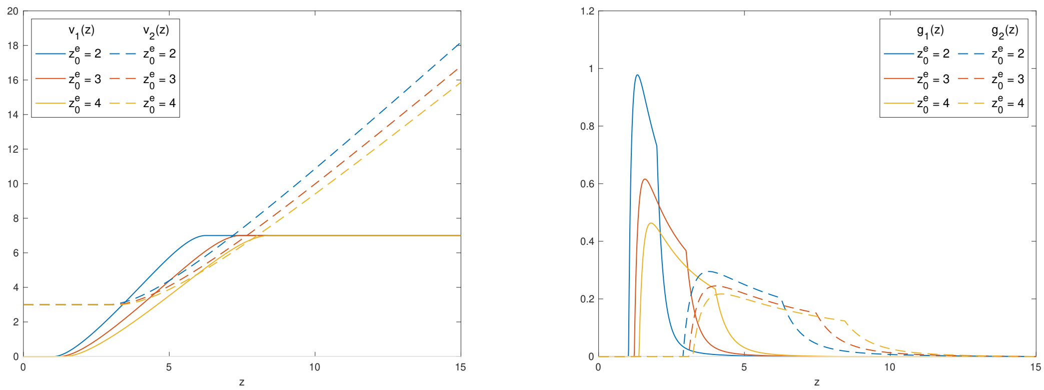

Figure 4.11: The value function (left) and the firm distribution (right) with the Kou model's Example 12

increases uncertainty in productivity.

Both Merton and Kou models notably influence the firm distribution, as depicted in Figure 4.2. The inclusion of jumps leads to a smoother spread of the probability density function across a broader range of productivities, resulting in a reduced maximum. Consequently, the significance of the kink phenomenon diminishes.

4.3.2.2 Example 13: The steady-state equilibrium with random entry productivities

In this example, we introduce randomness into the entry productivity in the steady-state version of the KFP problem (3.37). In particular, we consider a probability distribution for new establishments defined by the expression (1.19) with $I = 3$.

In this context, we will explore various combinations of entry productivities (z_i^e) and their associated probabilities (p_i^e).

As our initial dataset, we consider $\mathbf{z^e} = (2, 3, 4)$ and $\mathbf{p^e} = (0.25, 0.5, 0.25)$. In Tables 4.11, for the Merton model, we can observe that as the mesh size becomes finer, the values of ω_1, ω_2, $\underline{z}$, z_2^1 and z_1^2 tend to converge. The convergences for the Kou model have also been verified.

Table 4.11: Equilibrium wages and optimal exit productivities for $\mathbf{z^e} = (2, 3, 4)$ and $\mathbf{p^e} = (0.25, 0.5, 0.25)$ in the Merton model's Example 13

N_z	ω_1	ω_2	$\underline{z}$	z_2^1	z_1^2
6001	1.133619	1.890186	1.257500	3.127500	7.692500
12001	1.133893	1.890862	1.257500	3.130000	7.695000
24001	1.134341	1.891240	1.258750	3.130625	7.698125
48001	1.134406	1.891366	1.258750	3.131250	7.698125

Next, we take the finest mesh and present the previous results for the Merton model in Table 4.12. Moreover, we have included the results for $\mathbf{p^e} = (0.1, 0.8, 0.1)$ and $\mathbf{p^e} = (0.8, 0.1, 0.1)$ as in the steady-state PDEs model. Similarly, we provide numerical results for the Kou model in Table 4.13. Note that the values of ω_1, ω_2, $\underline{z}$, z_2^1 and z_1^2 are smaller in the case of the Kou model. Moreover, if we compare with the case without jumps, the absence of jumps provides smaller values of all magnitudes as illustrated by Table 4.3.

Table 4.12: Probabilities, wages and optimal exit productivities for $\mathbf{z^e} = (2, 3, 4)$ in the Merton model's Example 13

$\mathbf{p^e}$	ω_1	ω_2	$\underline{z}$	z_2^1	z_1^2
$(0.25, 0.5, 0.25)$	1.134406	1.891366	1.258750	3.131250	7.698125
$(0.1, 0.8, 0.1)$	1.117725	1.881395	1.240313	3.114688	7.585000
$(0.8, 0.1, 0.1)$	1.017800	1.819752	1.129375	3.012500	6.906875

In Figures 4.12 and 4.13, we present the computed value functions and firm density functions for both the Merton model and the Kou model. In the probability density function of firms for small establishments, we can observe a distinct kink at each possible entry productivity, resulting in a total of three kinks. The kink is more

Table 4.13: Probabilities, wages and optimal exit productivities for $\mathbf{z^e} = (2,\ 3,\ 4)$ in the Kou model's Example 13

$\mathbf{p^e}$	ω_1	ω_2	$\underline{z}$	z_2^1	z_1^2
$(0.25, 0.5, 0.25)$	1.130581	1.880599	1.254375	3.112813	7.640625
$(0.1, 0.8, 0.1)$	1.113720	1.870270	1.235625	3.095625	7.526563
$(0.8, 0.1, 0.1)$	1.013224	1.806826	1.124063	2.990625	6.847500

pronounced at the productivity with the highest probability. Moreover, at each entry productivity, the density function becomes singular, a consequence of employing combinations of delta functions in the source term g^e.

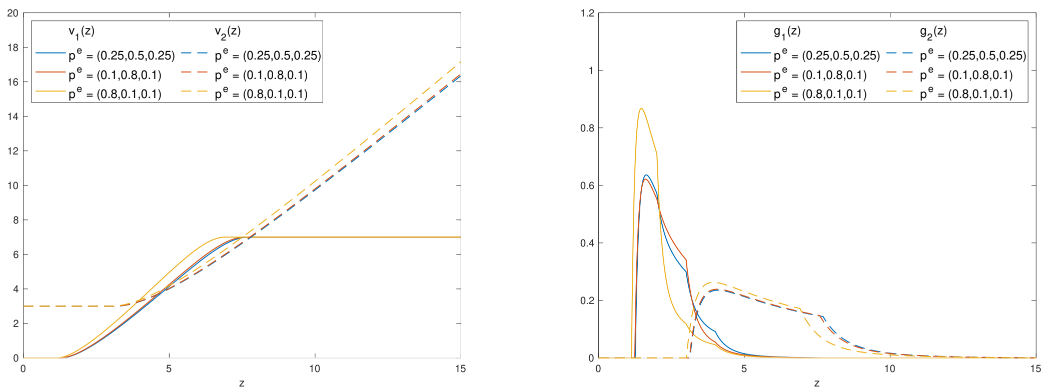

Figure 4.12: The value function (left) and the firm distribution (right) for $\mathbf{z^e} = (2,\ 3,\ 4)$ in the Merton model's Example 13

4.4 Numerical solution for the time-dependent PIDEs problem

In this section we address the numerical solution of the time-dependent equilibrium problem, which is mainly defined by equations (3.28) and (3.34) for small

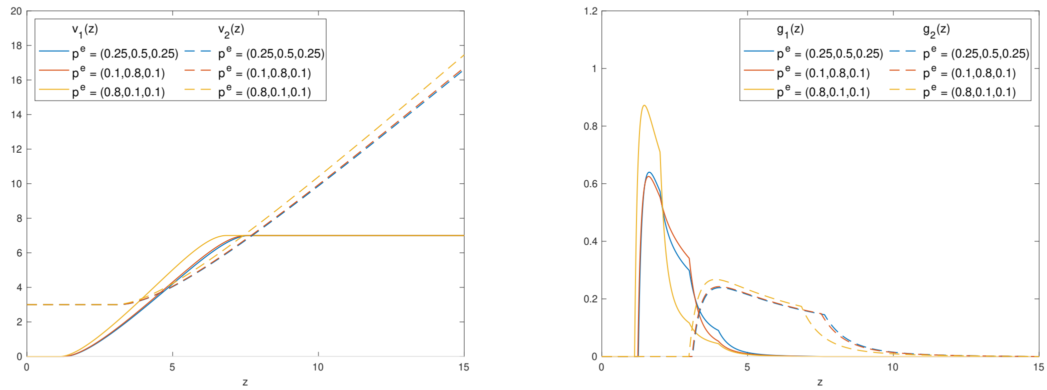

Figure 4.13: The value function (left) and the firm distribution (right) for $\mathbf{z^e} = (2, 3, 4)$ in the Kou model's Example 13

establishments, and (3.29) and (3.35) for large establishments. As in the steady-state problem, in the time-dependent equilibrium we pose a fixed point iteration between the numerical solution of the involved problems.

As we aim to show the convergence of the solution of the time-dependent problem to the solution of the corresponding steady-state one, we consider as final conditions for (3.28) and (3.29) their solutions of their steady-state problem. Concerning the initial conditions to complete equations (3.34) and (3.35), we assume that they are related to the productivities at which establishments enter each sector.

We first describe the additional numerical methods we incorporate in the time-dependent problems and secondly we show some numerical examples to illustrate the performance of the proposed methodology.

4.4.1 Numerical methods

For the numerical solution of problems defined by equations (3.28), (3.29), (3.34) and (3.35), we propose a Crank-Nicolson scheme for the time discretization, which will be combined with the finite difference methods we used for the spatial discretization in the steady-state problems. For this aim, we propose a similar numerical strategy to Section 4.1.1. Moreover, the AB scheme has been incorporated in order to treat integral terms explicitly.

4.4.1.1 Problem of evolutionary incumbent firms

As Section 4.2.1.1, we propose a uniform mesh for spatial and time discretizations, so that $[v_1]_k^n$ and $[v_2]_k^n$ representing the approximations of the solutions of problems (3.28) and (3.29) at the points (t^n, z_k).

To approximate problems (3.28) and (3.29) at the point (t_θ^n, z_k), where $k = 1, \ldots, N_z - 1$ and $n = 0, 1, \ldots, N_t - 1$, we introduce the θ-method ($0 \leq \theta \leq 1$). Nevertheless, the Crank-Nicolson scheme will be used in the practice.

After some reordering of terms, we get for (t_θ^n, z_k), with $k = 1, \ldots, N_z - 1$ and $n = 0, 1, \ldots, N_t - 1$, the expressions:

$$[\mathcal{L}_J^{H,1}]^\theta[v_1] \geq [\pi_1]_k^\theta, \quad s^\theta \leq [v_1]_k^\theta \leq [s_1^2]^\theta, \quad \Big([\mathcal{L}_J^{H,1}]_\theta^[v_1] - \pi_1^\theta\Big) \cdot (v_1^\theta - s) \cdot (s_1^2 - v_1^\theta) = 0,$$
$$[\mathcal{L}_J^{H,2}]_\theta[v_2] \geq [\pi_2]_k^\theta, \quad [v_2]_k^\theta \geq [s_2^1]^\theta, \quad \Big([\mathcal{L}_J^{H,2}]_\theta[v_2] - [\pi_2]_k^\theta\Big) \cdot ([v_2]_k^\theta - [s_2^1]^\theta) = 0,$$

such that $[v_i]_k^\theta$, $[\pi_i]_k^\theta$, s^θ, $[s_2^1]^\theta$ and $[s_1^2]^\theta$ are defined as in Section 4.2.1.1 and for the involved operator $[\mathcal{L}^{H,i}]^\theta[\cdot]$ given by (4.10), we have:

$$[\mathcal{L}_J^{H,i}]_k^n[v_i] = [\mathcal{L}^{H,i}]_k^n[v_i] - \lambda \int_{x_{\min}}^{x_{\max}} \frac{3F_k^{n+1}(v_i) - F_k^{n+2}(v_i)}{2} f(x)\,\mathrm{d}x, \quad i = 1, 2,$$

where $F_k^n(v_i) = v_i\big(t^n, z_k + \beta(t^n, z_k, x)\big) - v_i(t^n, z_k)\beta(t^n, z_k, x)\dfrac{\partial v_i}{\partial z}(t^n, z_k)$. Note that the AB scheme is applied.

Additionally, the final and boundary conditions for (3.28) and (3.29) are approximated by expressions (4.11) and (4.12), respectively. Thus, a fully discritized linear complementarity problem is represented as in (4.13) and (4.14).

After discretizing the time-dependent HJB formulations, we propose employing the ALAS algorithms previously mentioned in the context of PDEs for each time step.

4.4.1.2 Problem of evolutionary firm distribution

For small establishments, we impose $g_1(t,z) = 0$ on $[\mathcal{E}_1]_Z$ and $[\mathcal{E}_1^2]_Z$, and pose the PIDE of (3.34) on $[\mathcal{S}_1]_Z$, while for the large establishments, we impose $g_2(t,z) = 0$ on $[\mathcal{E}_2^1]_Z$ and pose the PIDE of (3.35) on $[\mathcal{S}_2]_Z$. Moreover, initial conditions for $g_1^0(z)$ and $g_2^0(z)$ are defined as in (4.15).

Moreover, to approximate problem (3.34) and (3.35), we utilize a time discretization method involving the θ-method. In practice, we will use Crank-Nicolson ($\theta = 0.5$) and the AB method.

After rearranging terms, we obtain a system of equations for (t_θ^n, z_k) which are solved sequentially for $n = 0, 1, \ldots, N_t - 1$:

$$[\mathcal{L}_J^{K,1}]^\theta[g_1] = \frac{\sigma_1^2(t^n, z_{\hat{k}}^n)}{2}\frac{\partial g_1}{\partial z}(t^n, z_{\hat{k}}^n) g^e(t^n, z_k), \qquad k = \widetilde{k} + 1, \ldots, k_1^2 - 1, \quad (4.20)$$

$$[\mathcal{L}_J^{K,2}]^\theta[g_2] = \frac{\sigma_2^2(t^n, z_{k_2^1}^n)^2}{2}\frac{\partial g_2}{\partial z}(t^n, z_{k_2^1}^n)\delta(z_k - z_{k_1^2}^n), \quad k = k_2^1 + 1, \ldots, N_z - 1, \quad (4.21)$$

such that for the involved operator $[\mathcal{L}^{K,i}]^\theta[\cdot]$ given by (3.19), we have:

$$[\mathcal{L}_J^{K,i}]^\theta[g_i] = [\mathcal{L}^{K,i}]^\theta[g_i] - \lambda \int_{x_{\min}}^{x_{\max}} \frac{3H_k^n(g_i) - H_k^{n-1}(g_i)}{2} f(x)\,\mathrm{d}x, \quad i = 1, 2,$$

where $H_k^n(g_i) = g_i\big(t^n, z_k - \beta(t^n, z_k, x)\big) - g_i(t^n, z_k)$.

Equation (4.20) is completed with $[g_1]_k^{n+1} = 0$, for $k = 0, \ldots, \widetilde{k}, k_1^2, \ldots, N_z$ and the initial condition is approximated by $[g_1]_k^0 = g_1^0(z_k)$, while the equation (4.21) is completed with $[g_2]_k^{n+1} = 0$, for $k = 0, \ldots, k_2^1, N_z$ and the initial condition is approximated by $[g_2]_k^0 = g_2^0(z_k)$.

The fully discretized problems can be written in matrix form, solving the resulting linear systems for each time step.

4.4.1.3 Evolutionary equilibrium problem

Given functions $\mu_1(t,z)$, $\mu_2(t,z)$, $\sigma_1(t,z)$, $\sigma_2(t,z)$, $\beta(t,z)$, $s(t)$, $s_1^2(t)$ and $s_2^1(t)$, along with fixed parameters ρ, e, c_f and λ. The Steffensen algorithm is proposed. We start with $\omega_1^0(t)$ and $\omega_2^0(t)$ given and for $m = 0, 1, 2, \ldots$, we follow:

1. Given the wages $\omega_1^m(t)$ and $\omega_2^m(t)$ at the mesh points in time, solve the backward-in-time HJB equations (3.28) and (3.29) using the Crank-Nicolson method ($\theta = 0.5$). This will yield the value function approximations v_1^m and v_2^m at the mesh points and the approximation of the optimal exit boundaries $\underline{z}^m(t)$, $[z_1^2]^m(t)$ and $[z_2^1]^m(t)$ at t^n for $n = 0, 1, \ldots, N_t$.

2. Given $\underline{z}^m(t)$, $[z_1^2]^m(t)$ and $[z_2^1]^m(t)$, solve the forward-in-time KFP problems (3.34) and (3.35) with $\theta = 0.5$. This will provide approximations of g_1^m and g_2^m at the mesh points.

3. Compute the wages $[\omega_1^m(t)]^1$ and $[\omega_2^m(t)]^1$ by employing the implicit formulas from (3.23).

4. Given the wages $[\omega_1^m(t)]^1$ and $[\omega_2^m(t)]^1$, we repeat Steps 1 to 4 for computing $[\omega_1^m(t)]_2$ and $[\omega_2^m(t)]_2$ and update the wages using (2.12).

When the difference between the current and previous approximations of $\omega_1^m(t)$ and $\omega_2^m(t)$ are smaller than the prescribed tolerance, the solution of the time-dependent equilibrium problem for two productive sectors is obtained.

4.4.2 Numerical results

This section discusses the time-dependent jump-diffusion equilibrium model for two productive sectors and provides validation for the proposed numerical solution. As the main objective is to illustrate the convergence of the solutions of the evolutionary equilibrium problem to corresponding ones of the steady-state, we assume that the productivity dynamics follows a geometric Brownian motion, with parameters μ_1, μ_2, σ_1^2, σ_2^2 and β given in Table 4.6.

4.4.2.1 Example 14: The time-dependent equilibrium with random entry productivities

In this example, the same parameters as those utilized in the steady-state case are considered and the initial condition for the distribution of firms is set to $I = 3$, with $\nu_0 = 0.44$ in expression (4.15).

Table 4.14: Wages and optimal exit productivities for $\mathbf{z^e} = (2, 3, 4)$ and $\mathbf{p^e} = (0.25, 0.5, 0.25)$ in the time-dependent Merton model's Example 14

t	$\omega_1(t)$	$\omega_2(t)$	$\underline{z}(t)$	$z_2^1(t)$	$z_1^2(t)$
0	1.296226	2.269128	1.398125	3.591250	8.137500
3	1.194054	2.134356	1.302500	3.407500	7.820625
6	1.143302	2.013059	1.265000	3.257500	7.718125
9	1.135650	1.930029	1.260000	3.166250	7.708750
12	1.136225	1.894864	1.260625	3.132500	7.710000
15	1.136257	1.890347	1.260625	3.129375	7.708750
SS	1.134436	1.891387	1.258828	3.131250	7.698281

Tables 4.14 and 4.15 provide a comprehensive overview of the computed wages and optimal exit productivities for both the Merton and Kou models at different times ($t = 0, 2.5, 5, 7.5, 10, 12.5$ and 15) for the case $\mathbf{z^e} = (2, 3, 4)$ and $\mathbf{p^e} = (0.25, 0.5, 0.25)$.

Moreover, same results have been illustrated for the choice $\mathbf{z^e} = (2, 3, 4)$ and $\mathbf{p^e} = (0.8, 0.1, 0.1)$ in Tables 4.16 and 4.17, for both Merton and Kou models. For all of them, we have included the values obtained for the steady-state equilibrium model in the last row for comparison.

Next, we have showcased the evolution of the value function and the probability distribution for both small and large establishments. Under $\mathbf{z^e} = (2, 3, 4)$, Figures 4.14 and 4.16 display this evolution for the Merton model with $\mathbf{p^e} = (0.5, 0.25, 0.5)$ and $\mathbf{p^e} = (0.8, 0.1, 0.1)$, respectively. Meanwhile Figures 4.15 and 4.17 illustrate

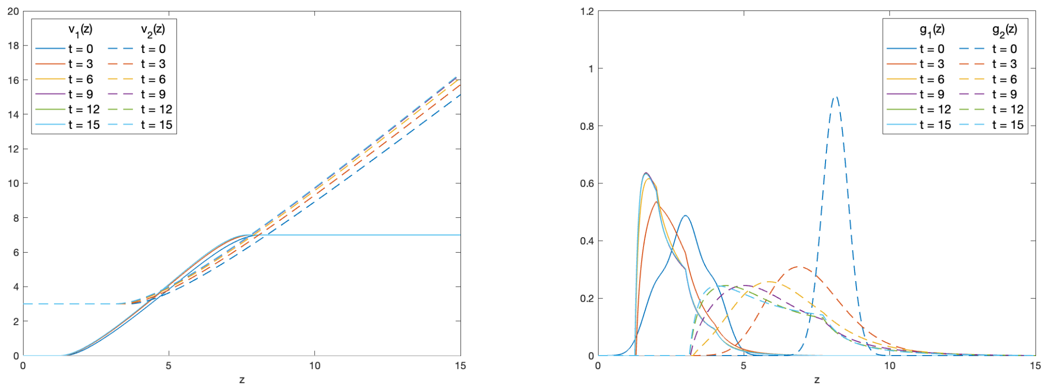

Figure 4.14: The time-dependent value function (left) and firm distribution (right) for $\mathbf{z^e} = (2, 3, 4)$ and $\mathbf{p^e} = (0.25, 0.5, 0.25)$ in Merton model's Example 14

Table 4.15: Wages and optimal exit productivities for $\mathbf{z^e} = (2, 3, 4)$ and $\mathbf{p^e} = (0.25, 0.5, 0.25)$ in the time-dependent Kou model's Example 14

t	$\omega_1(t)$	$\omega_2(t)$	$\underline{z}(t)$	$z_2^1(t)$	$z_1^2(t)$
0	1.296226	2.261199	1.396875	3.576250	8.085625
3	1.191936	2.125970	1.299375	3.391250	7.763750
6	1.139555	2.004171	1.260000	3.241875	7.658750
9	1.131207	1.920488	1.255000	3.149375	7.648750
12	1.131961	1.884610	1.255625	3.114375	7.650000
15	1.132032	1.879526	1.255625	3.110625	7.648750
SS	1.130591	1.880598	1.254375	3.112734	7.640625

the same for the Kou model. Notably, the graphics at $T = 15$ align with the computed steady-state representations (refer to Figures 4.12 and 4.13 for Merton and Kou models, respectively).

In Figure 4.18, the evolution with time of the free boundaries for the Merton (left), Kou (middle) and PDEs (right) models is presented for both sectors. This visualization allows us to observe the convergence of $\underline{z}(t)$, $z_1^2(t)$ and $z_2^1(t)$ towards

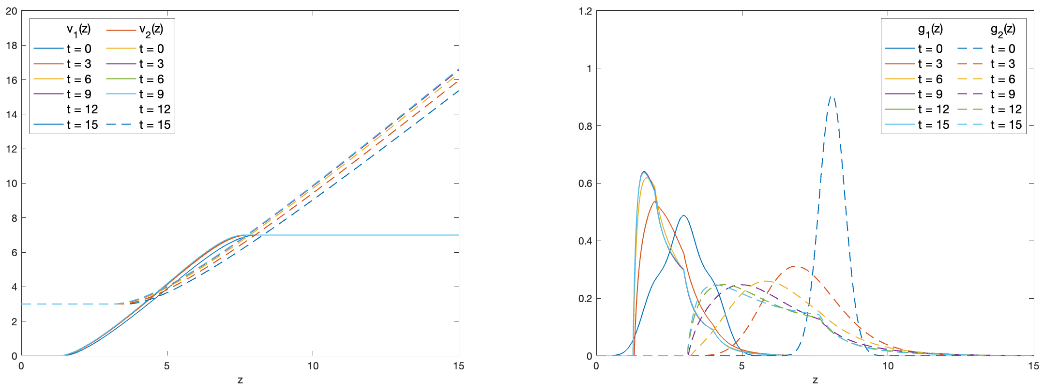

Figure 4.15: The time-dependent value function (left) and firm distribution (right) for $\mathbf{z^e} = (2, 3, 4)$ and $\mathbf{p^e} = (0.25, 0.5, 0.25)$ in the Kou model's Example 14

Table 4.16: Wages and optimal exit productivities for $\mathbf{z^e} = (2, 3, 4)$ and $\mathbf{p^e} = (0.8, 0.1, 0.1)$ in the time-dependent Merton model's Example 14

t	$\omega_1(t)$	$\omega_2(t)$	$\underline{z}(t)$	$z_2^1(t)$	$z_1^2(t)$
0	1.110345	2.121036	1.212500	3.191250	7.171250
3	1.051066	1.997167	1.156250	3.069375	6.993125
6	1.028555	1.892516	1.138125	3.040938	6.936875
9	1.021503	1.834538	1.132500	3.019610	6.920000
12	1.019481	1.822413	1.130625	3.014278	6.915000
15	1.018944	1.820165	1.130625	3.012500	6.913125
SS	1.017800	1.819752	1.129375	3.012500	6.906875

the steady-state case, as it is also numerically detailed in Table 4.14, Table 4.15 and Table 4.5. Notably, these free boundaries in the different modelling approaches exhibit a decreasing behaviour with respect to time until the curves transition into the corresponding straight line associated to the respective values of the steady state case.

Additionally, the corresponding exit regions for each productive sector are depicted

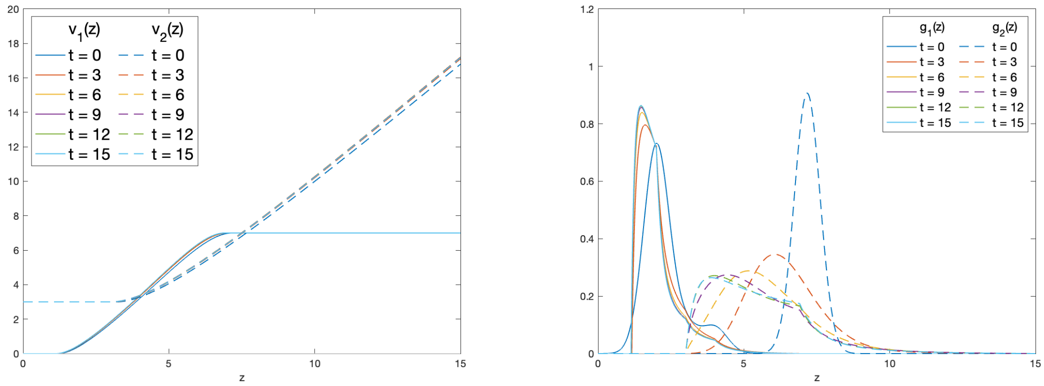

Figure 4.16: The time-dependent value function (left) and firm distribution (right) for the data $\mathbf{z^e} = (2,\ 3,\ 4)$ and $\mathbf{p^e} = (0.8,\ 0.1,\ 0.1)$ in Merton model's Example 14

Table 4.17: Wages and optimal exit productivities for $\mathbf{z^e} = (2,\ 3,\ 4)$ and $\mathbf{p^e} = (0.8,\ 0.1,\ 0.1)$ in the time-dependent Kou model's Example 14

t	$\omega_1(t)$	$\omega_2(t)$	$\underline{z}(t)$	$z_2^1(t)$	$z_1^2(t)$
0	1.110345	2.109220	1.211250	3.344375	7.123125
3	1.048644	1.985430	1.153125	3.182500	6.938125
6	1.024698	1.880820	1.133750	3.062500	6.878125
9	1.017036	1.823070	1.127500	3.005000	6.859375
12	1.014773	1.809504	1.125625	2.995000	6.854375
15	1.014136	1.807836	1.125000	2.992500	6.852500
SS	1.013224	1.806826	1.124063	2.990625	6.847500

in black, while stay regions are illustrated in white for each model.

Remark 4.4.1. *All computations in Sections 4.3.2 and 4.4.2 are obtained with a MATLAB implementation of the algorithms. The numerical solution of the evolutionary equilibrium problem with* 24001×12001 *mesh takes around 27000 seconds, while the stationary equilibrium problem with* 48001 *mesh points takes around 125*

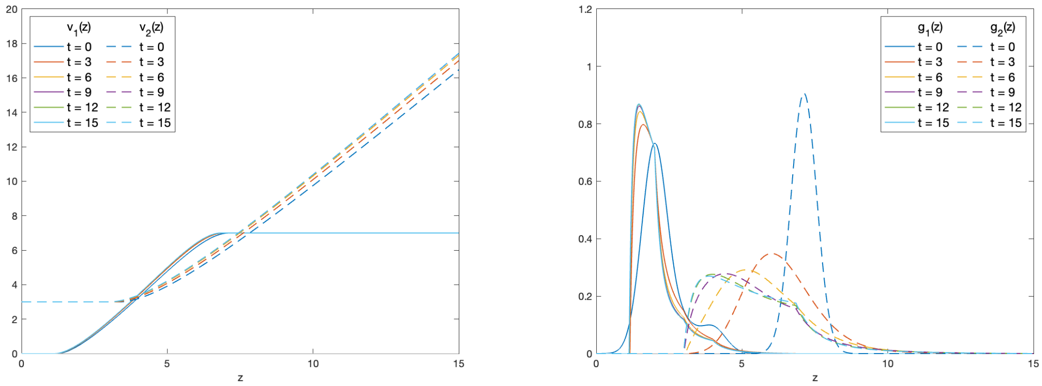

Figure 4.17: The time-dependent value function (left) and firm distribution (right) for the data $\mathbf{z^e} = (2, 3, 4)$ and $\mathbf{p^e} = (0.8, 0.1, 0.1)$ in the Kou model's Example 14

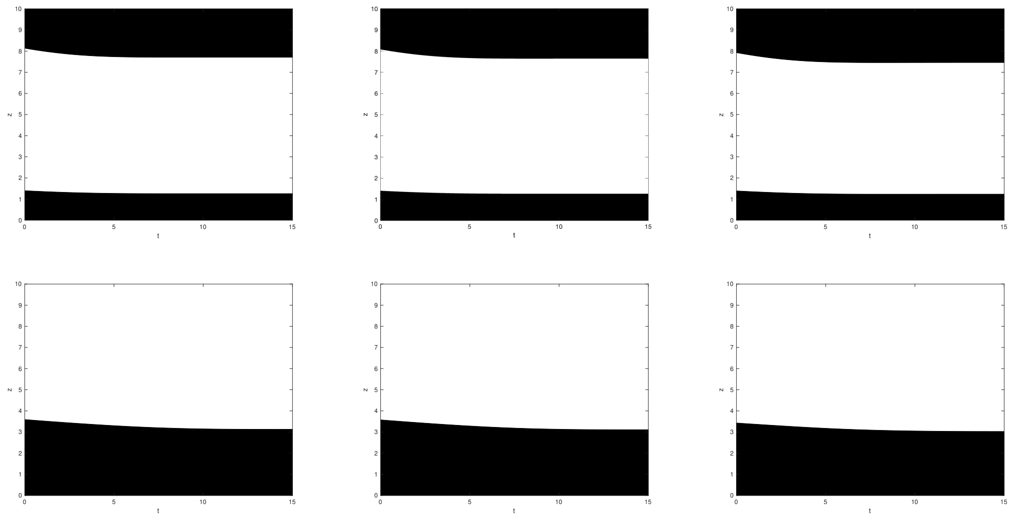

Figure 4.18: Approximated exit regions (in black) and stay regions (in white) for small (top) and large (bottom) establishments with Merton (left), Kou (middle) and PDEs (right) models based on the data $\mathbf{z^e} = (2,\ 3,\ 4)$ and $\mathbf{p^e} = (0.25,\ 0.5,\ 0.25)$

seconds on a MacBook Pro laptop. The CPU we use is a Apple M2 Chip with 8 GB RAM.

Conclusions

In this work we propose several original general equilibrium models for heterogeneous agents under rational expectations, allowing the possibility of exit or entry of new establishments. In the previous setting we consider problems posed in the presence of one sector or two sectors. In the case of one sector, the establishments that exit the sector just leave the economy and receive the subsidy. In the case of two sectors, the firms operating in the sector associated to small establishments can either leave the economy or move to the sector with large establishments after the payment of the conversion costs. In both cases, the model involves a problem of incumbent firms which is governed by HJB differential equations, a household problem, a problem that determines the probability distribution of firms which is governed by a KFP differential equation and a formulation of feasability conditions.

A first innovative aspect from the modelling point of view is related to the general definition of the stochastic dynamics of the productivity. Previous choices in the literature for this dynamics are based on Geometric Brownian motion or Ornstein-Uhlenbeck processes. In this work we propose to more general alternatives: a general Itô process or a Lévy process. While the first one implies that the paths of the stochastic productivity are continuous, the second one allow the possibility of jumps. Moreover, when considering the Itô process the models involve HJB and KFP partial differential equations (PDEs) while when considering Lévy processes we obtain the corresponding HJB and KFP partial integro-differential equations (PIDEs). Another innovative aspect is the possibility that firms enter the sector at a finite set of productivities with their corresponding probabilities, i.e., the probability density function of new establishments corresponds to a discrete random variable. This assumption also outperforms the assumption of entering at a prescribed deterministic productivity. In these more general modelling settings, even for the steady state problems we cannot obtain a semianalytical solution, so that numerical methods are mandatory to simulate the equilibrium models.

From the numerical simulation point of view, another relevant achievement comes from the proposal of appropriate numerical methods for solving the different subproblems that are involved in the several equilbrium problems that have been pose, either involving PDEs or PIDEs. In the steady state models, for the problems of incumbent firms that mainly consist of complementarity problems associated to HJB equations with one or two obstacles, we propose a combination of a finite differences schemes for discretization with an Augmented Lagrangian Active Set (ALAS) method for the nonlinearity related to the inequality constraints on the solution. For the problem of firms distribution suitable discretization methods for the KFP are proposed. For the time dependent problems we incorporate a time discretization based on a Crank-Nicholson scheme for the evolutive HJB and KFP equations. For those formulations involving PIDEs, the additional integral term is treated by an IMEX method based on an Adams-Bashford scheme for the integral term. Besides the previously enumerated methods for the differents subproblems, we propose a fixed point iteration for the equilibrium problems, which involves the sequential solution of the different subproblems at each iteration until convergence.

Numerical examples in these work have been designed to validate the numerical methods and the expected behaviour of the solutions of the different problems. For example, a semianalitical solution has been obtained for a particular steady state equilibrium problem and next validated by the proposed numerical methods. In all equilibrium problems, the convergence of the solution of the evolutive problem to the steady state one has been illustrated.

A main general conclusion is that as soon as we incorporate more general modelling issues and more general settings, the solution of the different equilibrium problems requires the use of appropriate numerical methods. The proposed set of numerical methods allows to obtain approximations of the solutions of the different mathematical models considered in this work, which provide the expected qualitative and quantitative behaviour. Although there is room to speed up the calculation, the computational times are reasonable, so that numerical algorithms seem fast enough and reliable.

Another conclusion is that the present work must be understood a scientific contribution to the study of stochastic models of general equilibrium with heterogeneous agents and opens the possibility of future research work in several directions.

First, concerning the equibrium models proposed in this work, the mathematical analysis to obtain the existence and uniqueness of solution is an open question that has not been addressed to our knowledge. Indeed, in [3] the authors point out that the existence and uniqueness of steady state and evolutive equilibrium models are open problems for stochastic processes different from the geometric Brownian motion. From the modelling point of view, a two factor model for productivity could be considered to incorporate stochastic volatility. A first possibility could be the Heston model. The author of the thesis has addressed this kind of models in the context of derivatives pricing in [6].

Secondly, concerning numerical methods, the use of machine learning methods based on physics-informed neural networks (PINNs) have been explored by using the methodology developed in [10] and [53]. Although the solution of some HJB and KFP PDE models have been obtained, the solution of the global equilibrium problem is a pending issue we hope to complete in the future.

Resumen extenso

En esta tesis estudiamos una clase de modelos de agentes heterogéneos de tiempo continuo con choques idiosincrásicos y mercados incompletos bajo expectativas racionales en un marco macroeconómico. Al igual que en Hopenhayn [30], consideramos una formulación de tiempo continuo en la que las empresas se enfrentan a choques idiosincrásicos de productividad. La evolución de la productividad es la única fuente subyacente de incertidumbre, modelada por un proceso estocástico tipo Itô o uno de Lévy. Suponemos que la industria está operada por agentes heterogéneos para relacionar los beneficios futuros (esperados) para las empresas, permitiendo la posibilidad de salida o entrada de nuevos establecimientos. En este escenario, consideramos problemas planteados en presencia de uno o dos sectores productivos. En el caso de un solo sector, los establecimientos que abandonan el sector simplemente salen de la economía y reciben subsidio. Sin embargo, en el caso de dos sectores, las empresas que operan en el sector asociado a pequeños establecimientos pueden salir de la economía o trasladarse al sector con grandes establecimientos después del pago de los costos de conversión.

En un marco macroeconómico de equilibrio general, el objetivo principal de esta tesis es proporcionar la modelización matemática tanto para los problemas de equilibrio estacionario como para los de equilibrio temporal, así como métodos numéricos adecuados para resolver los diferentes subproblemas involucrados en el problema de equilibrio global.

En primer lugar, nuestro estudio se centra en el problema de equilibrio que implica un sector productivo de la economía en un país. Al igual que en Weninger y Just

[55], asumimos que las habilidades de las empresas individuales siguen un proceso estocástico y que hay un costo operativo fijo para que las empresas permanezcan en la industria. Estas dos últimas suposiciones generan la evolución de la dinámica de las empresas a lo largo del tiempo. Por lo tanto, las decisiones racionales individuales no se basan solo en las ganancias actuales y toda la dinámica transitoria debe calcularse para capturar el comportamiento de las empresas y sus consecuencias en las variables económicas. Además, en vista de sus choques, las empresas deciden permanecer o salir. Las decisiones de salida se determinan de manera endógena por la decisión óptima en la que el costo de oportunidad de permanecer se tiene en cuenta mediante la existencia de un valor residual en el que las empresas abandonan la industria. Esta decisión se formula en términos de un problema de tiempo de parada óptimo. Además, las empresas que salen son reemplazadas por la entrada de nuevas empresas de manera que las tasas de salida y entrada se equilibren. De esta manera, la tasa de entrada de empresas también es endógena en niveles prescritos de productividad. En este sentido, consideramos dos ejemplos, un caso donde la entrada tiene lugar en una productividad dada por encima de la productividad óptima de salida, siguiendo a Luttmer [40], y un segundo caso donde las empresas ingresan en un conjunto finito de productividades con sus probabilidades correspondientes. Casos más generales podrían incorporarse mediante el uso de distribuciones de probabilidad adecuadas para la productividad de las empresas que entran. Además, en algunas industrias, estas productividades de entrada son proporcionadas exógenamente por modelos adecuados para incorporar los ingresos y, por lo tanto, los salarios y el trabajo (ver [16], por ejemplo, en el caso de pesquerías). A diferencia del trabajo de Guzzini y Pallestrini [29], no consideramos la interacción entre el shock idiosincrásico de las empresas y su estructura de red, lo que requeriría el uso de matrices de adyacencia de teoría de grafos para representar los vínculos entre las empresas.

Al igual que en Achdou et al. [3], asumimos que los individuos interactúan en mercados y toman decisiones para precios dados. Estos precios se determinan en un equilibrio general y dependen de toda la distribución de individuos en la economía y su evolución. Las decisiones de los individuos, junto con los choques idiosincrásicos, a su vez determinan la evolución de esta distribución. Los modelos matemáticos para tales economías pueden formularse principalmente en términos de un sistema de dos ecuaciones diferenciales parciales (EDPs) acopladas. Más precisamente, implican una EDP de Hamilton-Jacobi-Bellman (HJB) para el problema de empresas existentes, con restricciones de desigualdad de obstáculos en la solución. Esta ecuación de HJB hacia atrás en el tiempo caracteriza el valor óptimo de la función de utilidad asociada con la ganancia de la empresa a lo largo del tiempo con un proceso estocástico evolutivo de la productividad laboral. Además, una ecuación de Kolmogorov-Fokker-Planck (KFP) hacia adelante en el tiempo gobierna la evolución de la distribución de empresas. Cabe notar que el acoplamiento de estas dos ecuaciones para modelar el comportamiento de agentes heterogéneos se puede encuadrar en la teoría matemática de los Mean Field Games (MFG) desarrollada por Lasry y Lions en [39] y el sistema acoplado se conoce como un sistema MFG hacia atrás-adelante. Por ejemplo, este acoplamiento también surge en el modelo Aiyagari-Bewley-Hugget para caracterizar el ahorro óptimo y el comportamiento de consumo de individuos con ingresos estocásticos (ver Hugget [31] y Aiyagari [4], por ejemplo). Otras referencias adicionales de Mean Field Games son [8], [28], [27], por ejemplo. Se proponen métodos numéricos para el sistema MFG en [2]. Además, los modelos de equilibrio global se completan con el problema del hogar y las condiciones de viabilidad.

En nuestro modelo, las empresas individuales evalúan el valor esperado de permanecer en la industria en cada momento y lo comparan con el valor actual descontado de las ganancias asociadas con salir de la industria. Basándose en esta comparación, las empresas individuales deciden permanecer o salir de la industria. Tenga en cuenta que estos modelos con salida de empresas endógena también se investigan en el denominado marco de opciones reales (ver Dixit et al. [21], por ejemplo). Problemas análogos surgen en finanzas matemáticas, al valorar derivados financieros con oportunidades de ejercicio anticipado, como las opciones americanas (ver Wilmott et al. [56], por ejemplo).

En trabajos anteriores, como Luttmer [40] o Da-Rocha y Sempere [16], se asumió que el proceso estocástico de productividad sigue un movimiento Browniano geométrico y las nuevas empresas ingresan en una productividad dada por encima de la productividad de salida, de manera que en el caso de equilibrio estacionario podemos adaptar nuestro modelo para obtener una solución analítica para la ecuación KFP de un solo sector productivo y una solución semi-analítica para sus equilibrios. En general, las soluciones (semi-)analíticas para estas EDP no están disponibles. En Achdou et al. [1], los autores señalan que el desarrollo de métodos numéricos para resolver equilibrios estacionarios y dependientes del tiempo es una cuestión abierta cuando se consideran procesos estocásticos más generales que el movimiento Browniano geométrico para el problema de un solo sector productivo. Por lo tanto, nos enfocamos en el desarrollo de soluciones numéricas eficientes. Así, en el problema de las empresas existentes consideramos el uso del algoritmo de conjunto activo de Lagrangiano aumentado (ALAS) desarrollado en Kärkkäinen et al. [35] para resolver el problema de complementariedad lineal asociado con la ecuación HJB. Por ejemplo, en el contexto de problemas financieros, este algoritmo se ha utilizado en Bermúdez et al. [9] para la valoración de opciones de Amerasia, en Calvo et al. [13] para la valoración de planes de pensiones con jubilación anticipada y en Calvo et al. [11] para la valoración de opciones de tipo swing en mercados eléctricos. Para la ecuación KFP proponemos un método numérico adecuado y para el problema de equilibrio consideramos un método de Steffensen, desarrollado en [50], para acelerar la iteración de punto fijo, que proporciona convergencia de segundo orden en el algoritmo global. Además, los modelos dependientes del tiempo requieren métodos numéricos adicionales adecuados, por lo que incorporamos un esquema Crank-Nicolson para la discretización temporal que se combina con los métodos previamente indicados para los modelos de estado estacionario (ver Strikwerda [52], por ejemplo).

Además, la incorporación de saltos en la dinámica de la productividad sirve para modelar eventos significativos y abruptos que pueden tener un impacto profundo en los sistemas económicos. Tales eventos podrían incluir crisis globales, como se ha presenciado en los últimos años, con la pandemia de COVID-19 desde 2020, o eventos geopolíticos como la invasión de Ucrania en 2022, o burbujas en sectores específicos de la economía, que han tenido repercusiones en los mercados globales y sectores energéticos. Este enfoque de modelado, empleando procesos de difusión con saltos, está motivado por la necesidad de tener en cuenta estos eventos discretos e inesperados dentro del marco económico. Los modelos de difusión con saltos ya se han introducido en [22] para modelar la evolución del tamaño de una unidad económica, como una empresa o una ciudad, al analizar la presencia de power-law en la economía y las finanzas. También en [23], se considera un proceso de difusión con saltos para la dinámica de ingresos (en realidad para el logaritmo de los ingresos) al estudiar la dinámica de la desigualdad. Estos modelos tienen sus raíces en el trabajo de Merton [42] en 1976. En este modelo clásico, se asume típicamente que los tamaños relativos de los saltos siguen una distribución lognormal. Desde entonces, se han introducido en la literatura una amplia variedad de procesos de difusión con saltos, incluidos los procesos exponenciales de Lévy como los modelos Variance Gamma (VG), Normal Inverse Gaussian (NIG) y Carr-Geman-Madan-Yor (CGMY) (ver [15, 45, 49], por ejemplo). Esta tesis explora dos modelos específicos de difusión con saltos: el modelo clásico de Merton [42] y el modelo de Kou [38]. En este último, los tamaños relativos a los saltos siguen una distribución log-doble-exponencial. Estos modelos dan lugar a ecuaciones integro-diferenciales parciales (EIDP) dependientes del tiempo que rigen el equilibrio.

Al igual que en el caso de los modelos de EDPs, no se disponen de soluciones (semi-)analíticas para estas EIDPs generales. Por lo tanto, nos centramos en el desarrollo de soluciones numéricas efectivas para las EIDP de equilibrio asociadas tanto a los modelos de Merton como a los de Kou. Como en el problema de HJB con EDPs, utilizamos el algoritmo ALAS para tratar las fronteras libres en los problemas de empresas existentes. Este algoritmo ha demostrado ser efectivo en la resolución del problema de complementariedad lineal asociado a EIDPs y se ha aplicado en varios contextos, incluida la valoración de hipotecas de tasa fija, seguros y coaseguros, y opciones de tipo swing en mercados eléctricos, como se muestra en Calvo et al. [14] y Calvo et al. [12], respectivamente. Para la KFP con EIDPs, proponemos un método numérico adecuado y para el problema de equilibrio, consideramos el algoritmo de Steffensen como en el problema de EDPs. Además, también incorporamos un método de Crank-Nicolson para la discretización temporal, que se combina con los métodos mencionados anteriormente diseñados para modelos de estado estacionario. Además, incorporamos un tratamiento explícito del término integral, siguiendo el enfoque IMEX propuesto en [48], que utiliza el esquema de Adams-Bashforth.

Por otro lado, nuestro estudio se enfoca en el problema de equilibrio que implica la interacción entre dos sectores productivos de la economía en un país. Las empresas del primer sector tienen la opción de abandonarlo para ingresar al segundo sector (por ejemplo, cuando el primero entra en crisis), enfrentando los costos de conversión correspondientes. También, las empresas en el segundo sector tienen la opción de salir del sector ya sea cobrando un subsidio y saliendo de la economía, o pasando al primer sector afrontando los costos de conversión requeridos. Ejemplos recientes de estas situaciones aparecieron, por ejemplo, durante la última pandemia mundial, donde diferentes empresas adaptaron sus equipos de producción en sectores afectados por la crisis para fabricar mascarillas o trajes médicos de gran demanda durante la propagación del Covid-19. Otros ejemplos relacionados con empresas de un sector que se trasladaron a otro son las empresas constructoras de barcos que entraron en la producción de grandes estructuras (torres) altamente demandadas por los molinos de viento marinos cuando dejaron de ser competitivas en el sector naval. Además, la transición en la industria automotriz de la fabricación de automóviles de combustible diésel/gasolina a los eléctricos podría ser otro ejemplo.

Para modelar la evolución de los problemas de dos sectores productivos, nuestro enfoque se tiene que extender y adaptarse a las estrategias de modelado formuladas para problemas de un solo sector productivo. Esta adaptación se centra no solo en el enfoque de modelado sino también en la incorporación de metodologías numéricas adecuadas, asegurando la compatibilidad y efectividad dentro del contexto de la dinámica de dos sectores.

Las decisiones de salida en ambos sectores son determinadas internamente a través de procesos óptimos de toma de decisiones. Esto requiere considerar el costo de oportunidad de permanecer dentro de un sector, representado por un valor residual que indica el umbral en el cual las empresas optan por salir de cada sector. Los modelos matemáticos que gobiernan tales economías pueden formularse principalmente en forma de un sistema de cuatro EDPs o EIDPs acopladas. Más precisamente, estos modelos requieren un par de EDPs o EIDPs hacia atrás en el tiempo de tipo HJB, caracterizando los problemas de las empresas existentes para cada sector. Además, otro par de EDPs o EIDPs de tipo KFP hacia adelante en el tiempo rigen la evolución de la distribución de empresas dentro de cada sector. Estas ecuaciones acopladas modelan la dinámica de las empresas dentro de un contexto con dos sectores productivos.

Para la solución de equilibrio de los problemas de EDPs o EIDPs, se consideran estrategias numéricas similares al caso de un solo sector productivo. Para abordar el problema de las empresas existentes para pequeñas empresas, consideramos la aplicación del algoritmo ALAS adaptado para problemas de obstáculos bilaterales. Problemas similares surgen al resolver problemas óptimos de inversión bajo costos de transacción (ver [7, 18, 19], por ejemplo). Además, para manejar el problema de las empresas existentes para grandes empresas, proponemos emplear el algoritmo ALAS diseñado para problemas de obstáculos unilaterales. Ambas metodologías, desarrolladas por Kärkkäinen et al. [35], ofrecen soluciones efectivas para resolver problemas de complementariedad lineal asociados a EDPs y EIDPs. Además, en lo que respecta a la solución numérica de EDPs o EIDPs de KFP, consideramos el uso de técnicas numéricas apropiadas e para resolver el problema de equilibrio, se propone la implementación de una técnica de aceleración de Steffensen. Para los modelos dependientes del tiempo, incorporamos estrategias numéricas adicionales. Como en casos anteriores, para este propósito proponemos un esquema de Crank-Nicolson para la discretización del tiempo. Además, para abordar los problemas de PIDE, incorporamos un manejo explícito del término integral, que implica un esquema AB.

En base a lo anterior. Un primer aspecto innovador desde el punto de vista del modelado está relacionado con la definición general de la dinámica estocástica de la productividad. Elecciones previas en la literatura para esta dinámica se basan en el movimiento browniano geométrico o en procesos de Ornstein-Uhlenbeck. En este trabajo, proponemos alternativas más generales: un proceso de Itô general o un proceso de Lévy. Mientras que el primero implica que los caminos de la productividad estocástica son continuos, el segundo permite la posibilidad de saltos. Además, al considerar el proceso Itô, los modelos implican EDPs de HJB y KFP, mientras que al considerar procesos de Lévy obtenemos las correspondientes EIDPs de HJB y KFP. Otro aspecto innovador es la posibilidad de que las empresas ingresen al sector en un conjunto finito de productividades con sus respectivas probabilidades, es decir, la función de densidad de probabilidad de nuevos establecimientos corresponde a una variable aleatoria discreta. Esta suposición también supera la idea de ingresar en una productividad determinística prescrita. En estos ajustes de modelado más generales, incluso para problemas en estado estacionario, no podemos obtener una solución semianalítica, por lo que los métodos numéricos son obligatorios para simular los modelos de equilibrio.

Desde el punto de vista de la simulación numérica, otro logro relevante proviene de la propuesta de métodos numéricos adecuados para resolver los diferentes subproblemas involucrados en los diferentes problemas de equilibrio planteados, ya sea que involucren EDPs o EIDPs. Los ejemplos numéricos en este trabajo han sido diseñados para validar los métodos numéricos y el comportamiento esperado de las soluciones de los diferentes problemas. Por ejemplo, se ha obtenido una solución semianalítica para un problema de equilibrio estacionario particular y luego se ha validado mediante los métodos numéricos propuestos. En todos los problemas de equilibrio, se ha ilustrado la convergencia de la solución del problema evolutivo a la solución en estado estacionario.

Una conclusión general relevante es que tan pronto como incorporamos problemas de modelado y ajustes más generales, la solución de los diferentes problemas de equilibrio requiere el uso de métodos numéricos apropiados. El conjunto de métodos numéricos propuesto permite obtener aproximaciones de las soluciones de los diferentes modelos matemáticos considerados en este trabajo, que proporcionan el comportamiento cualitativo y cuantitativo esperado. Aunque hay margen para acelerar el cálculo, los tiempos computacionales son razonables, por lo que los algoritmos numéricos parecen lo suficientemente rápidos y confiables.

Otra conclusión es que este trabajo debe entenderse como una contribución científica al estudio de modelos estocásticos de equilibrio general con agentes heterogéneos y abre la posibilidad de futuros trabajos de investigación en varias direcciones.

En primer lugar, con respecto a los modelos de equilibrio propuestos en este trabajo, el análisis matemático para obtener la existencia y unicidad de solución es una pregunta abierta que no ha sido abordada, según nuestro conocimiento. De hecho, en [3] los autores señalan que la existencia y unicidad de modelos de equilibrio estacionario y evolutivo son problemas abiertos para procesos estocásticos diferentes al movimiento browniano geométrico. Desde el punto de vista del modelado, se podría considerar un modelo de dos factores para la productividad incorporando volatilidad estocástica. Una primera posibilidad podría ser el modelo de Heston. El autor de la tesis ha abordado este tipo de modelos en el contexto de valoración de derivados en [6].

En segundo lugar, con respecto a los métodos numéricos, se han explorado el uso de métodos de aprendizaje automático basados en redes neuronales informadas por la física (PINNs) utilizando la metodología desarrollada en [10] y [53]. Aunque se ha obtenido la solución de algunos modelos de EDPs para HJB y KFP, la solución del problema global de equilibrio es una cuestión pendiente que esperamos completar en el futuro.

El esquema de esta tesis es el siguiente:

En el Capítulo 1, proponemos modelos matemáticos para los problemas de equilibrio en el caso de un solo sector, donde las dinámicas de la productividad se basan en un proceso de Itô o un proceso de Lévy. Estos modelos involucran ecuaciones de HJB con problemas de frontera libre de tipo obstáculo único y ecuaciones de KFP.

El Capítulo 2 contiene la descripción del conjunto de metodologías numéricas para aproximar la solución de los modelos descritos en el capítulo anterior. Además, presentamos diferentes ejemplos numéricos que ilustran el rendimiento de los métodos y los modelos.

En el Capítulo 3, proponemos el enfoque de modelado para los problemas de equilibrio en el caso de dos sectores con dos dinámicas para la productividad. En este caso, los modelos involucran ecuaciones de HJB con problemas de frontera libre de obstáculos simples y dobles, y ecuaciones de KFP.

El Capítulo 4 describe el conjunto de métodos numéricos para resolver los modelos propuestos en el Capítulo 3 e incluye varios ejemplos de simulación numérica relacionados con los diferentes problemas de equilibrio en el caso de dos sectores.

Finalmente, se indican brevemente algunas conclusiones y posibles líneas futuras de investigación.

Resumo extenso

Esta tese estuda unha clase de modelos de axentes heteroxéneos de tempo continuo con choques idiosincráticos e mercados incompletos baixo expectativas racionais nun marco macroeconómico. Ao igual que en Hopenhayn [30], consideramos unha formulación de tempo continuo onde as empresas enfrontan choques idiosincráticos de produtividade. A evolución da produtividade é a única fonte subxacente de incerteza, modelada por un proceso estocástico tipo Itô ou un de Lévy. Supoñemos que a industria está operada por axentes heteroxéneos para relacionar os beneficios futuros (esperados) das empresas, permitindo a posibilidade de saída ou entrada de novos establecementos. Neste escenario, consideramos problemas plantexados na presenza dun ou dous sectores produtivos. No caso dun só sector, os establecementos que abandonan o sector simplemente saen da economía e reciben subvención. Porén, no caso de dous sectores, as empresas que operan no sector asociado a pequenos establecementos poden saír da economía ou trasladarse ao sector con grandes establecementos despois do pagamento dos custos de conversión.

Nun marco macroeconómico de equilibrio xeral, o obxectivo principal desta tese é proporcionar a modelización matemática tanto para os problemas de equilibrio estacionario como para os de equilibrio temporal, así como métodos numéricos axeitados para resolver os diferentes subproblemas involucrados no problema de equilibrio global.

En primeiro lugar, o noso estudo se centra no problema de equilibrio que implica un sector produtivo da economía nun país. Ao igual que en Weninger e Just [55], asumimos que as habilidades das empresas existentes seguen un proceso estocástico e hai un custo operativo fixo para que as empresas permanezan na industria. Estas dúas últimas suposicións xeran a evolución da dinámica das empresas ao longo do tempo. Polo tanto, as decisións racionais individuais non se basan só nos beneficios actuais e a dinámica transitoria debe calcularse para capturar o comportamento das empresas e as súas consecuencias nas variables económicas. Ademais, en vista dos seus choques, as empresas deciden permanecer ou saír. As decisións de saída determínanse de maneira endóxena pola decisión óptima na que o custo de oportunidade de permanecer se ten en conta mediante a existencia dun valor residual no que as empresas abandonan a industria. Esta decisión formúlase en termos dun problema de tempo de parada óptimo. Ademais, as empresas que saen son substituídas pola entrada de novas empresas de xeito que as taxas de saída e entrada se equilibren. Deste xeito, a taxa de entrada de empresas tamén é endóxena en niveis prescritos de produtividade. Neste sentido, consideramos dous exemplos, un caso onde a entrada ten lugar nunha produtividade dada por enriba da produtividade óptima de saída, seguindo a Luttmer [40], e un segundo caso onde as empresas ingresan nun conxunto finito de produtividades coas súas probabilidades correspondentes. Casos máis xerais poderían incorporarse mediante o uso de distribucións de probabilidade axeitadas para a produtividade das empresas que entran. Ademais, en algunhas industrias, estas produtividades de entrada son proporcionadas exóxenamente por modelos axeitados para incorporar os ingresos e, polo tanto, os salarios e o traballo (ver [16], por exemplo, no caso de pesquerías). Ao contrario do traballo de Guzzini e Pallestrini [29], non consideramos a interacción entre o choque idiosincrático das empresas e a súa estrutura de rede, o que require o uso de matrices de adxacencia de teoría de grafos para representar os vínculos entre as empresas.

Igual que en Achdou et al. [3], asumimos que os individuos interactúan nos mercados e toman decisións para prezos dados. Estes prezos determínanse nun equilibrio xeral e dependen de toda a distribución de individuos na economía e a súa evolución. As decisións dos individuos, xunto cos choques idiosincráticos, á súa vez déterminan a evolución desta distribución. Os modelos matemáticos para tales economías poden formulárense principalmente en termos dun sistema de dúas ecuacións diferenciais parciais (EDPs) acopladas. Máis precisamente, implican unha EDP de Hamilton-Jacobi-Bellman (HJB) para o problema de empresas existentes, con restricións de desigualdade de tipo obstáculo na solución. Esta ecuación de HJB cara atrás no tempo caracteriza o valor óptimo da función de utilidade asociada coa ganancia da empresa ao longo do tempo cun proceso estocástico evolutivo da produtividade laboral. Ademais, unha ecuación de Kolmogorov-Fokker-Planck (KFP) cara adiante no tempo rexe a evolución da distribución de empresas. Cabe notar que o acoplamento destas dúas ecuacións para modelar o comportamento de axentes heteroxéneos pódese encadrar na teoría matemática dos Mean Field Games (MFG) desenvolvida por Lasry e Lions en [39] e o sistema acoplado coñécese como un sistema MFG cara atrás-adiante. Por exemplo, este acoplamento tamén xorde no modelo Aiyagari-Bewley-Hugget para caracterizar o aforro óptimo e o comportamento de consumo de individuos con ingresos estocásticos (ver Hugget [31] e Aiyagari [4], por exemplo). Outras referencias adicionais de Mean Field Games son [8], [28], [27], por exemplo. Proponse métodos numéricos para o sistema MFG en [2]. Ademais, os modelos de equilibrio global complétanse co problema do fogar e as condicións de viabilidade.

No noso modelo, as empresas existentes avalían o valor esperado de permanecer na industria en cada momento e comparano co valor actual descontado das ganancias asociadas a saír da industria. Baseándose nesta comparación, as empresas individuais deciden permanecer ou saír da industria. Ter en conta que estes modelos con saída de empresas endóxena tamén se investigan no denominado marco de opcións reais (ver Dixit et al. [21], por exemplo). Problemas análogos xorden en finanzas matemáticas, ao valorar derivados financeiros con oportunidades de exercicio anticipado, como as opcións americanas (ver Wilmott et al. [56], por exemplo).

En traballos anteriores, como Luttmer [40] ou Da-Rocha e Sempere [16], asumíase que o proceso estocástico de produtividade segue un movemento Browniano xeométrico e as novas empresas ingresan nunha produtividade dada por enriba da produtividade de saída, de xeito que no caso de equilibrio estacionario podemos adaptar o noso modelo para obter unha solución analítica para a ecuación de KFP dun só sector produtivo e unha solución semi-analítica para o seu equilibrio. En xeral, as solucións (semi-)analíticas para estas EDPs non están dispoñibles. En Achdou et al. [1], os autores sinalan que o desenvolvemento de métodos numéricos para resolver equilibrios estacionarios e dependentes do tempo é unha cuestión aberta cando se consideran procesos estocásticos máis xerais que o movemento Browniano xeométrico para o problema dun só sector produtivo. Polo tanto, enfocámonos no desenvolvemento de solucións numéricas eficientes. Así, no problema das empresas existentes consideramos o uso do algoritmos de conxunto activo de Lagrangiano aumentado (ALAS) desenvolvido en Kärkkäinen et al. [35] para resolver o problema de complementariedade lineal asociado coa ecuación de HJB. Por exemplo, no contexto de problemas financeiros, este algoritmo utilizouse en Bermúdez et al. [9] para a valoración de opcións de Amerasia, en Calvo et al. [13] para a valoración de plans de pensións con xubilación anticipada e en Calvo et al. [11] para a valoración de opcións de tipo swing en mercados eléctricos. Para a ecuación KFP propoñemos un método numérico adecuado e para o problema de equilibrio consideramos un método de Steffensen, desenvolvido en [50], para acelerar a iteración de punto fixo, que proporciona converxencia de segundo orde no algoritmo global. Ademais, os modelos dependentes do tempo requiren métodos numéricos adicionais axeitados, polo que incorporamos un esquema de Crank-Nicolson para a discretización temporal que se combina cos métodos previamente indicados para os modelos de estado estacionario (ver Strikwerda [52], por exemplo).

Ademais, a incorporación de saltos na dinámica da produtividade serve para modelar eventos significativos e abruptos que poden ter un impacto profundo nos sistemas económicos. Tales eventos poderían incluír crises globais, como as que se presenciaron nos últimos anos, coa pandemia de COVID-19 desde 2020, ou eventos xeopolíticos como a invasión de Ucraína en 2022, ou burbullas en sectores específicos da economía, que tiveron repercusións nos mercados globais e sectores enerxéticos.

Este enfoque de modelado, empregando procesos de difusión con saltos, está motivado pola necesidade de ter en conta estes eventos discretos e inesperados dentro do marco económico. Os modelos de difusión con saltos xa se introduciron en [22] para modelar a evolución do tamaño dunha unidade económica, como unha empresa ou unha cidade, ao analizar a presenza de power-law na economía e nas finanzas. Tamén en [23], considérase un proceso de difusión con saltos para a dinámica de ingresos (en realidade para o logaritmo dos ingresos) ao estudar a dinámica da desigualdade. Estes modelos teñen as súas raíces no traballo de Merton [42] en 1976. Neste modelo clásico, supónse típicamente que os tamaños relativos dos saltos seguen unha distribución lognormal. Dende entón, introducíronse na literatura unha ampla variedade de procesos de difusión con saltos, incluídos os procesos exponenciais de Lévy como os modelos Variance Gamma (VG), Normal Inverse Gaussian (NIG) e Carr-Geman-Madan-Yor (CGMY) (ver [15, 45, 49], por exemplo). Esta tese explora dous modelos específicos de difusión con saltos: o modelo clásico de Merton [42] e o modelo de Kou [38]. Neste último, os tamaños relativos dos saltos seguen unha distribución log-dobre-exponencial. Estes modelos dan lugar a ecuacións integro-diferenciais parciais (EIDP) dependentes do tempo que rexen o equilibrio.

Do mesmo xeito que no caso dos modelos de EDPs, non se dispoñen de solucións (semi-)analíticas para estas EIDPs xerais. Polo tanto, centramonos no desenvolvemento de solucións numéricas efectivas para as EIDPs de equilibrio asociadas tanto aos modelos de Merton como aos de Kou. Do mesmo xeito que no problema de HJB con EDPs, utilizamos o algoritmo ALAS para tratar as fronteiras libres nos problemas de empresas existentes. Este algoritmo demostrou ser efectivo na resolución de problemas de complementariedade lineal asociado a EIDPs e aplicouse en varios contextos, incluída a valoración de hipotecas de taxa fixa, seguros e coaseguros, e opcións de tipo swing en mercados eléctricos, como se mostra en Calvo et al. [14] e Calvo et al. [12], respectivamente. Para a KFP con EIDPs, propoñemos un método numérico axeitado e para o problema de equilibrio, consideramos o algoritmo de Steffensen como no problema de EDPs. Ademais, tamén incorporamos un método de Crank-Nicolson para a discretización temporal, que se combina cos métodos mencionados anteriormente deseñados para modelos de estado estacionario. Ademais, incorporamos un tratamento explícito do termo integral, seguindo o enfoque IMEX proposto en [48], que utiliza o esquema de Adams-Bashforth.

Por outra banda, o noso estudo enfócase no problema de equilibrio que implica a interacción entre dous sectores produtivos da economía nun país. As empresas do primeiro sector teñen a opción de abandonalo para ingresar no segundo sector (por exemplo, cando o primeiro entra en crise), enfrontándose cos custos de conversión correspondentes. Tamén, as empresas no segundo sector teñen a opción de saír do sector xa sexa cobrando un subsidio e saindo da economía, ou pasando ao primeiro sector afrontando os custos de conversión requeridos. Exemplos recentes destas situacións apareceron, por exemplo, durante a última pandemia mundial, onde diferentes empresas adaptaron os seus equipos de produción en sectores afectados pola crise para fabricar máscaras ou traxes médicos de gran demanda durante a propagación do Covid-19. Outros exemplos relacionados con empresas dun sector que se trasladaron a outro son as empresas construtoras de barcos que entraron na produción de grandes estruturas (torres) altamente demandadas polos muíños de vento marítimos cando deixaron de ser competitivas no sector naval. Ademais, a transición na industria automotriz da fabricación de automóbiles de combustible diésel/gasolina aos eléctricos podería ser outro exemplo.

Para modelar a evolución dos problemas de dous sectores produtivos, o noso enfoque ten que extenderse e adaptarse ás estratexias de modelado formuladas para problemas dun único sector produtivo. Esta adaptación centráse non só no enfoque de modelado senón tamén na incorporación de metodoloxías numéricas axeitadas, asegurando a compatibilidade e efectividade dentro do contexto da dinámica de dous sectores.

As decisións de saída en ambos sectores son determinadas internamente a través de procesos óptimos de toma de decisións. Isto require considerar o custo de oportunidade de permanecer dentro dun sector, representado por un valor residual que indica o límite no cal as empresas optan por saír de cada sector. Os modelos matemáticos que gobernan tales economías poden formularse principalmente en forma dun sistema de catro EDPs ou EIDPs acopladas. Mais precisamente, estes modelos requiren un par de EDPs ou EIDPs cara atrás no tempo de tipo HJB, caracterizando os problemas das empresas existentes para cada sector. Ademais, outro par de EDPs ou EIDPs de tipo KFP cara adiante no tempo rexen a evolución da distribución de empresas dentro de cada sector. Estas ecuacións acopladas modelan a dinámica das empresas dentro dun contexto con dous sectores produtivos.

Para a solución de equilibrio dos problemas de EDPs ou EIDPs, considéranse estratexias numéricas semellantes ao caso dun só sector produtivo. Para abordar o problema das empresas existentes para pequenas empresas, consideramos a aplicación do algoritmo ALAS adaptado para problemas de obstáculos bilaterais. Problemas semellantes surxen ao resolver problemas óptimos de investimento baixo custos de transacción (ver [7, 18, 19], por exemplo). Ademais, para manexar o problema das empresas existentes para grandes empresas, propoñemos empregar o algoritmo ALAS deseñado para problemas de obstáculos unilaterais. Ambas metodoloxías, desenvolvidas por Kärkkäinen et al. [35], ofrecen solucións efectivas para resolver problemas de complementariedade lineal asociados a EDPs e EIDPs. Ademais, no referente á solución numérica de EDPs ou EIDPs de KFP, consideramos o uso de técnicas numéricas apropiadas e para resolver o problema de equilibrio, propónse a implementación dunha técnica de aceleración de Steffensen. Para os modelos dependentes do tempo, incorporamos estratexias numéricas adicionais. Como en casos anteriores, para este propósito propoñemos un esquema de Crank-Nicolson para a discretización do tempo. Ademais, para abordar os problemas de PIDE, incorporamos un manexo explícito do termo integral, que implica un esquema AB.

En base ao anterior. Un primeiro aspecto innovador dende o punto de vista do modelado está relacionado coa definición xeral da dinámica estocástica da produtividade. As escolles previas na literatura para esta dinámica baseáronse no movemento browniano xeométrico ou en procesos de Ornstein-Uhlenbeck. Neste traballo, propoñemos alternativas máis xerais: un proceso de Itô xeral ou un proceso de Lévy. Mentres que o primeiro implica que os camiños da produtividade estocástica son continuos, o segundo permite a posibilidade de saltos. Ademais, ao considerar o proceso de Itô, os modelos implican EDPs de HJB e KFP, mentres que ao considerar procesos de Lévy obtemos as correspondentes EIDPs de HJB e KFP. Outro aspecto innovador é a posibilidade de que as empresas ingresen ao sector nun conxunto finito de produtividades coas súas respectivas probabilidades, é dicir, a función de densidade de probabilidade de novos establecementos corresponde a unha variable aleatoria discreta. Esta suposición tamén supera a idea de ingresar nunha produtividade determinística prescrita. Nestes axustes de modelado máis xerais, incluso para problemas en estado estacionario, non podemos obter unha solución semi-analítica, polo que os métodos numéricos son obrigatorios para resolver os modelos de equilibrio.

Dende o punto de vista da simulación numérica, outro logro relevante provén da proposta de métodos numéricos axeitados para resolver os diferentes subproblemas involucrados nos varios problemas de equilibrio plantexados, xa sexan EDPs ou EIDPs. Os exemplos numéricos neste traballo foron deseñados para validar os métodos numéricos e o comportamento esperado das solucións dos diferentes problemas. Por exemplo, obtívose unha solución semi-analítica para un problema de equilibrio estacionario particular e despois validouse mediante os métodos numéricos propostos. En todos os problemas de equilibrio, ilustrouse a converxencia da solución do problema evolutivo á solución en estado estacionario.

Unha conclusión xeral relevante é que tan axiña como incorporamos problemas de modelado e axustes máis xerais, a solución dos diferentes problemas de equilibrio require o uso de métodos numéricos axeitados. O conxunto de métodos numéricos proposto permite obter aproximacións das solucións dos diferentes modelos matemáticos considerados neste traballo, que proporcionan o comportamento cualitativo e cuantitativo esperado. Aínda que hai margen para acelerar o cálculo, os tempos computacionais son razoables, polo que os algoritmos numéricos parecen abondamente rápidos e fiables.

Outra conclusión é que este traballo debe entenderse como unha contribución científica ao estudo de modelos estocásticos de equilibrio xeral con axentes heteroxéneos e abre a posibilidade de futuros traballos de investigación en varias direccións.

En primeiro lugar, con respecto aos modelos de equilibrio propostos neste traballo, o análise matemático para obter a existencia e unicidade de solución é unha pregunta aberta que non foi abordada, segundo o noso coñecemento. De feito, en [3] os autores sinalan que a existencia e unicidade de solución para modelos de equilibrio estacionario e evolutivo son problemas abertos para procesos estocásticos diferentes ao movemento browniano xeométrico. Dende o punto de vista do modelado, poderíase considerar un modelo de dous factores para a produtividade incorporando volatilidade estocástica. Unha primeira posibilidade podería ser o modelo de Heston. O autor da tese abordou este tipo de modelos no contexto de valoración de derivados en [6].

En segundo lugar, con respecto aos métodos numéricos, explorouse o uso de métodos de aprendizaxe automática baseados en redes neuronais informadas pola física (PINNs) utilizando a metodoloxía desenvolvida en [10] e [53]. Aínda que se obtivo a solución de alguns modelos de EDPs para HJB e KFP, a solución do problema global de equilibrio é unha cuestión pendente que esperamos completar no futuro.

O esquema desta tese é o seguinte:

No Capítulo 1, propoñemos modelos matemáticos para os problemas de equilibrio no caso dun só sector, onde as dinámicas da produtividade baséanse nun proceso de Itô ou un proceso de Lévy. Estes modelos involucran ecuacións de HJB con problemas de fronteira libre de tipo obstáculo único e ecuacións de KFP.

O Capítulo 2 contén a descrición do conxunto de metodoloxías numéricas para aproximar a solución dos modelos descritos no capítulo anterior. Ademais, presentamos diferentes exemplos numéricos que ilustran o rendemento dos métodos e os modelos.

No Capítulo 3, propoñemos o enfoque de modelado para os problemas de equilibrio no caso de dous sectores con dúas dinámicas para a produtividade. Neste caso, os modelos involucran ecuacións de HJB con problemas de fronteira libre de obstáculos simples e dobres, e ecuacións de KFP.

O Capítulo 4 describe o conxunto de métodos numéricos para resolver os modelos propostos no Capítulo 3 e inclúe varios exemplos de simulación numérica relacionados cos diferentes problemas de equilibrio no caso de dous sectores.

Finalmente, indícanse brevemente algunhas conclusións e posibles liñas futuras de investigación.

Appendix A

ALAS algorithms for obstacle problems

Algorithm 1: Algorithm for solving a unilateral obstacle problem

Input: S, A, f, $\beta > 0$, $itMax$

Output: V, $\mathcal{J}$

Initialize $V^0 = S$ and $P^0 = \min\{f - AV^0,\, 0\}$.

Determine the initial active and inactive sets:

$$\mathcal{J}^0 = \{n \in \mathcal{N} : [\mathcal{Q}^0]_n < 0\} \quad \text{and} \quad \mathcal{I}^0 = \mathcal{N} \setminus \mathcal{J}^0 = \{n \in \mathcal{N} : [\mathcal{Q}^0]_n = 0\},$$

where

$$\mathcal{Q}^0 = \min\{P^0 + \beta(V_1^0 - S), 0\},$$

Determine $(V^1,\, P^1)$ as the unique solution of the linear system:

$$\begin{aligned} &AV^1 + P^1 = f, && \\ &P^1 = 0, && \text{on} \quad \mathcal{I}^m, \\ &V^1 = S, && \text{on} \quad \mathcal{J}^m, \end{aligned}$$

Set $P^1 = \min\{P^1,\, 0\}$.

for $m = 1 : itMax$ **do**

$\quad \mathcal{Q}^m = \min\{P^m + \beta(V^m - S),\, 0\}$;

$\quad \mathcal{J}^m = \{n \in \mathcal{N} : [\mathcal{Q}^m]_n < 0\}$;

$\quad \mathcal{I}^m = \{n \in \mathcal{N} : [\mathcal{Q}^m]_n = 0\}$;

$\quad$ **if** $\mathcal{J}^m = \mathcal{J}^{m-1}$ **then**

$\quad\quad V = V^m$;

$\quad\quad \mathcal{J} = \mathcal{J}^m$;

$\quad\quad$ **break**

$\quad$ **else**

$\quad\quad$ Determine $(V^{m+1},\, P^{m+1})$ as the unique solution of the linear system:

$$\begin{aligned} &AV^{m+1} + P^{m+1} = f, && \\ &P^{m+1} = 0, && \text{on} \quad \mathcal{I}^m, \\ &V^{m+1} = S, && \text{on} \quad \mathcal{J}^m, \end{aligned} \tag{A.1}$$

$\quad\quad$ Set $P^{m+1} = \min\{P^{m+1},\, 0\}$.

$\quad$ **end**

end

Algorithm 2: Algorithm for solving a bilateral obstacle problem

Input: S, S_1^2, A_1, f^1, $\beta > 0$, $itMax$

Output: V_1, $\mathcal{J}_S$, $\mathcal{J}_{S_1^2}$

Initialize $V_1^0 = \dfrac{S + S_1^2}{2}$ and $\overline{P}^0 = f^1 - A_1 V_1^0$.

Determine the initial active and inactive sets:

$$\overline{\mathcal{J}}^0 = \mathcal{J}_S^0 \cup \mathcal{J}_{S_1^2}^0 \quad \text{and} \quad \overline{\mathcal{I}}^0 = \overline{\mathcal{N}} \setminus \overline{\mathcal{J}}^0,$$

where

$$\mathcal{J}_S^0 = \{n \in \mathcal{N} : [\overline{P}^0 + \beta(V_1^0 - S)]_n < 0\},$$
$$\mathcal{J}_{S_1^2}^0 = \{n \in \mathcal{N} : [\overline{P}^0 + \beta(V_1^0 - S_1^2)]_n > 0\}.$$

Determine $(V_1^1, \overline{P}^1)$ as the unique solution of the linear system:

$$A_1 V_1^1 + \overline{P}^1 = f^1,$$

where $\overline{P}^1 = 0$ on $\overline{\mathcal{I}}^0$, $V_1^1 = S$ on $\mathcal{J}_S^0$ and $V_1^1 = S_1^2$ on $\mathcal{J}_{S_1^2}^0$.

for $m = 1 : itMax$ **do**

  $\mathcal{J}_S^m = \{n \in \mathcal{N} : [\overline{P}^m + \beta(V_1^m - S)]_n < 0\}$;

  $\mathcal{J}_{S_1^2}^m = \{n \in \mathcal{N} : [\overline{P}^m + \beta(V_1^m - S_1^2)]_n > 0\}$;

  if $\mathcal{J}^m = \mathcal{J}^{m-1}$ **then**

    $V_1 = V^m$;

    $\mathcal{J}_S = \mathcal{J}_S^m$;

    $\mathcal{J}_{S_1^2} = \mathcal{J}_{S_1^2}^m$;

    break

  else

    Determine $(V_1^{m+1}, \overline{P}^{m+1})$ as the unique solution of the linear system

$$A_1 V_1^{m+1} + \overline{P}^{m+1} = f^1, \tag{A.2}$$

    where $\overline{P}^{m+1} = 0$ on $\overline{\mathcal{I}}^m$, $V_1^{m+1} = S$ on $\mathcal{J}_S^m$ and $V_1^{m+1} = S_1^2$ on $\mathcal{J}_{S_1^2}^m$.

  end

end

Bibliography

[1] Y. Achdou, F. J. Buera, J. M. Lasry, P. L. Lions, and B. Moll. Partial differential equation models in macroeconomics. *Phil. Trans. R. Soc. A*, 372:20130397, 2014.

[2] Y. Achdou and I. Capuzzo-Dolcetta. Mean field games: numerical methods. *SIAM Journal on Numerical Analysis*, 48:1136–1162, 2010.

[3] Y. Achdou, J. Han, J. M. Lasry, P. L. Lions, and B. Moll. Income and wealth distribution in macroeconomics. A continuous approach. *Review of Economic Studies*, 89:45–86, 2022.

[4] S. R. Aiyagari. Uninsured idiosyncratic risk and aggregate saving. *The Quaterly Journal of Economics*, 109:659–684, 1994.

[5] A. Almendral and C. W. Oosterlee. Numerical valuation of options with jumps in the underlying. *Applied Numerical Mathematics*, 53(1):1–18, 2005.

[6] I. Arregui and J. Ráfales. A stochastic local volatility technique for TARN options. *International Journal of Computer Mathematics*, 97:1133–1149, 2020.

[7] I. Arregui and C. Vázquez. Numerical solution of an optimal investment problem with proportional transaction costs. *Journal of Computational and Applied Mathematics*, 236:2923–2937, 2012.

[8] M. Bardi. Explicit solutions of some linear-quadratic mean field games. *Network Heterogeneous Media*, 7:246–261, 2012.

[9] A. Bermúdez, M. R. Nogueiras, and C. Vázquez. Comparison of two algorithms to solve a fixed-strike Amerasian options pricing problem. *In: International Series in Numerical Mathematics*, 154:95–106, Birkhauser, 2006.

[10] A. Borovykh, D. Kalise, A. Laignelet, and P. Parpas. Data-driven initialization of deep learning solvers for Hamilton-Jacobi-Bellman PDEs. *IFAC-PapersOnLine*, 55(30):168–173, 2022.

[11] M. C. Calvo-Garrido, M. Ehrhardt, and C. Vázquez. Pricing swing options in electricity markets with two stochastic factors using a partial differential equations approach. *Journal of Computational Finance*, 20(3):81–107, 2017.

[12] M. C. Calvo-Garrido, M. Ehrhardt, and C. Vázquez. Jump-diffusion models with two stochastic factors for pricing swing options in electricity markets with partial-integro differential equations. *Applied Numerical Mathematics*, 139:77–92, 2019.

[13] M. C. Calvo-Garrido, A. Pascucci, and C. Vázquez. Mathematical analysis and numerical methods for pricing pension plans allowing early retirement. *SIAM Journal on Applied Mathematics*, 73(5):1747–1767, 2013.

[14] M. C. Calvo-Garrido and C. Vázquez. Effects of jump-diffusion models for the house price dynamics in the pricing of fixed-rate mortgages, insurance and coinsurance. *Applied Mathematics and Computation*, 271:730–742, 2015.

[15] R. Cont and P. Tankov. Financial Modelling With Jump Processes, Chapman & Hall/CRC Financial Mathematics Series. *CRC Press*, 2004.

[16] J. M. Da-Rocha, R. Prellezo, J. Sempere, and L. Taboada Antelo. A dynamic economic equilibrium model for the economic assessment of the fishery stock-rebuilding policies. *Marine Policy*, 81:185–195, 2017.

[17] J. M. Da-Rocha and J. Sempere. ITQs, Firm dynamics and wealth distribution:

Does full tradability increase inequality? *Environmental and Resource Economics*, 68(2):249–273, 2017.

[18] M. Dai and F. Yi. Finite-horizon optimal investment with transaction costs: a parabolic double obstacle problem. *Journal of Differential Equations*, 246:1445–1469, 2009.

[19] M. H. A. Davis and A. R. Norman. Portfolio selection with transaction costs. *Mathematics of Operations Research*, 15:676–713, 1990.

[20] Y. d'Halluin, P. A. Forsyth, and K. R. Vetzal. Robust numerical methods for contingent claims under jump diffusion processes. *IMA Journal of Numerical Analysis*, 25(1):87–112, 2005.

[21] A. K. Dixit and R. S. Pindyck. *Investment under uncertainty.* Princeton University Press, Princeton, 1994.

[22] X. Gabaix. Power laws in economics and finance. *Annual Review of Economics*, 1:255–293, 2009.

[23] X. Gabaix, J. M. Lasry, P. L. Lions, and B. Moll. The dynamics of inequality. *Econometrica*, 84:2071–2111, 2016.

[24] R. Glowinski. *Numerical Methods for Nonlinear Variational Problems.* Springer, New York, 1984.

[25] R. Glowinski, J. L. Lions, and R. Trémolières. *Analyse Numérique des Inéquations Variationelles, Vol. 1.* Dunod, Paris, 1976.

[26] R. Glowinski, J. L. Lions, and R. Trémolières. *Numerical Analysis of Variational Inequalities.* North Holland, Amsterdam, 2000.

[27] D. A. Gomes, J. Mohr, and R. R. Souza. Discrete time, finite state space mean field games. *Journal Mathématiques Pures et Appliquées*, 93:308–328, 2010.

[28] O. Guéant. A reference case mean field models. *Journal Mathématiques Pures et Appliquées*, 92:276–294, 2009.

[29] E. Guzzini and A. Palestrini. Growth in total factor productivity and links among firms. *J. Econ. Interact. Coord.*, 11:35–55, 2016.

[30] H. A. Hopenhayn. Entry, exit and firm dynamics in long run equilibrium. *Econometrica*, 60:1127–1150, 1989.

[31] M. Hugget. The risk-free rate in heterogeneous-agent incomplete-insurance economies. *Journal of Economic Dynamics and Control*, 17:953–969, 1993.

[32] K. Ito and K. Kunisch. *Lagrange Multiplier Approach to Variational Problems and Applications*. SIAM, Philadelphia, 2008.

[33] K. Ito and K. Kunish. Semi-smooth Newton methods for variational inequalies of the first kind. *Mathematical Modelling and Numerical Analysis*, 37:41–62, 2002.

[34] K. Ito and K. Kunish. Semi-smooth Newton methods for state-constrained optimal control problems. *Systems and Control Letters*, 50:221–228, 2003.

[35] T. Kärkkäinen, K. Kunisch, and P. Tarvainen. Augmented Lagrangian active set methods for obstacle problems. *Journal of Optimization Theory and Applications*, 119(3):499–533, 2003.

[36] D. Kinderlehrer and G. Stampacchia. *An Introduction to Variational Inequalities and their Applications*. Academic Press, Boston, 1982.

[37] P. Kloeden and E. Platen. *Numerical Solution of Stochastic Differential Equations*. Springer, Berlin, 1992.

[38] S. G. Kou. A jump-diffusion model for option pricing. *Manage. Sci.*, 48(8):1086–1101, 2002.

[39] J. M. Lasry and P. L. Lions. Mean field games. *Japanese Journal of Mathematics*, 2(1):229–260, 2007.

[40] G. J. Luttmer. Selection, growth and the size distribution of firms. *Quaterly Journal of Economics*, 122:1104–1144, 2007.

[41] G. J. Luttmer. Models of growth and firm heterogeneity. *Annu. Rev. Econ.*, 2(1):547–576, 2010.

[42] R. C. Merton. Option pricing when underlying stock returns are discontinuous. *J. of Financ. Econ.*, 3(1-2):125–144, 1976.

[43] T. Mikosh. *Elementary Stochastic Calculus with Finance in View.* World Scientific Press, Singapur, 1998.

[44] B. Oksendal. *Stochastic Differential Equations. An introduction with applications.* Springer, Berlin, 1995.

[45] A. Pascucci. *PDE and Martingale Methods in Option Pricing.* Bocconi University Press, Springer, Milan, 2011.

[46] J. Ráfales and C. Vázquez. Equilibrium models with heterogeneous agents under rational expectations and its numerical solution. *Communications in Nonlinear Science and Numerical Simulation*, 96:105673, 2021.

[47] J. Ráfales and C. Vázquez. Jump diffusion productivity models in equilibrium problems with heterogeneous agents. *(Submitted for publication)*, 2023.

[48] S. Salmi and J. Toivanen. IMEX schemes for pricing options under jump-diffusion models. *Appl. Numer. Math.*, 84:33–45, 2014.

[49] W. Schoutens. *Lévy processes in finance: pricing financial derivatives.* Wiley Online Library, 2003.

[50] J. Steffensen. Remarks on iteration. *Scandinavian Actuarial Journal*, 1933(1):64–72, 1933.

[51] N. Stokey. *The Economics of Inaction.* Princeton University Press, Princeton, 2009.

[52] J. C. Strikwerda. *Finite Differences Schemes and Partial Differential Equations*. Wadsworth Publisher, Belmont (USA), 2008.

[53] R. van der Meer, C. W. Oosterlee, and A. Borovykh. Optimally weighted loss functions for solving PDEs with neural networks. *Journal of Computational and Applied Mathematics*, 405:113887, 2022.

[54] C. Vázquez. An upwind numerical approach for an American and European option pricing model. *Applied Mathematics and Computation*, 97:273–286, 1998.

[55] Q. Weninger and R. E. Just. Firm dynamics with tradable output permits. *American Journal of Agricultural Economics*, 84(3):572–584, 2002.

[56] P. Wilmott, S. Howison, and J. Dewynne. *Option pricing: Mathematical models and computation*. Oxford Financial Press, Oxford, 1996.